Practical Implementation of Hybrid Energy Systems for Small Loads in Rural South Africa

By

Kelebogile Confidence Meje

Dissertation submitted in fulfilment of the requirements for the degree:

Master of Engineering

in

Electrical Engineering

In the Department of Electrical, Electronic and Computer Engineering

Faculty of Engineering, Built Environment and Information Technology

Central University of Technology, Free State

Supervisor: Ms. L. Bokopane

Co-Supervisor: Prof. K. Kusakana

May 2021

DECLARATION

I, KELEBOGILE CONFIDENCE MEJE, student number , do hereby declare that this research project, which has been submitted to the Central University of Technology Free State, for the degree: Master of Engineering in Electrical Engineering, is my own independent work and complies with the Code of Academic Integrity, as well as other relevant policies, procedures, rules and regulations of the Central University of Technology, Free State. This project has not been submitted before by any person in fulfilment (or partial fulfilment) of the requirements for the attainment of any qualification.

K.C. MEJE

Date: 2021

DEDICATION

I dedicate this dissertation to Jesus Christ the son of the living God, the author and finisher of our faith, the visible image of the invisible God, the first born of all creation, in him all things hold together. To my husband, Itumeleng Meje, my children, Tshimologo and Onalerona Meje, for their tolerance, support, love, understanding and prayers throughout my studies. My Aunt Masenate Kgware, who initially believed in me and later developed the zeal to focus on my studies. Finally, to my Mother, Mamokete Kgware and siblings, Dimakatso and Tsholofelo Kgware, for their continuous support.

ACKNOWLEDGMENTS

First of all, I would like to give the entire Honour, the Glory and all the Praise to the Father, Son of the Living God (Jesus Christ) and the Holy Spirit for making everything possible for me by giving me and the absolute strength in this study in the mighty name of JESUS!

I further express my sincere appreciation to my supervisors Ms. Lindiwe Bokopane and Prof. Kanzumba Kusakana, who were constant with their mentorship and guidance throughout the process of my studies. Their continuous support and knowledge were appreciated. They provided me with motivation and on-going inspiration throughout this study. To Dr. Mukwanga Siti and Thato Ratau, for their contribution, inspiration and support in advancing my studies

Finally, I acknowledge the support and assistance provided to me by the Central University of Technology, Free State (CUT). CUT has been tremendously generous in supporting my academic efforts and many of my colleagues and friends have contributed ideas, feedback and advice.

Thank You.

LIST OF ABBREVIATIONS

AC	Average Consumption
ACMG	Alternating Current Microgrid
ACDCMG	Hybrid Microgrid
AGC	Automatic Generation Control
APD	Afternoon Peak Demand
ANN	Artificial Neural Network
BEE	Base Electric Energy
BES	Battery Energy Storage
BT	Battery
CELs	Controllable Energy Loads
CHP	Combined Heating Power
C&I	Commercial and Industrial
CO_2	Carbon Dioxide
COE	Cost of Energy
CS	Cuckoo Search
DC	Direct Current
DCMG	Direct Current Microgrid
DG	Diesel Generator
DGs	Distributed Generations
DS	Distributed Storage
DoE	Department of Energy
DERs	Distributed Energy Sources
DESs	Distribute Energy Sources
EE	Excess Energy
EMS	Energy Management System
EOP	Evening Off Peak
EP	Evening Peak
ESSs	Energy Storage Systems
ESKOM	Electric Supply Commission

FCs	Fuel cells
FLC	Fuzzy Logic Controller
FS	Free State
GAs	Genetic Algorithms
HC	High Consumption
HK	Hydrokinetic
HKT	Hydrokinetic Turbine
HRES	Hybrid Renewable Energy System
HRS	Hybrid Renewable System
HS	Hybrid System
HVAC	Heating, Ventilation and Air Condition
IC	Integrated Circuit
IDE	Integrated Development Environment
IEEE	Institute of Electrical and Electronic Engineers
IGBT	Insulated-Gate Bipolar Transistor
IRP	Integrated Resources Plan
KZN	Kwa-Zulu Natal
LC	Low Consumption
LCD	Light Emitting Diode
LEC	Level Energy Costs
LEM	Local Energy Market
MC	Morning Consumption
MD	Morning Demand
MG	Microgrid
MINLP	Mixed Integer Non-linear Programming
MILP	Mixed Integer Linear Programming
MP	Morning Peak
MPC	Model Predictive Control
MOP	Morning Off Peak
MPPT	Maximum Power Point Tracking
Mt	Million Tonnes

NF	Neuro Fuzzy
NR	Newton Raphson
PCC	Point Common Coupling
PI	Proportional Integral
PID	Proportional Integral Derivative
PSO	Particle Swarm Optimization
PSP	Power Supply Probability
PV	Photovoltaic
PWM	Pulse Width Modulation
RE	Renewable Energy
RES	Renewable Energy Source
RESs	Renewable Energy Sources
RT	Real-Time
RT-LAB	Real-Time Laboratory
SA	South Africa
SHS	Solar Home Systems
SoC	State of Charge
SoH	State of Health
SRE	Stand-alone Renewable Energy
STATCOM	Synchronous Compensator
SVC	Static Var Compensator
SVPWM	Space-Vector Pulse Width Modulation
USB	Universal Serial Bus
VHC	Very High Consumption
VLC	Very Low Consumption
VSI	Voltage Sourced Inverter
WAMS	Wide Area Measurements Systems
WT	Wind Turbine

NOMENCLATURE

$P_{PV,system}$	Output Power of the whole PV System
$P_{PV,\frac{module}{U}}$	Nominal Output Power of one PV Panel
η_{PV}	Number of PV Panels in Parallel
$P_{WT,system}$	Output Power of the Wind System
$P_{\frac{WT}{U}}$	Nominal Output Power of the one Wind Turbine
η_{WT}	Number of Wind Turbines Connected in Parallel
$P_{HKT,system}$	Output Power of the Hydrokinetic System
$P_{\frac{HKT}{U}}$	Nominal Output Power of the one Hydrokinetic Turbine
η_{HKT}	Number of Hydrokinetic Turbines Connected in Parallel
P_{DG}	Output Power of the Diesel Generator, which is a percentage of the maximum DG Power
$P_{DG,max/U}$	Maximum Nominal DG Power
X_{DG}	DG Output decision variable between 0-1. 0 Corresponds to no DG output and 1 to maximum output
P_{bat}	Instantaneous Output Power, which is a percentage of the maximum battery Power at that time t
$P_{bat,\max/U}$	Maximum Battery Power at that time t
$X_{bat\ t}$	Battery Output decision variable between [0, 1] as for the DG
η_{bat}	Number of Battery Strings in Parallel
v_o^*	Output voltage
v_{ref}	Output voltage reference at no load
R_D	Output impedance
i_o	Output current
i_{max}	Maximum Output current
v_n	Nominal output voltage
k_p' , k_i'	Control parameters

i_G^*	Current flow
ε_v	Limits

ABSTRACT

Hybrid renewable energy systems (HRESs), are alternative off-grid methods of generating power to remote rural areas, where power lines are not economically viable. Most of the research studies on renewable hybrid systems or microgrids (MGs) in South Africa, focus mainly on the optimal sizing and optimal control of different systems, by making use of renewable energy simulation softwares, however, there is a lack of research carried out on the implementation of these hybrid systems in real time.

The aim is to develop a real time control method for an isolated hybrid system submitted to a variable load, as well as resources. The first step towards achieving this aim, was to critically review available published research works, to describe recent developments in improving the optimum operating concept of microgrid controllers for stand-alone or grid-connected systems. Secondly, to investigate any real-time implementation established by either hierarchical or distributed control. Then to, analyze their reliability and functionality in practical set up of the controller, in managing power in the system to the variable load.

The study provided a brief overview of microgrid prototype systems, microgrid controls, operating modes and multi-DER microgrid types built into a hybrid system, which introduces a number of strategies or techniques for managing remote rural application prototypes in an isolated or grid-connected system. However, hierarchical control was found to be more appropriate for large microgrids with multiple types of distributed energy resources (DERs), compared to distributed control, particularly when combined with energy storage systems (ESSs), in isolated mode.

The rising of hybrid system controllers in real-time renewable energy for the optimum energy management system (EMS), required the design of a real-time controller to operate the entire system in real time. Increasing popularity of renewable energy (RE) has a control strategy that determined the overall efficiency of the hybrid system (HS), although the energy management system of these systems is particularly complex to be managed.

The study's main contribution is to investigate the feasible controller and, later, to present an advanced control strategy for managing and controlling the flow of hybrid renewable energy with a diesel generator (DG) and battery (BT) as a backup in a rural

application of SA. EMS would be implemented, using a fuzzy logic controller (FLC) in MATLAB / SIMULINK. This study analysed input and output variables for the design of a controller, with a set of rules and a three-dimension (3D) surface. Simulation results of related studies with different objectives were analysed, with the aim of sussing out an appropriate controller for the current study.

Arduino Mega was used for coding and uploaded to the implementation of practical implementation of the study. The system operated successfully by supplying the load. This study finally answered the question of the feasibility of the controller in real-time applications.

CONTENTS

LIST OF FIGURES

LIST OF TABLES

CHAPTER 1: INTRODUCTION

1.1. BACKGROUND

South Africa's (SA's) substantial challenge, is that it uses a significant amount of energy, due to statistical population growth occurring in the country. This constant increase in load demand is one of the factors that contributes to the disruption and lack of sustainability on the local grid [1]. Energy provision plays a crucial role in improving the lives of the rural community. It may create and sustain several developments and economic transformation. These developments are generally not possible without sustainable energy [2]. More so, the energy demands in the country are largely met by non-renewable energy resources, such as coal and nuclear. Recent studies indicate that 72.1% of the primary consumption was met by coal whilst nuclear contributes to approximately 4.2% of the generation. These fossil fuels are significantly polluting the environment negatively with tonnes of carbonaceous material, estimated to be approximately 224 million tonnes (Mt) of coal annually. SA is becoming one of the leading carbon dioxide (CO_2) emitters, largely due to heavy dependence on fossil fuels. Africa is ranked amongst the 5th in the World's top largest carbon dioxide emitters accounting for 35% of emissions [3].

The Department of Energy (DoE), confirmed the common vision of improving SA's energy mix, by having clean energy by 2030 and a large portion of Intergraded Resources Plan (IRP), is allocated to renewables by the government [4]. SA has several types of renewable energy (RE) resources, that have the potential to contribute significantly to the country. In particular, solar, wind, waves and biomass power, as they are suitable for off-grid and small-scale solution [5, 6]. RE increases access to electricity in rural areas where power lines are prohibited. Moreover, the energy demand in the country is largely met by non-renewable energy resources, such as coal and nuclear. RE is the most appropriate energy option for the reduction of CO_2 emissions, relieve climate change [7]. It further increases the usage of natural energy resources.

There are a number of stand-alone renewable energy (SRE) systems that cannot meet the load at all, due to the variability of the load and resources. Stand-alone RE microgrid systems, have been successfully implemented in other parts of the world, such as Europe,

Asia, North America, as well as Australia, and SA is catching up on this trend [8]. The first pilot project to electrify a sparsely located area, with the use of photovoltaic (PV) battery backup system, was implemented by SA utility power provider ESKOM. The electrification took place in Ficksburg, in the Free State (FS) province [9]. However, one of the solutions to replace stand-alone renewable energy systems, is the use of a hybrid system, which minimizes the shortcomings of each renewable energy source (RES) used individually [10].

Several studies have been carried out, with regards to optimal sizing and optimal control of hybrid systems in SA [11]. The systems were tested on simulations, in most of the cases and were not built physically. Therefore, it is still challenging to see how a hybrid system would perform in real time, under variable load and resource in the South African context.

The HRES concept is gaining popularity in remote rural areas, for their electrifications and, on the other hand, generating low-carbon emissions [12, 13], by moving away from the traditional energy network. RE has many applications and has been used in various part of the country for the electrification of isolated homes, vehicles, etc [14]. The combination of RE and storage is increasingly offering a preferable solution to the problem caused or created by conventional power, particularly, the integration of solar and wind power that has been vastly used worldwide [14] for electrification The involvement of more than one type of RE sources plays a crucial role and appropriate storage may improve HRES's efficiency and reliability to a greater extent [15]. It has been pointed out in [16], that it is of importance to include storage devices in remote locations, due to the fluctuating nature of the RES generated power. Energy management (EM) was performed by [17], before using three different controllers, such as FLC [18, 19] , neural network [20] and genetic algorithm [21], in the HRES. FLC was considered among the most recent developments in control techniques and strategies, required to achieve load balancing [22], [23]. The implementation of FLC is used to manage the flow of energy in the extended hybrid renewable system (HRS), which has been investigated in order to satisfy the load of the isolated ones in other parts of the world. EMS was further, used to optimally share power between the different components within the RE [24]. A number of techniques have previously been used to manage the flow of energy in the HS and previous work has shown that FLC may manage complex systems [24-26]. The study's main contribution, is to investigate the feasible controller and, subsequently, present an advanced control strategy

to manage and control the flow of hybrid renewable energy with DG and BT as a backup, in rural SA applications.

1.2. PROBLEM STATEMENT

Most studies related to hybrid systems conducted in SA are simulation based and focus on the feasibility of hybrid renewable systems. As a result, there is a lack of performance analysis of such a system operating in real-time condition.

1.3. OBJECTIVES OF THE STUDY

The aim of the study is to design and implement a controller for a hybrid renewable energy system in real time. The system consists of solar PV, Wind, Pico-Hydrokinetic and a Diesel Generator with a battery storage system.

Objectives of the study are as follows:

- To review current status regarding the development of a stand-alone renewable hybrid system, with a diesel generator and battery storage system, within rural electrification in SA.
- To develop a Fuzzy logic controller in Simulink, to optimally manage the operation of the proposed system.
- Perform simulations of the proposed system managed by the developed controller under variable resources and load demand conditions.
- To build a prototype and conduct an analysis, to verify the simulation results.

1.4. OUTCOMES OF STUDY:

- The FLC controller model for optimal management of the hybrid renewable system with DG and battery storage.
- A prototype of hybrid system that may be used for performance analysis of the system under different operating conditions.
- A Masters dissertation and publications.

1.5. RESEARCH METHODOLOGY

To achieve the objectives of the study, the methodology is as follows:

1.5.1 Literature Review

The review provided a brief overview of microgrid prototype systems, microgrid controls, operating modes and multi-DER microgrid types built into a hybrid system, that introduced a number of strategies or techniques for managing remote rural application prototypes in an isolated and grid-connected system. The review further described recent development studies, aimed at improving the optimum operation principle of microgrid controllers for stand alone, hybrid and grid-tied connected systems, for real-time implementation of the system by means of hierarchical control or distributed control strategy for a reliable and optimal energy management system.

1.5.2 System Modeling

The optimal energy management controller was developed and modeled HRES in SIMULINK, using fuzzy logic in the following pattern:

- Input and output variables using membership functions.
- Fuzzy logic control (FLC) rules and surface.
- Switching times developed.
- Variable load system built.
- Modelling of PV/PHK/WT/DG/BT hybrid system in SIMULINK.

1.5.3 Simulations

This section examined the viable controller, before introducing an advanced control strategy, to manage and control the flow of hybrid HRE, with DG and BT as a backup, in rural application of SA. The results analysed the input and output variables for the design of a controller, with a set of rules and surfaces and EMS's were further implemented, using

a FLC in SIMULINK, to demonstrate the performance that is acceptable in managing the power flow between the sources under various load demands, while storing energy in the battery.

1.5.4 Practical setup

Laboratory built practical experiment was carried out, using the following methods and considering the essential software and hardware tools:

- Proteus design suite used to perform simulation, by testing the functionality and demonstrating the result of the proposed system.
- Arduino IDE was used to write the code.
- Arduino MEGA, which is the microcontroller of the system, was programmed to control and monitor the entire system, by sending a signal to the sources and determine which source should take the load.
- SD card for storing or logging data from the system to the microcontroller.
- Relays used to open and close the renewable energy sources (RESs) switches and backup system for power supply and determine when to switch ON/OFF under the command/ influence of the microcontroller.
- LCD used to display the proposed system's real time event parameters.
- Heatsink was installed in the circuit to dissipating heat from the transistors.
- Voltage regulator used to regulate the voltage to acceptable voltage, used by the controller.
- Resistors to limit current.
- Diodes to avoid back feed.
- LED's representing the load.

1.6. HYPOTHESIS

- Both the developed FLC model and the prototype system may minimize the use of the DG and maximize the available RE resources.

1.7. LIMITATIONS OF THE STUDY

This research work has been carried out, considering the following limitations:

- The system will consist of PV, PHK, WT and backup system, and will not be connected to the grid.
- Data acquisition from renewable resources and load demand will not be collected, however, it will make use of the existing data.
- The optimal sizing will not be a part of the work.

1.8. PUBLICATIONS DURING THE STUDY

Conference papers:

- Meje, K.C., Bokopane, L. and Kusakana, K., 2018, October. Practical implementation of hybrid energy systems for small loads in rural south Africa. In *2018 Open Innovations Conference (OI)* (pp. 293-298). IEEE.
- Meje, K.C., Bokopane, L. and Kusakana, K., 2020, October. Microgrids control strategies: A survey of available literature. *In 2020 International Conference on Smart Grid and Clean Energy Technologies (ICSGCE)* (pp. 167-173). IEEE.
- Siti, M.W., N.T. Mbungu, K Meje, K.C., Naidoo, R.M., Bansal, R.C., Kusakana, K., 2020, December. Industrial load demand management with PV-battery systems using fuzzy logic and optimisation-based implementation. *In 2020 international Conference on Applied Energy (ICAE2020).*

Journal papers:

- Meje, K., Bokopane, L., Kusakana, K. and Siti, M., 2020. Optimal power dispatch in a multisource system using fuzzy logic control. *Energy Reports*, 6, pp.1443-1449.
- Kelebogile Confidence Meje, Lindiwe Bokopane, Kanzumba Kusakana, Mukwanga Siti, 2021. "Real-time power dispatch in a standalone hybrid multisource distributed energy system using an Arduino board". Accepted in *Energy Reports*.

1.9. DISSERTATION LAYOUT

This dissertation is structured as follows:

Chapter 1 introduces the dissertation, which presents background, problem statement, objectives, research output, methodology of the study, hypothesis and limitations of the study.

Chapter 2 provides a detailed review of existing microgrid prototype control for optimum operation and classifies their disadvantages and benefits. In order to select and make use of a good performing controller in real-time. It further identifies the gaps and potential avenues for future research work in this field.

Chapter 3 the FLC is developed in Simulink, to control the proposed hybrid to supply the load with varying supply.

Chapter 4 the simulations are performed with MATLAB and the results are analysed.

Chapter 5 a prototype of the system is built, the controller tested in real-time, and performance functionality analysed under various operating conditions.

Chapter 6 concludes the practical work and indicates future studies to be carried out.

CHAPTER 2: LITERATURE REVIEW

2.1. INTRODUCTION

This chapter aimed at analyzing the existing microgrid systems in power grids and DER systems and, subsequently, to identify a viable technique for the design and implementation of real-time controllers for MG hybrid systems. It further introduces numerous strategies or techniques, to manage the prototypes for rural remote rural application in an isolated and grid connected system. This Chapter further describes recent development studies aimed at improving the optimum operation principle of microgrid controllers for stand-alone, hybrid and grid-tied connected systems, for real-time implementation of the system through either a hierarchical control or distributed control strategy, for a reliable and optimal energy management system

2.2. MICROGRID SYSTEMS

Throughout the years, MGs have been given multiple definitions of the same meaning. In a study conducted by [27, 28], it was defined as a "small-scale power grid capable of operating independently or collaboratively with other small power grids; a localized power station with its own generation and storage resources and definable boundaries," composed of a variety of components such as controllable energy loads (CELs) and distributed energy resources (DERs). While in another study it was said to be “a group of interconnected loads and distributed energy resources within clearly defined electrical boundaries that act as a single controllable entity with respect to the grid” [29, 30] or “cluster of distributed generations(DGs), energy storage and load within clearly defined electrical boundaries, which act as a single controllable entity, with respect to the grid” [31-33].

The common factor that all of these studies have highlighted is that MG's are able to effectively integrate various sources of DGs, in particular RESs, for the supply of emergency power switching between island and grid connected modes by controlling multiple DERs and CELs with either centralized or decentralized control systems. In addition, literature refers to components, such as DERs in MGs, that may be either

distributed generations (DGs) or distributed storage (DS) and are often used to supply microgrid energy, as indicated in [13-14,34-36]. These components include PV, WT, Combined Heating Power (CHP), Fuel Cells (FCs) and ESSs, CELs including Heating, Ventilation and Air Conditioning (HVAC) [37-39]. MGs may be integrated into the main power grid of the area and are often referred to as a hybrid microgrid [40-42]. They have the ability to operate in both grid-connected and isolated modes to improve power quality, overall system efficiency, local generation management and energy security for critical loads, by managing multiple loads [43, 44].However, the benefit of microgrids further includes:

- Enabling the modernization of grid and multi-smart grid technologies integration.
- Improve the distributed and RES's integration, which helps to reduce peak loads and losses, as a result of near-demand location generation [29, 45, 46].

Generators and system isolation from the utility grid generally halts the burden of control issues for the grid, by integrating vast numbers of renewable energy [47, 40, 15]. The integration of these different renewable technologies, together with deployment of the smart grid, differentiates the microgrid from conventional power systems. In turn, it introduces new challenges for power management, control, design of the control and protection systems, which includes bidirectional power flow, stability issues, modelling, low inertia and uncertainty[40, 48]. The EMS has currently been responsible for energy management and control operations in the traditional power system, to advance the EMS so that it may meet emerging challenges, as emphasized by [49, 50]. The advancement of EMS presents a new opportunity to address the paradigm mentioned above. In previous researches, researchers were tasked with the responsibility for energy management and control operations in the traditional power system. In recent studies, researchers currently encompass or include both supply and demand side management, while adhering to the system constraints, in order to achieve an economical, sustainable and reliable operation of MG[51, 52].

2.3. MICROGRIDS OPERATION MODES

MGs are basically classified on the basis of i) Mode of operation ii) Types iii) Source iv) Scenario and v) Size [53]. This section of the paper will highlight and address what other researchers have stated, in terms of modes of operations in MGs, that may be grid-connected and isolated mode. In order to promote RESs, to generate electricity or power by means of renewable energy, which may be produced by either solar, biomass, wind, small hydro power or integration of all renewable energy sources into a single MG system. However, there are different types of MG scenarios, identified as: remote off-grid, community, campus or institutional, military base that fall under the residential scenario. Furthermore, there are commercial and industrial(C&I), with various basic microgrid components itemized as: local generation, consumption, energy storage and PCC [54-56]. MG technologies are categorized as AC, DC and AC/DC hybrid systems, with different control methods. In addition, microgrids have different sizes, ranging from less than 10 kW to more than 1 MW, as shown in Figure 2.1. below, which includes various designs, depending on the size of the MG system.

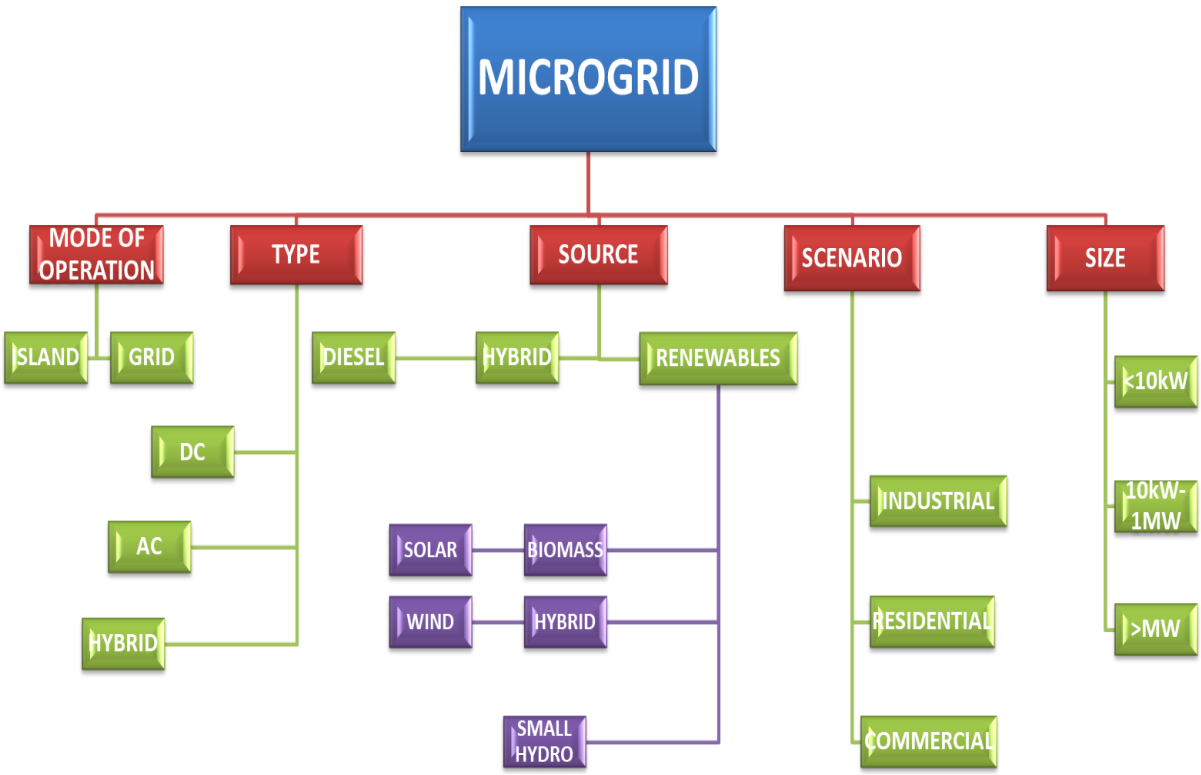

Figure 2.1: Microgrid classification

2.3.1 Islanded mode

The islanded operation is primarily intended for the reliability of the microgrid and for continuous power supply to as many loads as possible, after the microgrid is disconnected from the main grid [57-59] and switched to island mode or any unusual conditions that occur on the grid. The primary function of a microgrid, is to satisfy all its load and the grid requirements. Researchers have not addressed much, in terms of the development of more simulation platforms, suitable for the identification of microgrid control requirements and the evaluation of microgrid dynamic behaviour, under several conditions [60, 61]. As with many computer simulations, the time of execution is limited by slow computational speed, contributing to unrealistic output Real-time (RT) simulation. Therefore, it introduces faster computational speed, allowing for more accurate solutions that require further investigation in the field of real-time control. Taking into consideration that microgrid design takes advantage of RT, by implementing dynamic state of the art space-average models, which allow for a smoother simulation platform to run RT OPAL-RT 5600 [62-64]. It is a challenge to provide constant voltage at a stable frequency with appropriate synchronization between each DG in a microgrid. Nevertheless, it is of importance to place more emphasis based on the utility grid's complexity, which requires careful research and evaluation, prior to real-time implementation. Microgrid challenges were addressed by OPAL-RT real-time simulation technology, for power balance, frequency regulation, voltage and sysnchonization in an island microgrid with a master/slave controller. Nonetheless, further investigation should be carried out on a real-time controller, using an advanced real-time platform known as the Real-Time Laboratory (RT-LAB) [65, 66].

Lopes et al. suggested that, under certain conditions, a low voltage distribution network with a significant amount of smaller dispersed generation, could be operated as an isolated system. The control techniques for dealing with island operations and exploiting the resources of the local generation in such a system are a way of assisting in the resoration of the power system following a global outage. According to the researcher's findings, storage systems play a critical role in the success of power restoration of islanding systems. The viability of such practices was demonstrated using numerical simulation, to derive and evaluate a set of rules and conditions to be checked by the MG components, during the

restoration phase. A successful verification established a significant contribution and demonstrated the importance of expanding micro-generation resources [67-70].

2.3.2 Grid- connected mode

MGs connected to the main power grid, are known as grid-connected systems [60, 61]. In grid-connected operation, all DGs are under active and apparent (P/Q) power control. The MG operates as the current controller and injects power into the main utility grid, depending on the power generated. The DGs droop control model may remain unchanged for grid-connected and islanded mode, making it easy for a smooth transfer between the two modes[68, 71,72]. When the microgrid is grid-connected to the grid, the grid provides stable voltage, frequency support, and generally does not exercise any specific control. Figure 2.2 indicates that, when MGs are operated in the grid-connected mode, they are simply connected to the grid at the PCC.

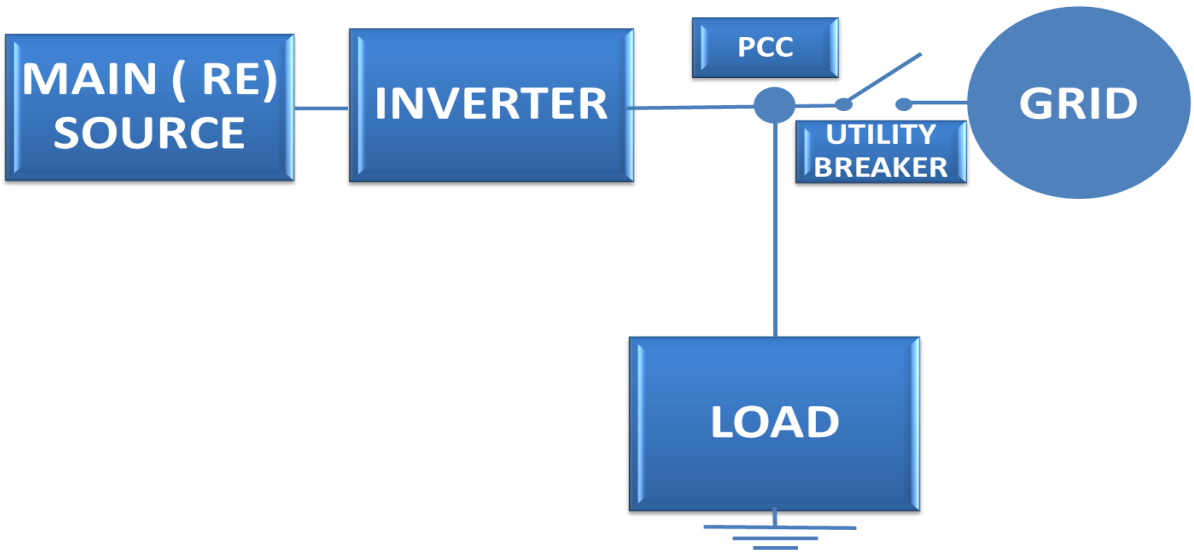

Figure 2.2: Isolated and grid connected mode transition

In this mode, the connection between the ACMG and the utility grid plays a significantly important role in determining the control system. The connection made is by means of switchgear, which further plays an important role in the power grid, as it determines the speed and voltage magnitude of the MG. Based on the Maximum Power Tracking (MPPT),

DGs provide maximum output power into the grid. However, limited power is set by higher control levels and the electrical controller generally used at the PCC [73, 74]. Nonetheless, under this mode, ACMG may draw a certain amount of power from the utility grid, in order to supply the loads while maintaning a balanced voltage and frequency. As a matter of fact, from the work of other researchers, MG control is similar to an independent mode, with the utility grid acting as one of its DGs.

In addition, a grid-connected mode could provide an optimal dispersion and when the MG is connected to the grid, it acts as a controllable load or source, that should not actively control the voltage at the PCC [75-77] and begin to create challenges.

2.4. TYPES OF MICROGRID

This section presents various types of MG technologies, including ACMG, DCMG and AC/DC hybrid microgrid (HADMG). From a historical point of view, the AC power network has been the standard choice of commercial energy systems, to power light bulbs in most households, since the late 19th Century [78-81], which has been a simple method supplying power. It has the ability to transmit electricity over a long distance and can be used in a carbon-driven system, such as coal and fuel fossils. The AC power networks have existed for more than a century, along with the market-dominated AC loads. As a result, the individual AC microgrid is lower in efficiency, as there are more energy losses leading to multiple conversions and disadvantages are caused by syncing, reactive power and stability requirements [82-85].

DC-based microgrids are gaining interest due to the advantages they offer over their counterparts (no reactive power, or synchronization, an increasing number of dc devices, etc.). Given the ratio of DC loads and DERs, DCMGs may potentially be more effective than ACMGs, eliminating the need to synchronize generators that minimize the use of converters. It allows for the connection of different types of DERs and loads to a MG common bus, with simplified interfaces, which further reduces the losses associated with AC-DC power conversion [86-88]. Nevertheless, the generation of power from sources such as DG, PV panels, small hydro turbine with synchronous generator and electrical loads results in a combination of DC and AC power. Generally, independent DCMGs cannot eliminate any losses resulting from multi-stage conversions, although the losses that

result in conversions of DC/DC are lower than those resulting from conversation of DC/AC or AC/DC. Independent ACMGs, on the other hand, have AC loads that solely require one conversion stage, similar to DCMGs. [89-91].

More so, HADMG is more beneficial than other types of microgrid technology, making it easier to connect multiple renewable AC and DC power sources and loads to the power system, in order to reduce conversion losses. The current grids in use are AC grids, however current electrical loads, such as solar-powered or DC-powered equipment and distributed renewable energy generation are ensuring that DC microgrids more appealing. Nevertheless, for DC and AC loads, the individual ACMG and DCMG each require multiple energy transmissions for the consumer's. To avoid significant losses of energy in multiple conversions, HADMG appears to be the best solution. [83-85] are currently supported as the optimal approach to use, as they combine primary advantages of ACMG and DCMG.

2.4.1 AC microgrids

Under AC microgrid type, all DERs and loads are connected to the AC bus, as indicated on the AC microgrid block diagram, shown in Figure 2.3. AC generating unit and energy storage systems are connected to the AC bus via DC-to-AC inverters, where AC-to-DC rectifiers are used to supply DC loads, similar principal applies from DC to AC rectifiers to the load [92-94], as most microgrids are currently using a conventional AC grid system. Now that a large number of renewable sources are generating, DC voltages and power converters will be required to convert power from DC to AC power, resulting in power losses. Researchers have therefore established that DC devices undergo mutiple conversion phases for the use of AC grid connection. However, it is critical to consider that the multiple phases of conversion have a significant impact, by reducing the systems's reliability and overall efficiency [95- 98].

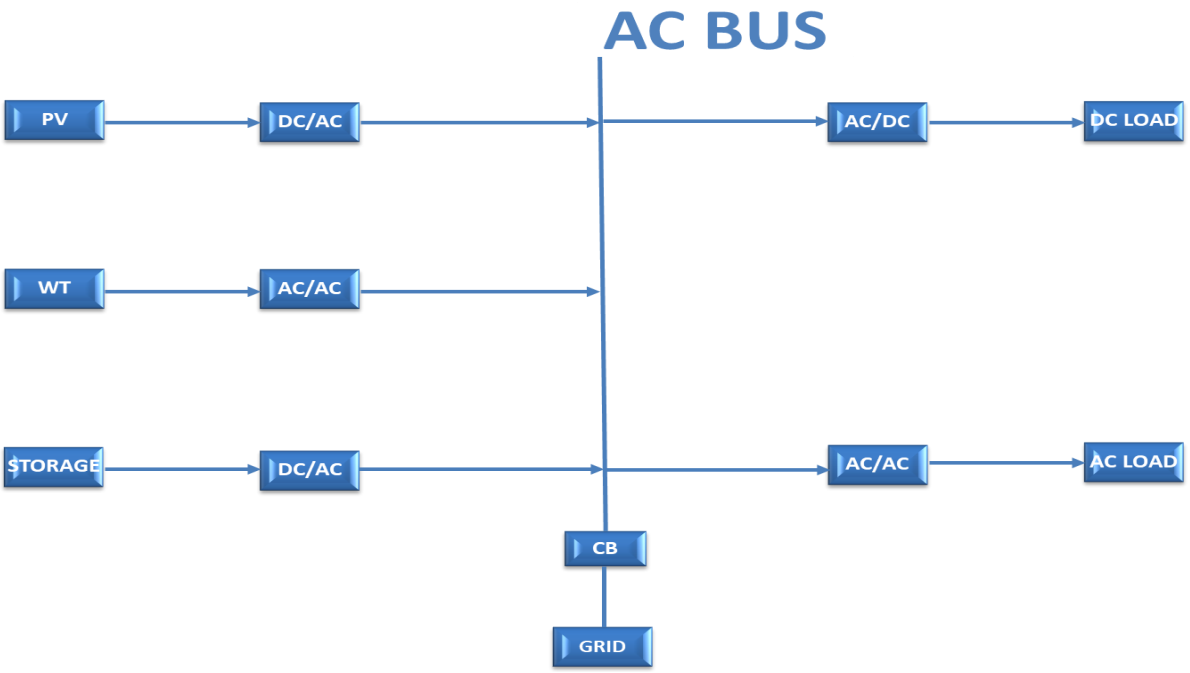

Figure 2.3: AC microgrid block diagram

2.4.2 DC microgrids

The DC microgrid layout in Figure 2.4, utilizes a DC microgrid bus to avoid many of the power conversion steps required when using an AC bus, potentially leading to a higher energy efficiency and improved economic performance [99-101]. Many researchers have discovered that DC microgrid technology is becoming more desirable in the traditional electrical grid system, due to its natural connection with RESs, electrical loads and energy storage systems [95, 102, 103]. In the recent past, there has been an improvement in research. Whereby, the works has been observed in the area of DCMG, bringing this technology closer to practical implementation.

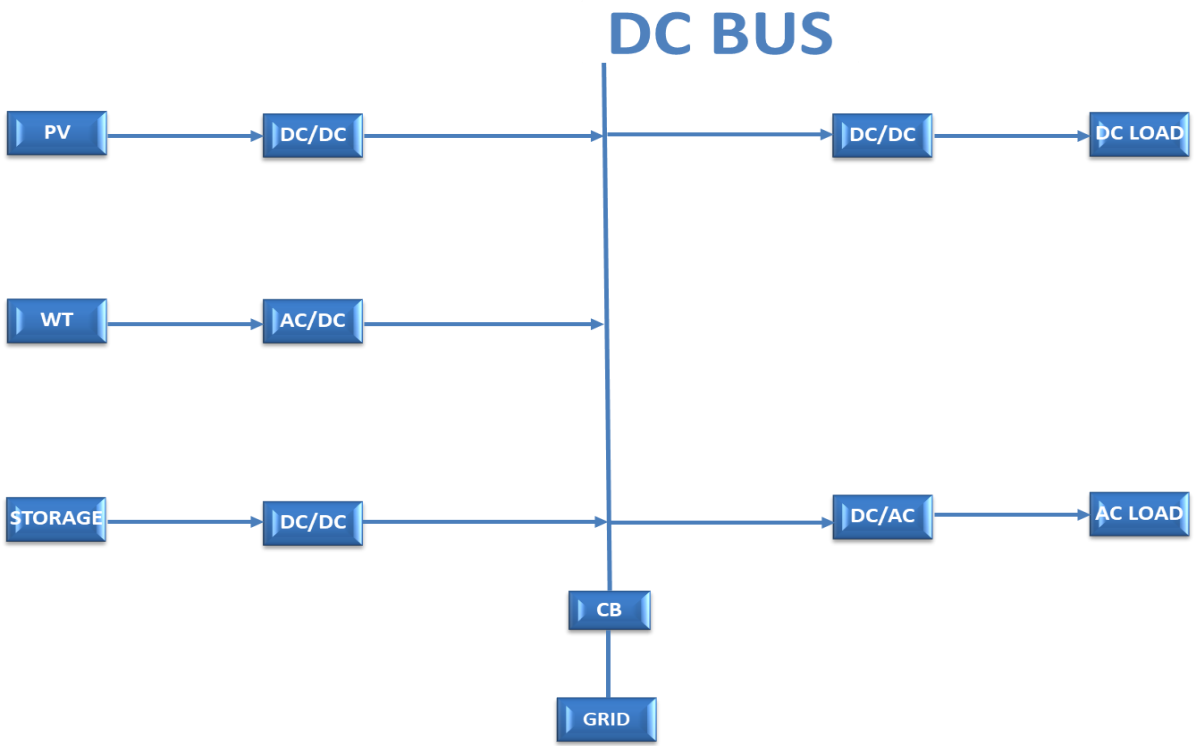

Figure 2.4: DC microgrid block diagram

2.4.3 AC/DC hybrid microgrids

This idea provides a new example of how the distributed generation operation is defined. For the purpose of utility, MG may be considered as a controlled power system unit [104-106]. Improvement of local reliability, reduction of feeder losses, support for local voltages and increased efficiency through waste heat recovery scheme, creates correction of voltage sag. The microgrid or distribution network subsystem will help create less problems for utility network than conventional micro generation and loads are appropriately and intelligently conducted. AC/DC hybrid microgrid is used as an optimal approach, to combine the primary advantage of AC and DC microgrid [107-109].

2.5. MICROGRID CONTROL STRATEGIES

The basic concepts and control architecture of microgrids have advanced communication and information technology used in smart grids for future microgrids, allowing for high penetration of a renewable energy system stated by [110]. The two main

control structures in microgrids are hierarchical control and distributed control. Both controls are essential for the operation of the microgrids to be reliable and efficient [111]. However, again: centralized and decentralize [89, 92] are two distinct approaches to MG control [112, 113].

- Centralized approach

With a centralized approach, all the data has been gathered and calculated at a single point, with the communication between each control unit. In reality, the fully centralized approach is not feasible, as there is a huge amount of data and computation at the central controller [114].

- De-centralized approach

Each control unit relies on local measurement in a decentralized approach. Similarly, fully decentralization is not possible, as using solely local measurement is not sufficent for the operation of the MG [115], so we should compromise both of those approaches, which may be achieved by hierarchical control schemes [116].

2.5.1 Hierachical control

The automatic generation control (AGC) signal for generators is updated every half a second to a few seconds, to maintain the system frequency and voltage at nominal values under hierarchical control structure [117]. In order to send dispatch signals and collect status and measurement of local units, the central controller may communicate with local energy resource controllers on the microgrid. In local controllers, the stability control function is implemented, to balance and share power in real time. Hierarchical control requires only vertical communication and requires no peer-to-peer communication, which reduces communication system requirements. Figure 2.5. shows the diagram of a microgrid, with structure of the hierarchical control.

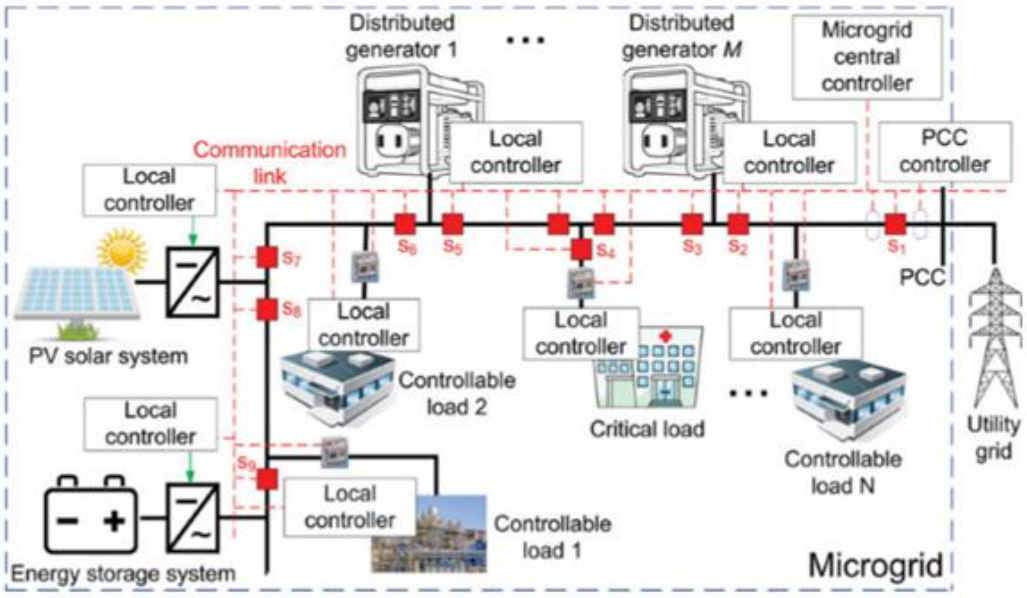

Figure 2.5: Microgrid with hierarchical control structure [111]

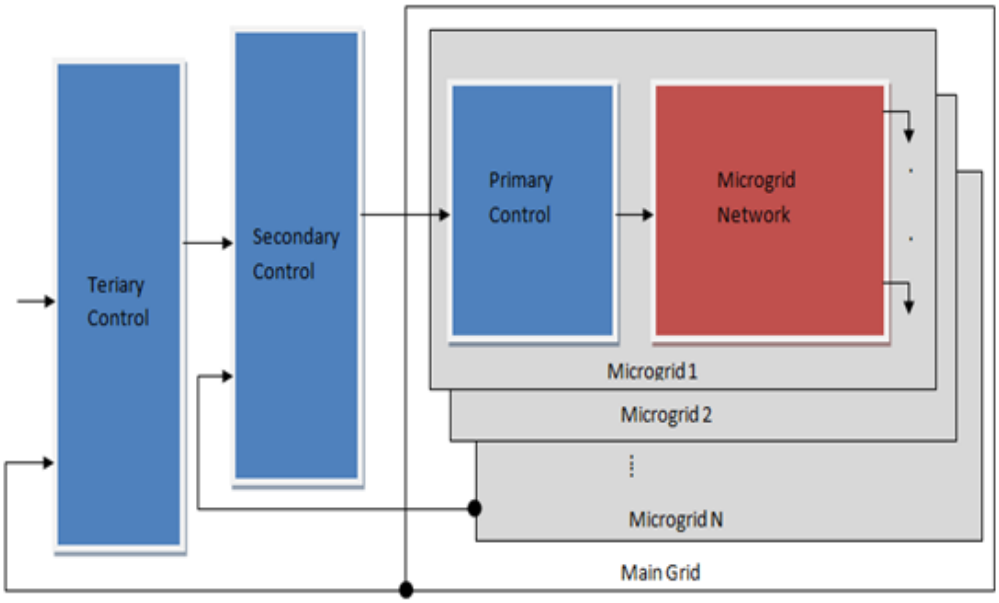

Figure 2.6: Hierarchical control levels [40]

The operational structure of the hierarchical control system is divided into 3 levels: primary, secondary and tertiary control [118].The system information flows from the primary level to the tertiary level; the decision signals flow from the tertiary level to the primary level to meet the overall operation objectives, as indicated in Figure 2.6.

- Inner control

Determination of operating condition of DER units is the function of this layer. Current and voltage, feedback, linear and nonlinear loops may be carried out, to manage output voltage and current, while maintaining a stable system [119] and these inner check loops are often called zero-level control loops.

- Primary control

Primary control aims at dealing with controlling and sharing power between DERs. Primary control sends the setting values for inner control. The droop control method is often used in this level, to emulate physical behaviours that stabilize the system [120]. This primary control level adjusts the voltage reference provided to the inner current and voltage control loops (level 0). It includes a virtual output impedance loop that may be used to express the output voltage as:

$$v_o^* = v_{ref} - R_D.i_o \tag{2-1}$$

Where: i_o is the input current; R_D is the output impedemce and v_{ref} is the output voltage reference at no-load. Assuming that: ε_{ref} at v is the maximum allowed voltage deviation, R_D and v_{ref} must be designed as the following:

$$v_{ref} = v_n - \varepsilon_v/2; \tag{2-2}$$

$$R_D = \varepsilon_v/i_{max} \tag{2-3}$$

v_n being the nominal output voltage and i_{max} the maximum output current. Thus, the current sharing between two converters may be expressed as follows:

$$\Delta i_o = \Delta v_o^*/R_D.i_o \tag{2-4}$$

In primary control there are two methods, namely: droop-based methods and non-droop-based methods, indicated below.

➢ Droop-based method

Droop-based methods imitate the behaviour of synchronous generators in the power system. That is, the deviation in frequency appears when there is an imbalance between the input mechanical power and its output electric active power; the similarity with voltage and reactive power. This method is based solely on local measurement, which avoids the need for communication. The droop control is commonly used to achieve the power balance in the power system of islanded mode [20].

➢ Non-droop-based method

Non-droop-based method focuses on a centralized perspective and master slave is a typical example of this method.

- Secondary control

Ensures that the electrical levels into the microgrid are within the required values. In addition, it may include a synchronization control loop to seamlessly connect or disconnect the microgrid to the distribution system [120]. Secondary control has responsibilities for both the reliable and economical operation of the MG and usually takes seconds to minutes (that is, lengthier than the former), to justify the stabilized dynamics and structures of the primary and secondary control loops. Hence, the set-point of primary control is determined through secondary control as a centralized controller. It restores the microgrid voltage and frequency as an integrated device and compensates for deviations triggered by load changes or by renewable sources [121] (see Figure 2.7).

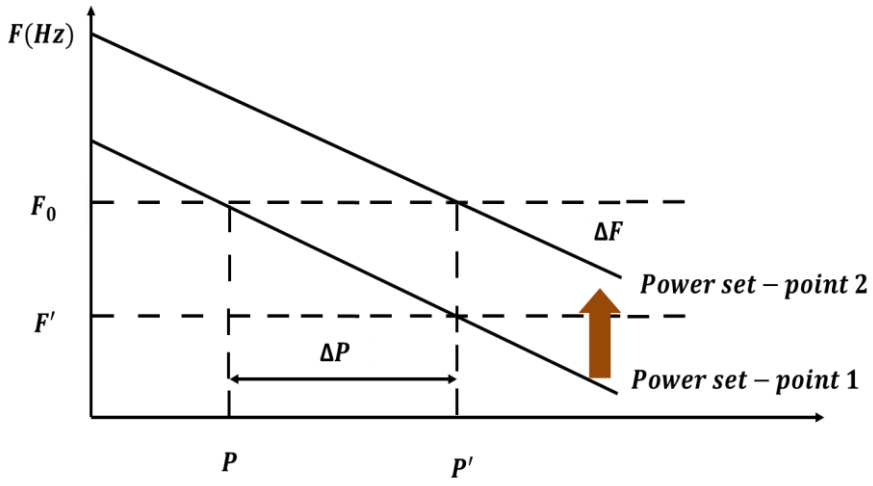

Figure 2.7: Secondary control for frequency [121].

To solve the problem of the voltage deviation, the controller may be expressed as follows:

$$\delta v_o = k_p(v^*_{MG} - v_{MG}) + k_i(v^*_{MG} - v_{MG})dt \quad (2\text{-}5)$$

k_p and k_i being the control parameters of the secondary control compensator, δv_o must be limited not to exceed the maximum voltage deviation. Finally, Eq. (2-6) becomes:

$$v^*_0 = v_{ref} + \delta v_o - R_D.i_o \quad (2\text{-}6)$$

- Tertiary control

The tertiary control is more related to economic optimization, based on energy prices and electricity market and it determines the import or export of energy for the MG. The controller could be used to handle a cluster of interconnected microgrids, to create what is called "microgrid clustering", which could behave as a virtual power plant and continue to supply the critical loads, at the least. During the situation, the central controller should select one of the microgrids as the slack (i.e. master) and the rest as PV and load buses, in accordance with a predefined algorithm and the existing system conditions (i.e. demand and generation). In this case the control should be in real time or, at least, high sampling rates [122].

This control is the last (and slowest) level of control, that takes into account economic concerns in the microgrid's optimal operation (sampling time is minutes to hours) and manages the power flow between the microgrid and the main grid [120]. The level, however, often means predicting the weather, electricity price and loads for a generator delivery scheme, that achieves financial efficiency in the coming hours or days [123].The energy production level controls the power flow between the microgrid and the grid. The controller may be expressed as follows:

$$\delta v_o = k'_p(i^*_G - i_G) + k'_i(i^*_G - i_G)dt \tag{2-7}$$

k'_p and k'_i being the control parameters of the tertiary control compensator. Here, δv_o is further saturated, in case of being outside of the limits of $\pm\varepsilon_v$. Notice that, depending on the sign of i^*_G, the power flow may be exported $i^*_G > 0$ or $i^*_G < 0$ imported.

2.5.2 Distributed generation control

Distributed control is another control structure for microgrids. The distributed control structure, particularly for the small and remote microgrids, makes DER configurations, in small microgrids, an attractive solution. The main feature and structure of a distributed control systems, are illustrated in Figure 2.8. There is no central controller, however, a central monitoring computer is available in the system, to monitor the entire system's operation. Monitoring of communication, diagnostics and visual analyses, peer-to-peer (horizontal) communication are the key part for the integration of various distributed resources, in order to achieve an overall operational aim [111].

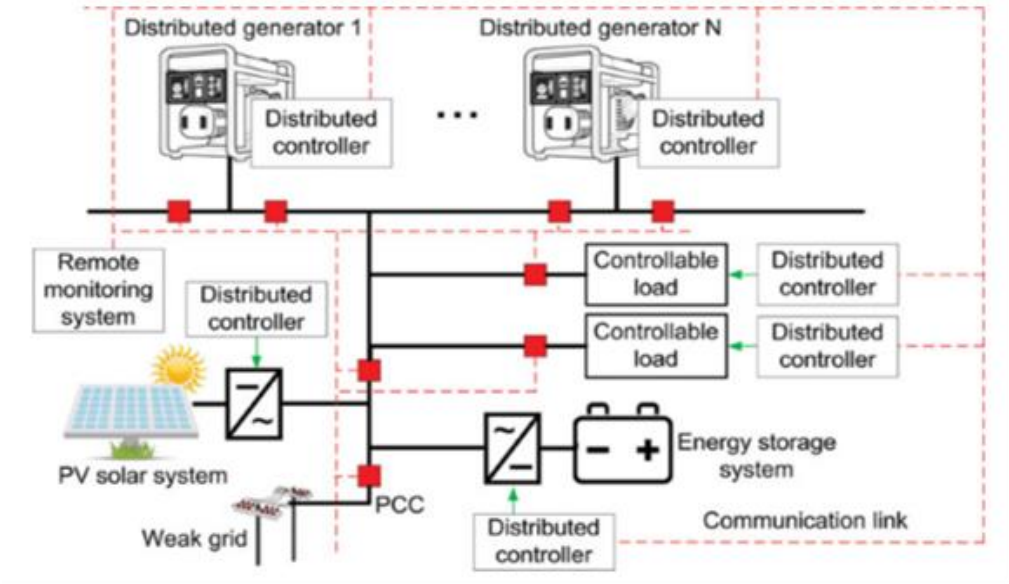

Figure 2.8: Microgrid with dictributed control structure [111]

2.6. MICROGRIDS POWER SHARING CONTROL STRATEGIES

The alternating nature of renewable energy has been identified as inconsistent between collected and consumed energy in individual homes, which reduces efficiency, as this significantly reduces the maximal rate of renewable energy penetration. However, introduced methods to minimize large range of losses, by balancing the locally recovered energy from microgrid systems; (i) by creating a novel energy sharing system, (ii) developed greedy matching algorithm and (iii) designed a practical transmission scheduling. Up to at least 60% of the solar system's energy losses were reduced from the AC lines without the need for large battery systems. They further evaluated their system, using practical traces of collected solar energy and homes energy demand in Amherst, MA [123].

2.6.1 Standalone system controllers

An advanced PV-Wind energy conversion system optimization method, has been used in PV-Wind standalone system by advancing the control strategies of DC-DC and AC-DC controllers. The method was, however, used to consider the optimal sizing of the system, and designed a system that reduced the total costs of the system [124]. One of the

researchers, designed a stand-alone hybrid system consisting of a PV power system, wind power system and a battery storage system, using a novel controller linking the two technologies or sources to supply the load under variable weather condition in MATLAB and Simulink. The simulation results indicated that the developed controller was significantly effective for hybridized system, proved only on simulations. They recommended that more real-time controllers to be implemented in remote rural areas for hybrid microgrid systems in Africa[124].

The EMS algorithm based on the local energy market (LEM) and EMS algorithm, based on mixed integer non-linear programming (MINLP), for a microgrid in island mode, were proposed by considering a direct scenario with real data, to test the performance and accuracy of the proposed algorithm. Simulation results indicated that EMS, based on MINLP, is an effective algorithm compared to EMS, based on LEM, with a total cost of energy (COE) reduction of 15% [125].

In addition, an optimal control based on the fuzzy logic of an extraordinary EMS, for the standalone system incorporated of wind turbine/photovoltaic/hydrogen/battery HRES). The selected control was utilized to maintain the state-of-charge (SOC) of the battery, to ensure that the load demand was constantly met, to optimize the utilization cost and ESS lifespan. However, the simulation results indicated, that compared to the ordinary EMS, the control based on fuzzy logic saved the costs by 13% and the control was found to be the viable control for standalone HRES [126].

2.6.2 Hybrid system controllers

In terms of energy management as one the roles that controllers play in hybrid microgrid systems, Olatomiwa et al. indicated that the majority of renewable energy systems that integrate more than one RES with backup and intermittent drawbacks of these renewable energy sources. Have, however, the exclusive design that was considered to be part of the hybrid system. Even though, the design of the control of the system increases the total cost of the standalone or grid-connected hybrid system. Energy management strategies have therefore been used in the smart grid and special attention has recently been paid to controlling the energy flow among various components such as energy source, storage device and load system, incorporated in one system. The results of the study

indicated that the centralized controller was selected, installed and programmed with a monitor, such as SCADA, to control the system according to an optimized strategy. Recommendations were, however, made to further improve the reliability of the hybrid system [25].

A fully integrated system of RES, in particular, solar PV, wind and hydropower, in a mini-grid was introduced for the practical implementation of two economical HS for small off-grid loads. An experimental test was carried out in the village of Nepal, on one of the two hybrid energy systems selected. Results showed that the hybrid charge controller (HCC), the grid-tied inverter (GTI) and the appropriate load controller may be hybridized by the selected three-hybrid renewable energy system [127].

Upadhyay et al. developed a hybrid energy system with an optimum solar PV/MHG/BGG/BMG/Battery storage, using a variety of energy management strategies, such as cycle charging strategy, load-following strategy and peak-shaving strategy in rural Indian villages. Particularly, genetic algorithm, particle swarm and biogeography have been used as an optimization technique, by returning the ratio of energy index at 1. Based on the results, it was concluded that cycle charging strategy is 5.64/kWh less expensive than peak-shaving and load-following strategies. However, the system should include a diesel generator, to meet any system's energy shortage [128].

The performance of the FLC for off-grid hybrid power system energy management, battery state-of-charge (SOCs) and other sources of energy from the hybrid off-grid system, has been evaluated in this regard. The FLC tested, revealed the cuckoo search (CS) algorithm simulation results; CS is better than particle swarm optimization (PSO) for the fuzzy system controller. As a result, the controller was found to maintain its performance and flexibility, by managing to minimize the loss of power supply probability (PSP), excess energy (EE) and level energy costs (LEC) [129].

A hybrid grid energy system with renewable energy sources, which optimizes the generation of energy and load management has been commonly experiencing technical difficulties. Then, by combining power generation with optimal load management, an optimal energy management strategy was suggested. The formulated optimization problem is indicated as: operating constraints for generating, storage deficit and load units as a mixed-integer linear programming (MILP) problem. The MILP model was used to relieve the peak power demand and power deficit by integrating power reduction strategies; a

temporary pause and multiple power supplies algorithms for the load. However, the simulation results revealed that the optimal power reduction was achieved as desired and allowed scheduled operation to take place without any hindrance or sacrificing efficiency [130].

2.6.3 Grid-connected system controllers

In terms of the maximum power, size and cost, the design and installation of the PV connected network system was analyzed using the inverters optimized for single phase balancing. On the basis of available solar radiation and demand under a grid-tied system, this interactive system was controlled. However, the results have shown that the system is able to supply most of the peak loads in a small household, under certain conditions, by providing power back into the grid [126].

The small PV system model presented comprises of a solar photovoltaic Silicon cell system with sun tracking, the battery storage utilized to store excessive energy, a DC to AC converter and a microcontroller. The PV system supplies the residential energy as the primary electricity source. The system controller was designed in a case whereby, if the demand for the load exceeds the PV system energy available, the controller switches to the power supply line for additional power. If the demand for power dropped below the photovoltaic system's energy, the controller would switch off the power from the utility. In real residential applications, the designed system is recommended; however, both solar and microcontroller panels should be adapted and modified to meet the desired applications' power demand [131].

In distributed generation and smart grid, the grid connected inverters are now increasingly used. However, their compatibility with the grid utility and maintaining the harmonic contents of output current is the key challenge for grid-connected systems. The inverter switching is based on the Selective Harmonic Elimination PWM method, where Newton Raphson (NR) methods calculate switching angles. In the grid-linked inverter system, it is found that the proposed method via MATLAB/Simulink has two important benefits. The modulation index is controlled first, then the active power flows on the grid side, and the harmonics and THD are reduced from the current in the common connection point, which reduced filter inductor costs and sizes [132].

Integrated control strategies, particularly under unbalanced grid conditions for the inverter connected to a three-phase grid was examined. PWM's three-phase voltage sourced inverters (VSI), is commonly used in energy generation systems, based on renewables, to perform advanced energy management and power flow control, e.g. wind energy and solar power systems smoothing control, as well as fast battery energy storage (BESS) charge and discharge control. The proposed control methods have found that the grid-based inverter may effectively remove active and reactive power oscillations individually or simultaneously, however, the three-phase inverter power streams are distorted if both are active and reactive power oscillations are eliminated simultaneously [133].

Inverter technologies, which may deliver high efficiency conversion with high power factors and low harmonic distortions for safety and reliability of the energy system, for grid interconnection, play an important role. With the current control technical inverter, the possibility of compensation for low order harmonics for high power quality generation in the grid may be eliminated by a steady state error and fast transient reaction [134].

An improved controlling scheme for two-stage grid-tied PV power systems, maximum power point tracking (MPPT), DC-Link voltage adjustment, and network current synchronization are proposed for this control scheme. The proposed controlling strategy was evaluated by numerical simulations in a MATLAB/Simulink TM (R2009b, MathWorks, Natick, MA, USA) and the designed control approach provided accurate maximum power point (MPP) tracking, with lower power oscillation with a fast and precise DC-Link control, under different irradiation conditions, compared to conventional control schemes [135].

2.7. SUMMARY

The AC microgrid's standalone mode of operation is the most difficult from a control point of view, requiring DGs to balance active and reactive power, either through the use of local controllers or central controllers. Unbalanced currents would circulate between them, if the voltage amplitude, phase angle or frequency of any DG varied widely. As a result, AC microgrid control's hierarchical structure is often used to optimize local behaviour against grid-wise synchronization. The DC microgrid has not been fully used in

residential or commercial areas. Existing applications have shown that it is a promising solution for future smart grids, however, hybrid AC/DC is gaining more popularity, as it combines the main advantages of AC and DC microgrids.

As a result, it appears that the combined AC/DCMG is the best solution for avoiding huge loss of energy due to multiple conversions. Nonetheless, a number of technical issues that should be addressed in the practical implementation of hybrid AC/DCMG microgrids, as they have been highlighted as critical issues and challenges from various research, to be able to develop new controller developments. Wide area measurement systems (WAMS) should be investigated for the efficient and proper use of hybrid MGs in the future. It was important to know more about real-time implementation by using Opel real-time (RT) master/slave control on Opel LAB, an advanced method of managing the controller in MG islanded mode for stability and control reliability in the system. The aim of this study is to review most of the existing microgrid systems in power system networks and DER's systems. The review further discusses the basics of various modes of microgrid integration, with a published academic survey of the basic background, practical requirements, historical events, current state and technologies. Reasonable evaluation of different techniques was further carried out for the verification of optimum techniques in identifying the feasible MG controllers in isolated locations applications, in various connections. The information collected, provides modern technology research relevant to the next generation MG and energy storage system challenges, in terms of the controller in the system. It is based on the number of research articles published in recent years and provides updates on emerging issues that will be identified and used to assist in advancing and enhancing the performance of MG controllers.

The studies mostly dealt with controllers designed for the transition that occurs between the grid-connected system integrated with renewable DG technologies, with a view to minimizing the operating costs of MG systems, by developing different types of designs and controls according to their operating mode, in order to accommodate the transition between grid-connected and islanding mode, when the system is connected to the power grid. Generally, the islanding detector was developed when MG was connected, to the utility grid. The benefit of the study is therefore the design of appropriate controller for an islanding mode operation, integrated with a diesel generator and energy system storage (ESS), with the aim of electrifying approximately +/- 6 households, as opposed to one

household, for each study and often simulating South African (SA) prototypes, instead of real-time implementation. Investigations will be further conducted, on the basis of reliability and feasibility of the islanded connected mode controls, looking at recent developments in DCMG than the ACMG type-renewable energy sources (RES), that are currently preferable solutions worldwide.

CHAPTER 3: SYSTEM MODELING

3.1. INTRODUCTION

The main objective of this Chapter, is to design and develop a mathematical model for the controller in MATLAB and achieve the optimal energy management performance of the standalone HRES microgrid system. The controller optimizes the energy on a day-to-day operation of the HRES, by maximizing the use of the RS, while minimizing the use of the battery and diesel generator to supply the required energy, without interruption for small scale load applications in rural SA. Various methods of optimization have been developed by several researchers over the years. These methods are dynamic programming, fuzzy logic, neural network, Quasi-Newton method, etc. Each method is developed for a particular application, similarly with the control algorithms. Proportional integral (PI), proportional integral derivative (PID), fuzzy logic controller (FLC) and model predictive control (MPC) are some of the most commonly used control algorithm. Among numerous other algorithms, FLC and PID are the widely used by the industries and the researchers, as they are considered to be the optimal recent algorithms, due to their costs. In comparison, the most widely used control algorithm, FLC, is therefore, a selected optimization solver, since it is more efficient when compared to PID and it may take approximately 70% more control time than PID, achieve significant performance enhancements, mitigate power quality problems, meet the desired performance with a complex and uncertainty plant and is further a feasible algorithm to be used in the study, to verify the developed proposed system, using MATLAB and hardware experiments in the following Chapters. The optimal energy management controller is developed and modelled HRES in SIMULINK, using fuzzy logic in the following pattern: input and output variables using membership functions, fuzzy logic control (FLC) rules and surface, switching times system designed, variable load system built and the modelling of a PV/PHK/WT/DG/BT hybrid system.

3.2. SYSTEM CONFIGURATION

3.2.1 System description

Figure 3.1 illustrates the proposed schematic diagram of the PV/PHK/WT hybrid microgrid power system with BT and DG as a backup and arrows indicating the direction of power flow, whilst indicating the direction of the signal. The controller receives or sends a signal to any of the RE sources, including the DG and battery bank; when to be ON/OFF, by optimizing the power flow. As the load demand begins to escalate, the controller will inform the DG or battery to act as a backup, in order to maintain a balanced hybrid system. During daytime solar PV, PHK and WT are the sources of energy with power P_{PV}, P_{PHK} and P_{WT} for the load. Excess power generated by these technologies is stored in the BT system. The WT and PHK operate during the night, while solar PV is off. The backup system includes DG and BT, operating in the following pattern: BT (P_{BT}) is the source of energy; whenever a fault occurs on the system, it supplies the load to its maximum discharge when necessary. Similar to DG (P_{DG}), where it turns on whenever there is a short fall of all sources and serves the load and simultaneously charges the battery.

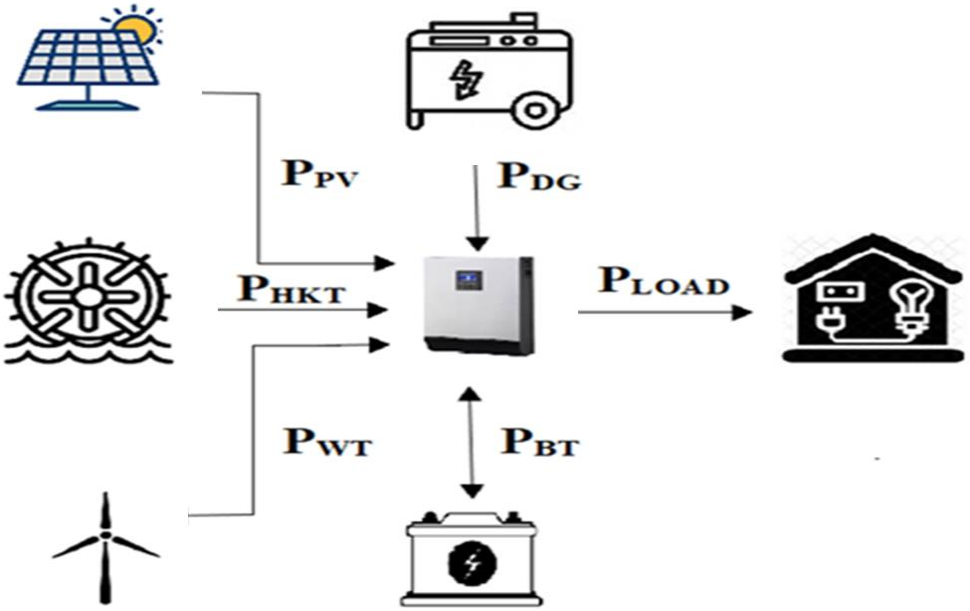

Figure 3.1: Schematic diagram of PV/PHK/WT/DG/BT power system with controller

The power management strategy of PV/PHK/WT, with a backup for a microgrid power system, is implemented, as shown in Figure. 3.1. The power flow is based on FLC, to balance the power through the expressed Eq. (3-1) below:

$$P_{PV} + P_{PHK} + P_{WT} + P_{BT} + P_{DG} = P_L \quad (3\text{-}1)$$

P_{PV} denotes power extracted from the PV to the load and stored in the battery during the day; $P_{PHK} + P_{WT}$ denotes power generated from PHK and WT throughout the day and at the same time stores. Power P_{DG} denotes power from the diesel generator; P_{BT} denotes power from the battery (may also be negative); P_L is the power demand from the AC load.

3.3. FUZZY INTELLIGENT CONTROLLER

Fuzzy has been widely used for controlling processes in different industries and systems, due to its characteristic abilities that are simple and independent to complex mathematical methods and systems, high adaptability, low sensitivity, performance enhancement, less distortion, high efficiency, harmonic mitigation, lower current fluctuation, decision boundaries, quality power flow management amongst hybridised sources for variable load in standalone systems, etc. [136, 137]. This control unit has a high degree of flexibility similar to its rule-based inference system and the ability of this controller to make quick decisions on the basis of problem constraints and sudden conditions that have made FLC the preferable choice for online systems, in particular, online control of hybrid power systems[138].

Recent work hybridised two or more intelligent controls, such as PID's, genetic algorithms (GAs) for adding more quality performance [139]. FLC, however, performs better at the weakness of each system, providing sufficient outcome or results [140] and was further used by [141] for an energy management strategy in an alternative hybrid system and an EMS was designed to achieve the main objective. Due to the difficulty of the load, the development of the FC resulted in the success of the power system control, the results have demonstrated that the FLC based management strategy does not only

supply the load, but further maintain the battery nearly charged, to ensure discharge readiness and improvement of the performance [141].In addition, FLC was used to collect and transfer the data for the applications in an intelligent hardware and software control system for the Arduino platform, while control signals for the technological process were to be generated on the basis of lab-VIEW related Software [138].

The fuzzy logic-based energy management control technique is described in detail in this section, whereby the average maximum load demand for six households is 1.14 kW (refer to Figure. 4.3). With regards to the design of a fuzzy logic controller for the proposed rural microgrid system, the controller should be used for energy management, by sending signals to all hybrid system components at a specified time.

3.3.1 Optimization technique for HRES

The fuzzy intelligent controller has three inputs and two outputs, shown in Figure. 3.2. The inputs are power generated by each of the RESs, such as PV, PHK and WT, load demand (power consumption) and the time at which the sources are operational. The outputs determine the status of the two backups that operate during short fall, faults or any emergency (BT and the DG) to the load, in order to satisfy the load power demand, by managing and controlling the energy required. This involvement of an energy management controller, sends/receives signals to or from any of the RES and back-up systems, notifies the sources on when to be ON / OFF, in order to maintain the energy required to meet the load demand continuously, despite the fluctuation of the sources.

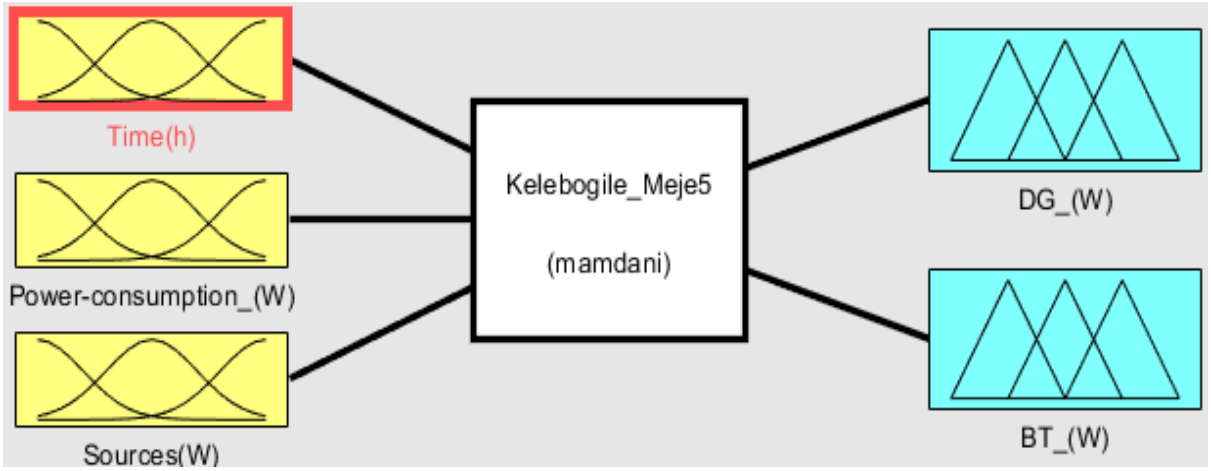

Figure 3.2: Block diagram of FLC energy management electrical system

3.3.2 Fuzzy logic application

Figure 3.3. depicts the fuzzy logic controller's overall block diagram that takes the three inputs, processes the information and produces an output in terms of the timeframe to determine; as and when the DG or BT can take over the load depending on the demand in each and every 24 hours. The input and output variables are defined in detail in the section below.

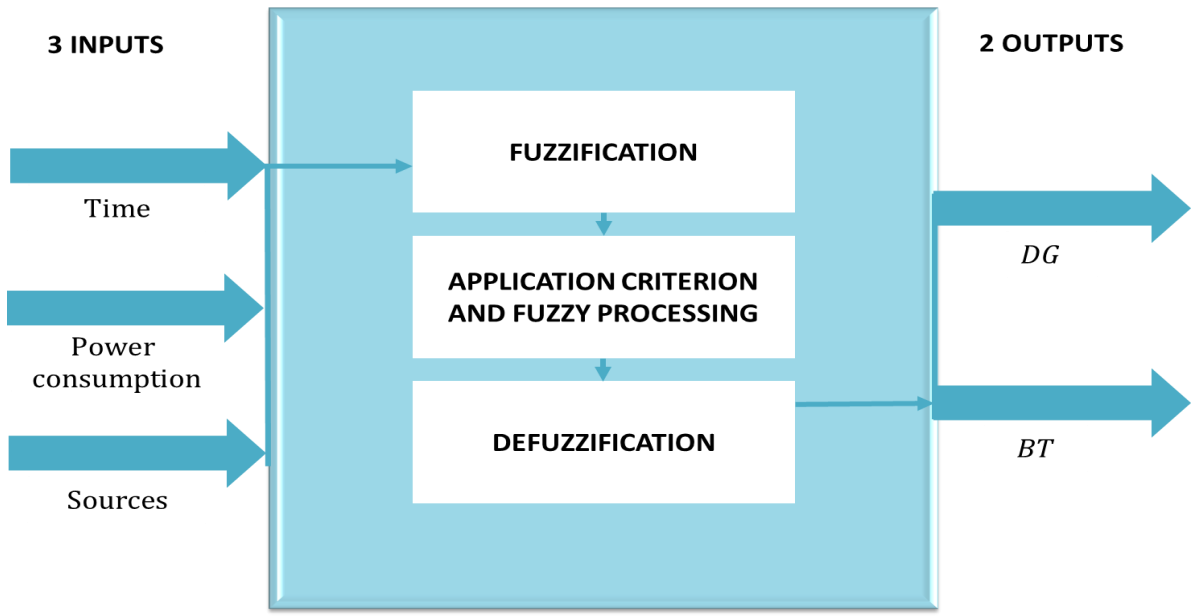

Figure 3.3 Fuzzy logic controller block diagram

3.3.2.1 Timeframes definition

The fuzzification process is described below, where the daily timeframes are first defined in six categories, as shown in Table 3.1 and visualized in Figure 3.6.

Table 3.1: Fuzzificaton of timeframes

Description of Input 1 (Time)	Nomenclature of fuzzy	Time range (24 hrs)
Morning Off Peak	MOP	00:00 -4:00
Morning Peak	MP	03:30 -6:00
Morning Demand	MD	05:30-16:00
Average Peak Demand	APD	15:30-17:00
Evening Peak	EP	16:30-22:00
Evening Off Peak	EOP	21:30-23:00

3.3.2.2 Power consumption definition

The power consumption is defined, as shown in Table 3.2, whereby the sources are expected to meet the demand from a particularly low consumption to high consumption.

Table 3.2: Fuzzificaton of power consumption

Description of Input 2 (Power consumption)	Nomenclature of fuzzy	Power consumption range (kW)
Very Low Consumption	VLC	0-400
Low Consumption	LC	350-600
Medium Consumption	MC	450-660
Average Consumption	AC	550-780
High Consumption	HC	750-1080
Very High Consumption	VHC	1050-1140

3.3.2.3 RE sources definition

As shown in Table 3.3 RE sources are defined, where they are the primary energy supply to the load throughout the day. Depending on when the load starts to consume power, the sources takes over the load accordingly, to minimize the backup system supply.

Table 3.3: Fuzzificaton of RE sources

Description of Input 1 (Time)	Nomenclature of fuzzy	Time range (24 hrs)
Pico-Hydrokinetic	PHK	00:00 -4:00
Wind Turbine	WT	03:30 -6:00
Pico-Hydrokinetic+ Photovoltaic	PHK+PV	05:30-16:00
Photovoltaic	PV	15:30-17:00
Wind turbine	WT	16:30-22:00
Pico-hydrokinetic	PHK	21:30-23:00

3.3.2.4 Fuzzification input and output of the controller

The configuration of the fuzzy logic controller includes the input and output variables indicated in Table 3.4, below. Load consumption (kW), renewable energy sources (kW) and time (hrs) are selected input variables, with a diesel generator (kW) and battery (kW) as output variables. FLCs have the potential to work with data that is incorrect and that does not require an accurate mathematical model [23]. At a particularly low, average or medium consumption, the renewable energy system (RES) is expected to be able to meet the load demand, without a backup over a specific period, as shown in Table 3.4. The backup system may solely work in unforeseeable circumstances, if either of the RES is unable to function.

Table 3.4: FLC input and output variables

Input 1(Time in hrs.)	Input 2(Power consumption in W)	Input 3 (RES in W)	Output (Backup in W)
MOP (00:00 -4:00)	VLC (0-400)	PHK	BT
MP (03:30 -6:00)	LC (350-600)	WT	BT
MD (05:30-16:00)	MC (450-660)	PHK+PV	BT
APD (15:30-17:00)	AC (550-780)	PV	BT
EP (16:30-22:00)	HC (750-1080)	WT	DG
EOP (21:30-23:00)	VHC (1050-1140)	PHK	DG

3.3.3 Membership function

The membership functions selected for inputs are triangular and have six labels VL, L, M, A, H and VH under three input categories, which stand for Very low, Low, Medium, Average, High Value, respectively shown in Figure 3.4. The outputs further have four membership functions under BT and two membership functions under DG, that represent when the backup system is able to start operation under faulty or emergency conditions to the load, shown in Figure 3.5.

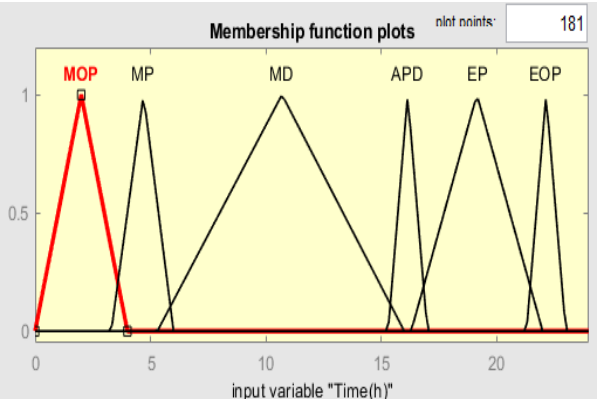

(a)

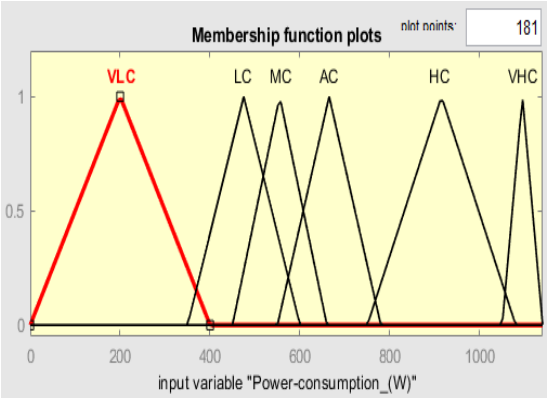

(b)

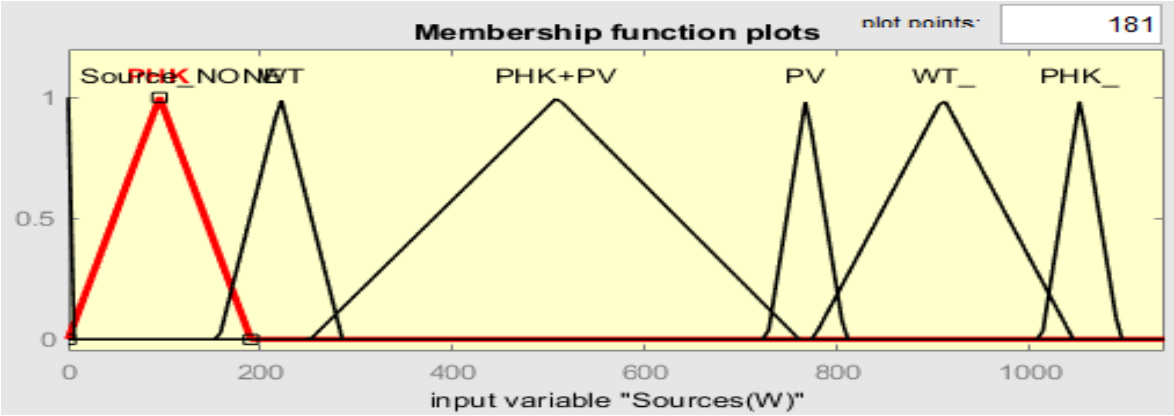

(c)

Figure 3.4: Input membership fucntion, (a) time (b) power consumption (c) source

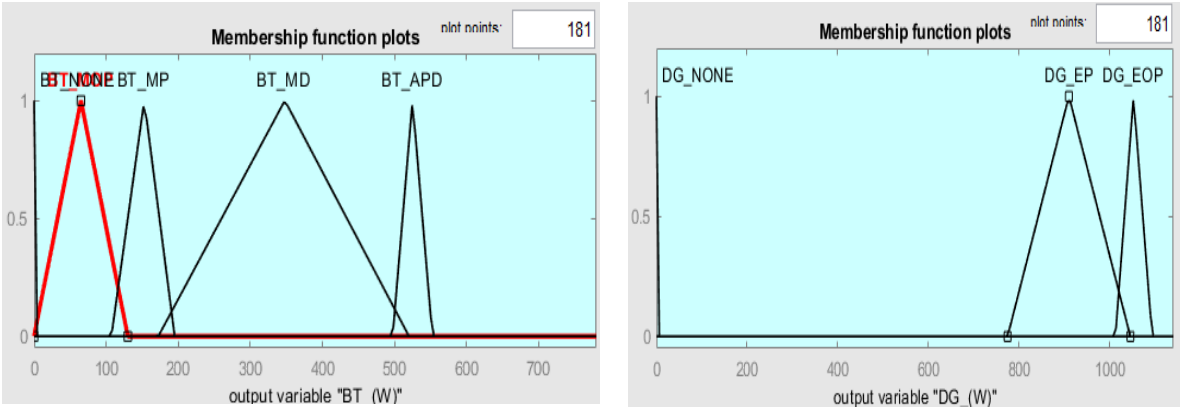

(a) (b)

Figure 3.5: Output membership funtion (a) BT (b) DG

3.3.4 Fuzzy logic rules

The fuzzy controller rules determine how design constraints are to be applied and decided [142]. The rules of the designed fuzzy intelligent controller may be established on the basis of objectives and constraints which are briefly mentioned: 1) meeting the load power demand; 2) the priority to use resources to feed the load, in the order of the PHK, WT, PV, BT and the DG; 3) the priority of the use of resources for charging the battery in the order of PHK, WT, PV and DG during RES energy supply absence; 4) attempting to maintain the battery constantly charged. The use of DG and storage power, will take place only in the absence of the three integrated renewable energy sources of the proposed system; 5) avoiding the use of DG, is merely to minimize the fuel costs and CO_2 emissions.

Approximately eighteen sets of IF-THEN rules, governing three input and two output variables that are available for fuzzy rule editor in MATLAB, used to prepare the modelling of the designed hybrid controller in SIMULINK. Figure 3.6; lists these rules and all of them may be adjusted and easily viewed for the expected results; they are designed according to the five constraints mentioned above.

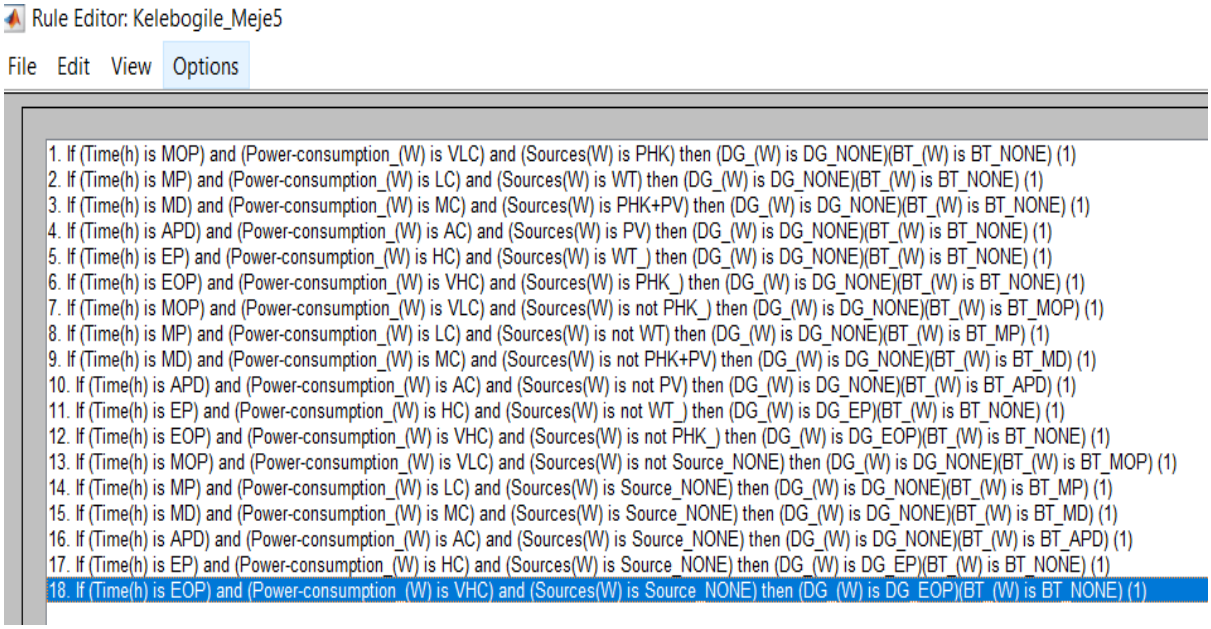

Figure 3.6: FLC rules for input and output variables

3.4. HYBRID POWER SYSTEM MODEL

The studied overall microgrid hybrid power system consists of PV/PHK/WT, a backup system such as battery storage and DG, with a fuzzy intelligent controller modelled in MATLAB/SIMULINK, as shown in Figure 3.7. It is designed to avoid power flow imbalances that may occur during the fluctuating load demand. Fuzzy intelligent controller ensures that the signal sent/received is transmitted to the correct component at the correct time, during a certain load consumption. However, whenever there is a loss of sufficient power to provide the load, the backup system receives a signal sent by the FLC to satisfy the load demand. On the basis of the proposed method, the fuzzy intelligent controller plays the role of the hybrid power system energy management.

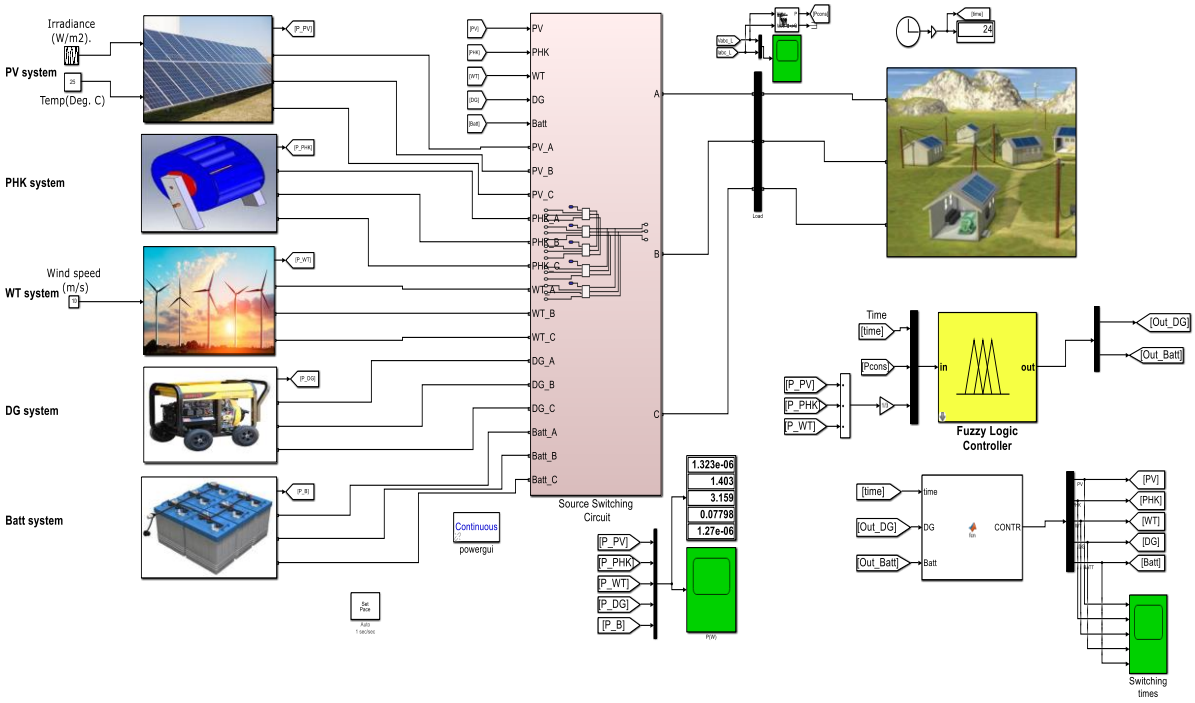

Figure 3.7: SIMULINK model of overall PV/PHK/WT with backup power system

3.4.1 Solar PV modeling

The mathematical model presented for the PV array consists of sustainable power solutions (SPS) and implements a PV array a 16-series and 1 parallel connected PV modules. It enables the modelling of a variety of preset PV modules available from the National Renewable Energy Laboratory (NREL) system Advisor Model (Jan. 2014) [143], as well as the user-defined PV module. The PV array block has two inputs that allow for the supply of varying solar irradiance (input I_r in W/m2) and temperature (input T in deg. C) data. The PV array consists of a single string of SunPower SPR-415-WHT-WHT-D modules, which are connected in parallel with sixteen strings in a series. At 25 ^{0}C, with a solar irradiance of 1000 W/m^2, the string may produce up to 4 080W. The PV system generation consists of several existing components from the MATLAB/SIMULINK software library, to simulate the solar PV system. Figure 3.8, shows the block diagram of the equivalent circuits used for simulation in the library. However, the equivalent circuit of the solar PV system is segmented into a two-level converter; SVPWM generator (2-level) illustrates the behaviour of the solar cells and operating principle.

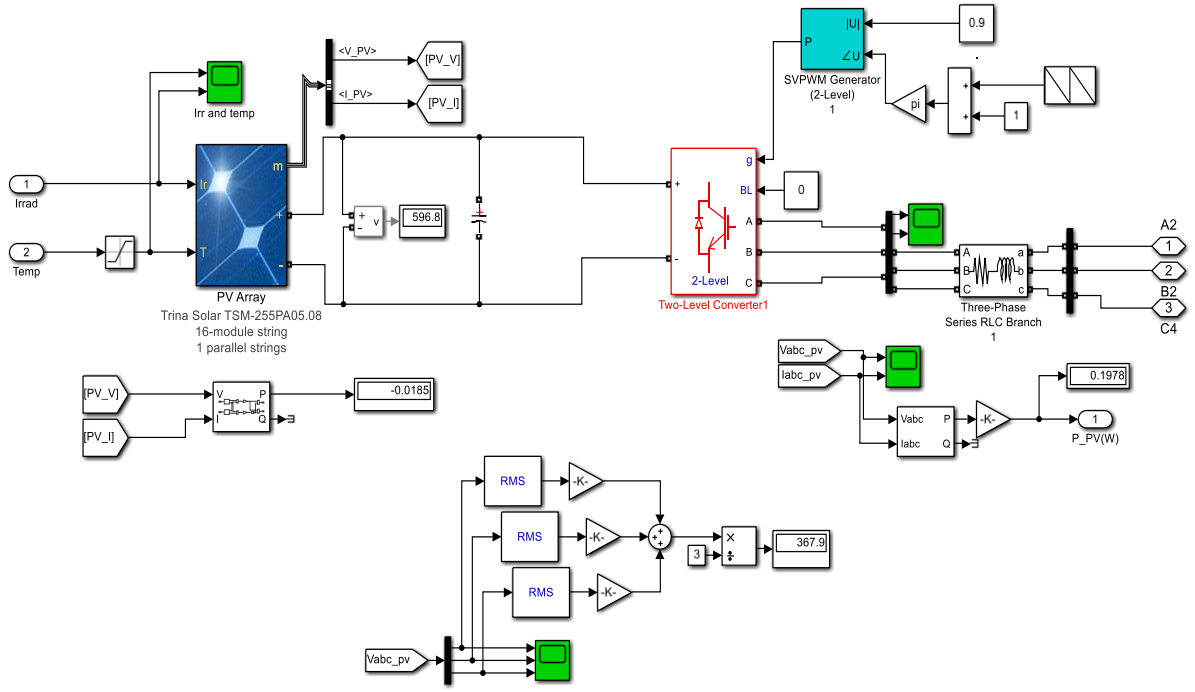

Figure 3.8: Simulation diagram of solar PV system generation

3.4.1.1 Two- level converter

The switching devices converter is modelled with an insulated-gate bipolar transistor (IGBT), which is controlled by firing pulses generated by a Pulse Width Modulation (PWM) generator. This model provides the most accurate simulation results.

3.4.1.2 SVPWM generator (2 level)

It uses the space-vector pulse width modulation (SVPWM) technique to generate the pulses for three-phase and two-level DC/AC converters. The converter switches are represented by the following equivalent circuit, in Figure 3.9 [144]:

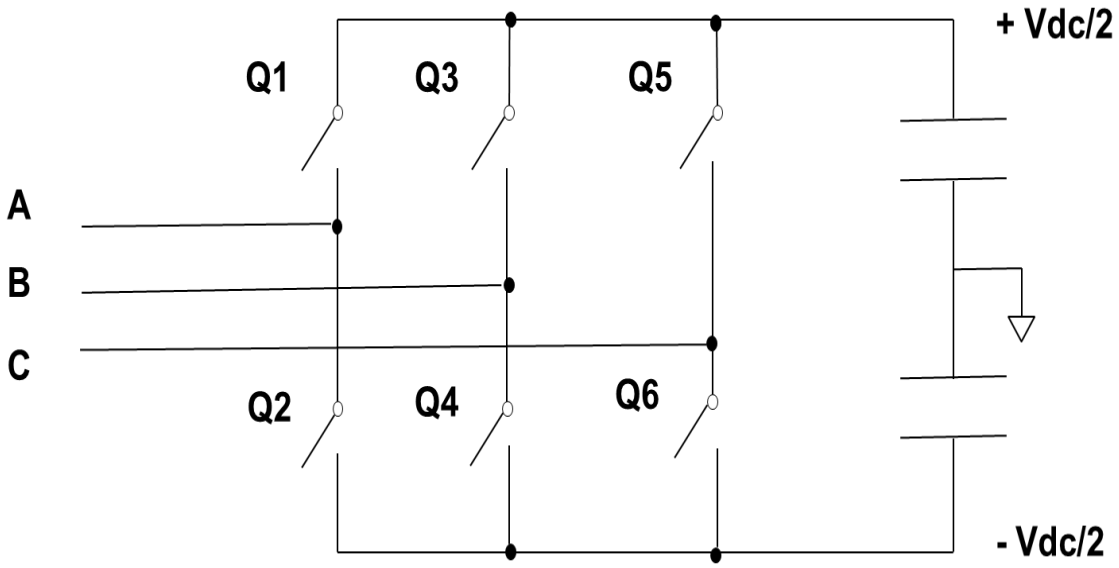

Figure 3.9: Converter switches [145]

3.4.1.3 Operation principle

PV modules convert solar radiation directly into electricity, using the photovoltaic effect; the conversion efficiency may be between 15-19% [145]. The output power from the whole PV system may be expressed as:

$$P_{PV,system} = P_{PV,module/U} \times \eta_{PV} \quad (3\text{-}2)$$

Where:

$P_{PV,system}$ denotes the total PV system output power; $P_{PV,module/U}$ denotes the nominal output power of a single PV panel and η_{PV} denotes multiple PV panels connected in parallel.

3.4.2 PHK modeling

In this section, the mathematical model of PHK in Figure 3.10 below, consists of an existing SIMULINK library block, that implements a 3-phase synchronous machine in the d,q rotor reference frame by combining an existing hydraulic turbine and governor, excitation system and synchronous machine. The stator's windings are wye-connected to a

500VA,400V and 50 Hz internal neutral point. With the help of a hydraulic turbine model designed by the institute of electrical and electronic engineers (IEEE) Working Group (1992), [146] under MATLAB simulation software and available on the Mathworks website, [147]. A comprehensive review of a pico-hydrokinetic system modelling was handled at this level. The model takes into account the dynamics of the stator, field and damper windings. The equivalent circuit of the model is represented in the rotor reference frame (qd frame). All rotor parameters and electrical quantities are viewed from the stator. They are identified by primed variables [148-150], with the following subscripts :

- d,q : d and q, denotes the quantity of the axis,
- R,s : R and s, denotes the quantity of rotor and stator,
- l, m — l and, m denotes the inductance of magnetizing and leakage,
- f,k — f and k, are the field and damper winding quantity.

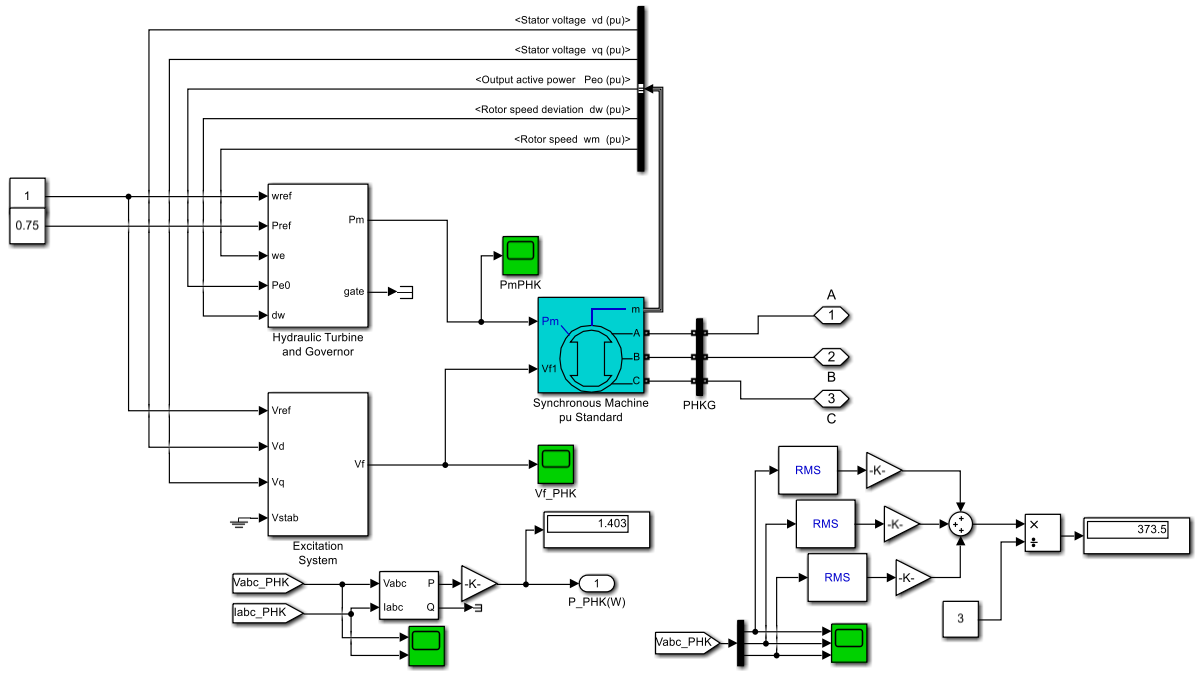

Figure 3.10: Simulation diagram of PHK system generation.

3.4.2.1 Hydraulic turbine and governor

A non-linear hydraulic turbine model, a PID governor and a servomotor, as described in Figure 3.11 and are implemented in the hydraulic turbine and governor block [146].

Figure 3.10 illustrates the summary of the input/output to the hydraulic model and are in the following pattern:

- ω_{ref}: the speed of the reference in pu.
- P_{ref}: mechanical power reference in pu.
- ω_e: machine current speed in pu.
- P_e0: the machine's electrical power in pu. This is applicable, if the gate position is used as an input to the feedback loop, instead of the deviation of power and the entry may be left disconnected.
- dw: deviation of speed in pu.
- Pm: the synchronous machine block, which is measured in pu and has a mechanical power Pm.
- Gate: Opening of the gate in pu.

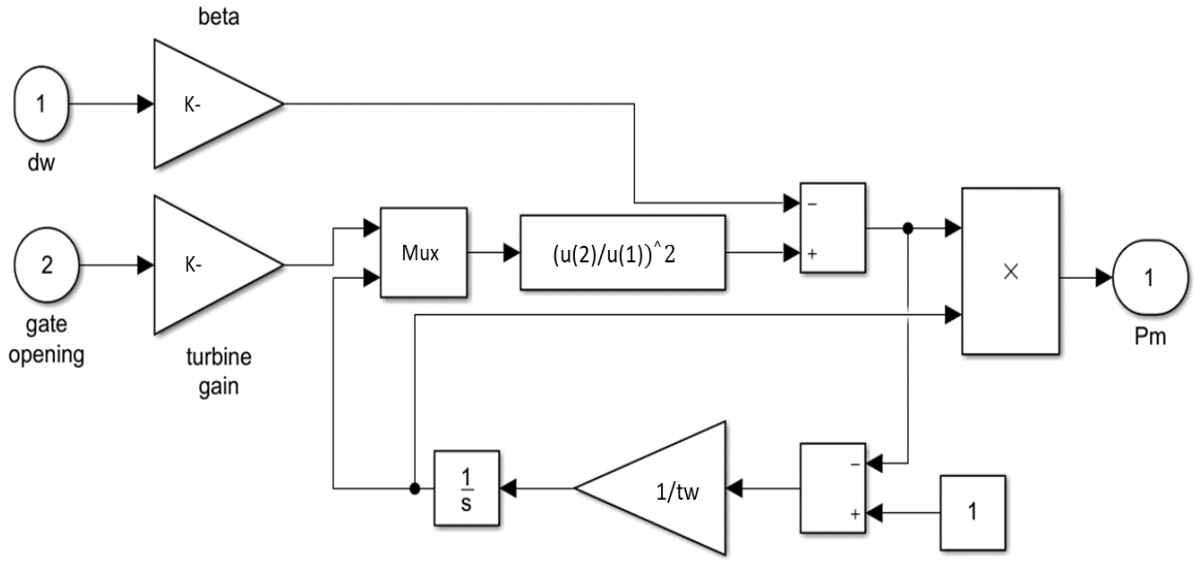

Figure 3.11: Hydraulic turbine model [146].

The gate servomotor model is modelled by a second-order system shown in Figure 3.11, with a turbine model input, including the gate servomotor (per unit of full gate opening), a blade servomotor stroke (per unit of full blade stroke) and the output of the turbine model was the turbine power (per unit of turbine megawatt capacity). At full gate opening at a specified head, the turbine megawatt capacity was defined at a full gate opening at a specified head. The input of the blade controller was the stroke of the gate servomotor (per unit full gate opening), then, the output of the blade was the stroke of the blade

servomotor (per unit of full stroke)[151, 152]. Servomotor was used to control the flow of water in small hydropower, by controlling the rotational motion of the spear valve [153].

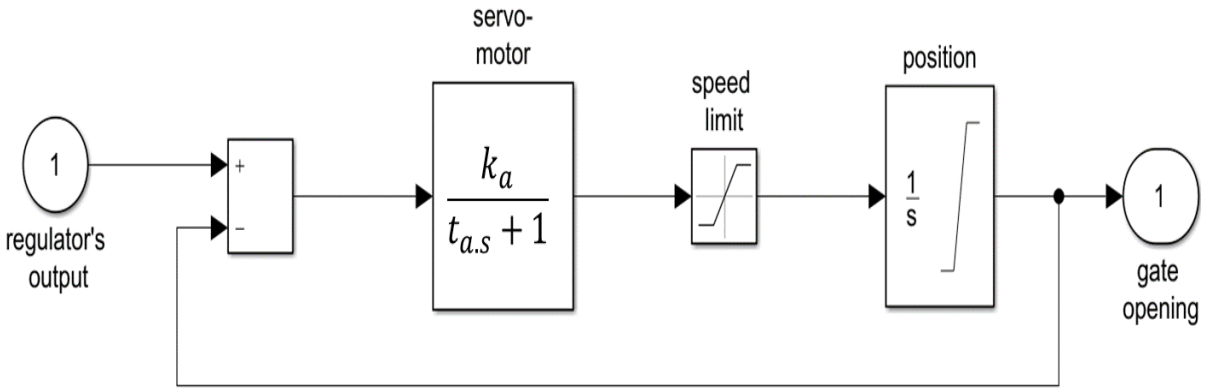

Figure 3.12: Gate servomotor model [146]

3.4.2.1 Excitation system

Provide an excitation system for a synchronous machine and regulate its terminal voltage in the mode of generation [154]. The basic elements that make up the excitation system block are the voltage regulator and the exciter, indicated in Figure 3.13 and the exciter is represented by the following transfer function between the exciter voltage v_{fd} and regulator's output e_f:

$$\frac{v_{fd}}{e_f} = \frac{1}{K_e + sT_e} \tag{3-3}$$

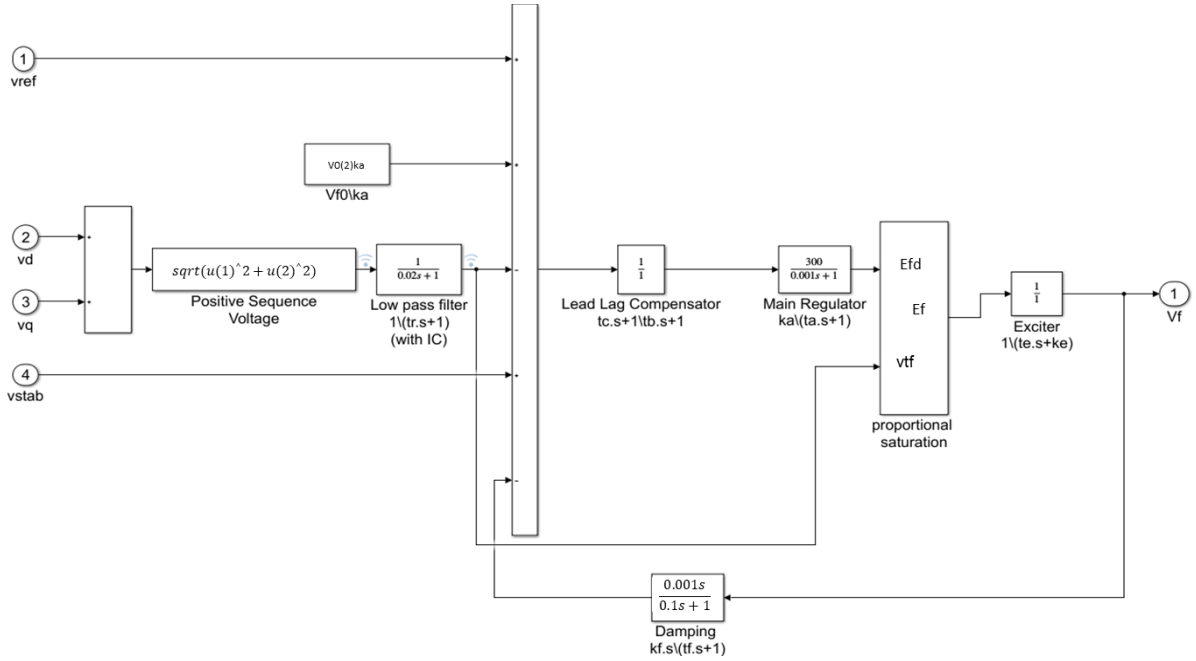

Figure 3.13: Voltage regulator and exciter

3.4.2.1 Operation principle

Hydro kinetic technology is obtained from waves, tides, ocean currents and a natural flow of water in rivers. However, the focus of the study is the application in running water rivers only, as it was indicated to be suitable for small-scale electrification[155]. Therefore, hydro kinetic energy conversion systems convert the energy in moving water to mechanical and then electricity. The output power from the hydrokinetic system, it may be expressed as:

$$P_{HKT,system} = P_{HKT/U} \times \eta_{HKT} \quad (3\text{-}4)$$

Where:

$P_{HKT,system}$ denotes the total output power of the hydrokinetic (HKT) system; $P_{HKT/U}$ denotes the nominal output power of a single HKT and η_{HKT} denotes multiple HKT connected in parallel.

3.4.3 WT modelling

WT's Asynchronous Machine/ induction machine implements a three-phase asynchronous squirrel cage machine, modelled in a selectable dq rotor reference frame. Stator and rotor windings are connected in wye to an internal neutral point. It operates in generator mode rated at 1.35kVA, 400V. The mode of operation is dictated by the sign of the mechanical torque (Tm) and the Tm is negative, so the machine acts as a generator, as shown in Figure 3.14.

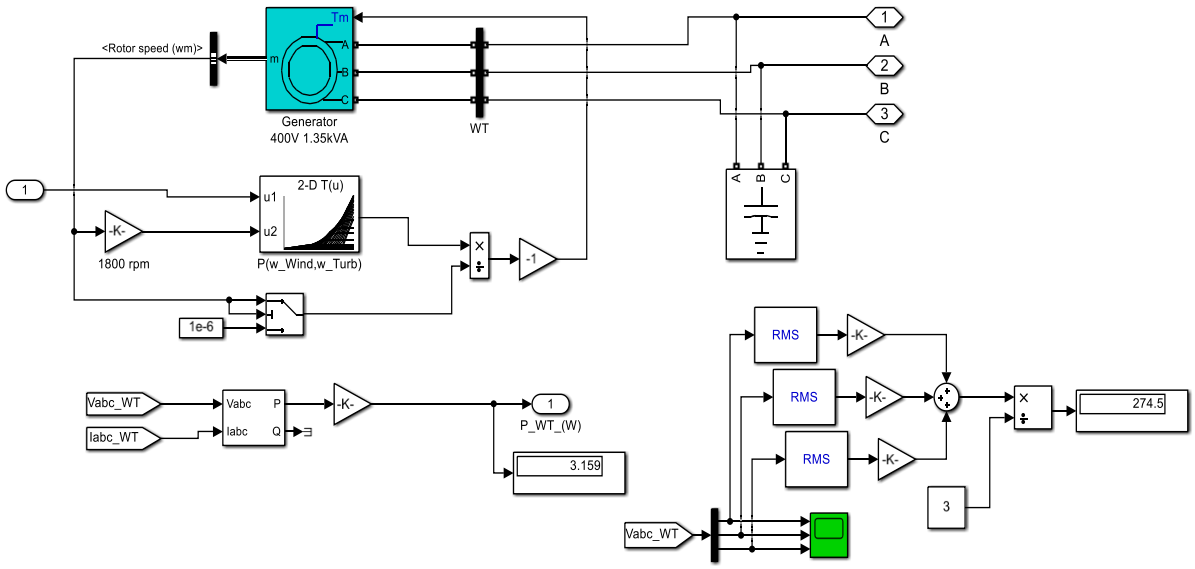

Figure 3.14: Simulation diagram of WT system generation

3.4.3.1 Operation principle

Wind energy conversion systems convert the energy in moving air to mechanical and then electricity. The output power from the whole wind system may be expressed as:

$$P_{WT,system} = P_{WT/U} \times \eta_{WT} \quad (3\text{-}5)$$

Where:

$P_{WT,system}$ denotes the total output power of the wind system; $P_{WT/U}$ denotes nominal output power of a single WT and η_{WT} denotes multiple WT connected in parallel.

3.4.4 DG Modelling

This block in Figure 3.15, implements a synchronous machine, diesel engine and governor system from the SIMULINK library.

3.4.4.1 Diesel engine governor

The first input is the reference speed and the second input is the measured speed. The output is the mechanical power of the diesel engine. The engine inertia should be combined with the inertia of the generator. The model consists of a regulator represented by the following transfer function:

$$H_c = K(1 + T3.s)/(1 + T1.T2s^2) \quad (3\text{-}6)$$

The trotte actuator is implemented as:

$$H_a = K(1 + T4.s)/[s(1 + T5.s)(1 + T6.s) \quad (3\text{-}7)$$

3.4.4.1 Synchronuos machine

Implement a 3-phase synchronous machine modeled in the reference of the dq rotor. Stator windings are connected in wye to an internal neutral point, which is rated at 1.425kVA, 400V.

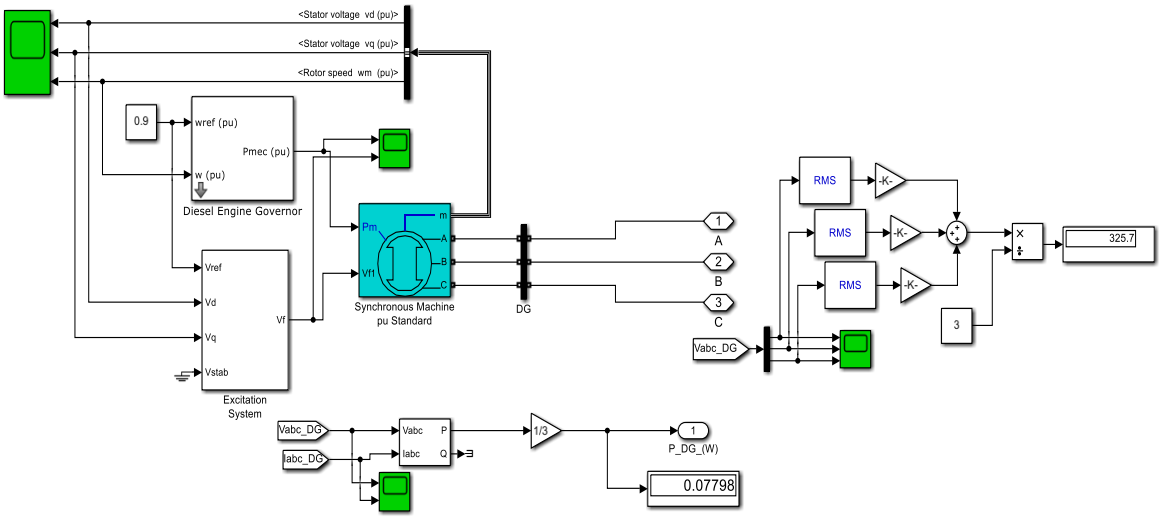

Figure 3.15: Simulation diagram of DG system generation

3.4.4.2 Operation principle

Diesel generators are general diesel engines coupled to generators. DGs are the most common way of providing AC power to isolated areas not connected to the grid [43]. Output power from the DG depends on variables, expressed as:

$$P_{DG} = P_{DG,max/U} \times X_{DG} \tag{3-8}$$

Where:

P_{DG} denotes the DG output power; $P_{DG,max/U}$ denotes maximum nominal DG power and X_{DG} denotes DG's output decision variable, which ranges from 0 to 1. 0, indicating DG with no output and 1 indicating the maximum output.

3.4.5 BT modelling

3.4.5.1 Battery type

This implements two generic battery models for the most popular battery types in Figure 3.17. Temperature and aging (due to cycling) effects may be specified for Lithium-Ion battery types. With a nominal voltage of 12V, 800Ah, 50% initial state of charge (SoC)

and battery response time of 15 second. The battery discharge depends on the nominal parameters of the batteries. Figure 3.16 shows the equivalent circuit that the block models. This model may have a sufficient accuracy and be easily implemented in the battery management systems to dynamically predict the battery voltage and use this equivalent circuit model to model battery dynamics. Mathematical and equivalent circuit models may be used, however, equivalent circuit was proven by [156] to be a better performing model, at the cost of increased complexity

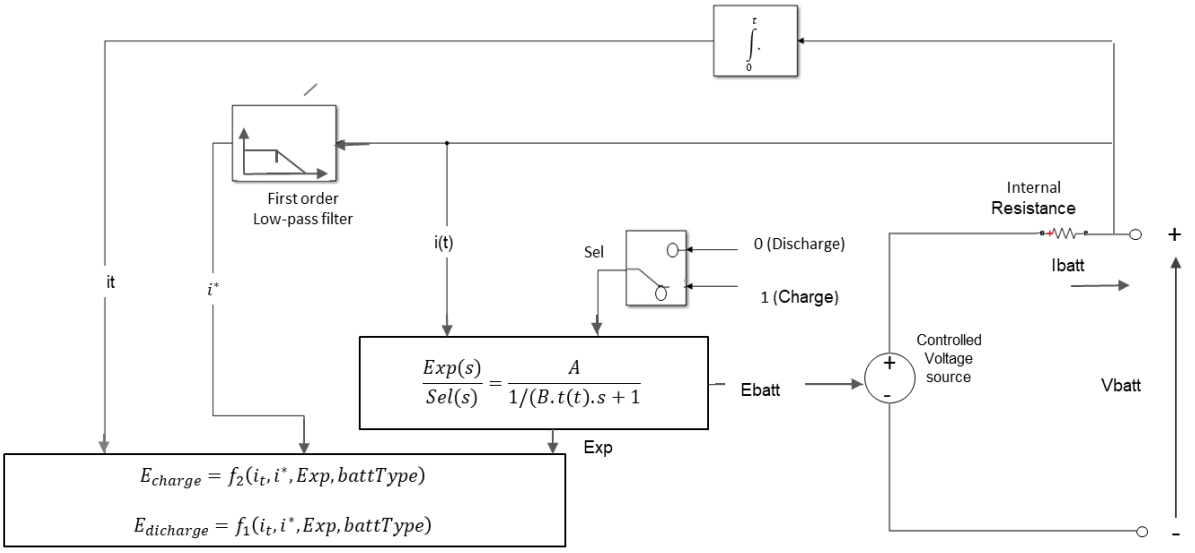

Figure 3.16: Generic dynamic model of a battery equivalent circuit.

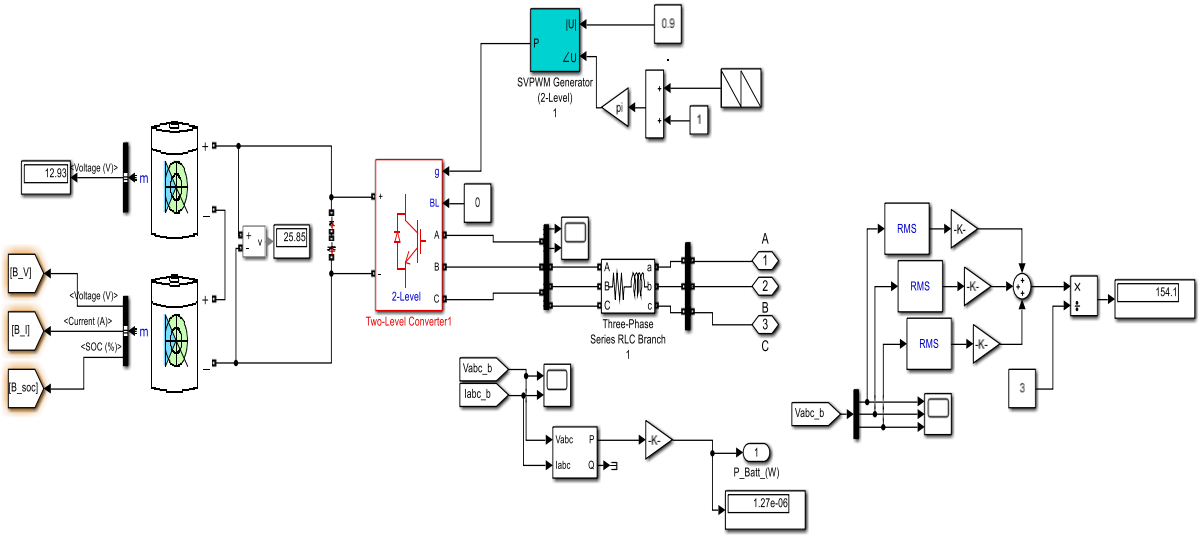

Figure 3.17: Simulation diagram of BT system generation

3.4.5.2 Operation principle

Batteries are devices that are used to store energy. The deep cycle lead-acid battery type is the most extensively used as a storage system or back-up in combination with renewable energy sources [157]. The maximum available power of the battery in percentage may be expressed as:

$$P_{Bat} = P_{Bat,max/U} \times X_{Bat} \times \eta_{Bat} \quad (3\text{-}9)$$

Where:

P_{Bat} denotes the instantaneous output power, which at time (t) is expressed as a percentage of the battery's maximum power; $P_{Bat,max/U}$ denotes the battery's maximum power at time (t), while X_{Bat} raises the output decision variable of the battery ranging between [0, 1]. A nominal voltage of the DC bus, which is a constant, dictates the number of batteries in series. The instantaneous output power of the entire battery bank is determined by variables such as the battery type and size (η_{Bat} , size, type) and the quantity of battery strings connected in parallel η_{Bat}.

3.5. MODELLING OF LOAD SYSTEM

The Figure in Appendix A shows approximately five different non-linear load categories, ranging from VL, L, M, A, H, to VH, expected to be met by all hybrid renewable energy sources, visualized in Table 3.4. The load varies with the supply; however, the artificial intelligent controller is required to maintain this imbalance of the system as anticipated. As the load switch closes, as demanded by the end user, the controller detects a signal of the system and responds accordingly, so that the required source is in operation at the time, even though WT and PHK are able to operate throughout the day, the idea is to investigate how the controller behaves when the system is hybridized with different sources detected by the controller.

3.6. SWITCHING SYSTEM

The PV/PHK/WT/DG/BT involves approximately five switches that are used to control the switching ON and OFF of each component. Each switch closes or opens each component according to the availability of resources. They have been developed in FLC, as presented in Figure in Appendix B. These switches are controlled externally in response to the change in load demand, with the switches closing or opening, depending on the power consumption varying from VLC to VHC. Allowing all RES to generate power to the load, including the back-up system, accordingly in emergency situations.

3.7. MATLAB FUNCTION CODE

The hybrid power system, consisting of approximately three renewable sources and two backup systems, as mentioned above, makes use of the IF/END function code in Appendix C. Firstly, the MATLAB function controller is initialized, to set the programmed switch to zero (0), which symbolizes an OFF/OPEN state and one (1) indicates an ON/CLOSE state. If the time is between 00:00 and 4:00am, then the second source will start receiving a signal from the FLC, in order to respond accordingly, in the same way as the 3rd to the 4th source of supply, with respect to time. The MATLAB function code is linked to the internal switch, to control it externally by controlling the entire microgrid hybrid renewable system via the FLC. The controller responds to each signal sent and received by the load demand. Each component is allocated a specific time to operate and when the energy should or should not be stored or discharged by the batteries, similarly with the DG, while charging the battery, the primary idea is to minimize the use of DG and BT and to maximize the use of hybridized RES.

3.8. SUMMARY

There are various cases and scenarios in which FLC was used to control and mitigate the risks that could be experienced by the different systems and are still found to be the optimal performing artificial intelligent control used in simulations and later used in real

time experiments, as most researchers have recently considered FLC to be the optimal and most viable option to be used in real time systems. In future work and better development, any algorithm should be integrated with a different artificial intelligence algorithm, rather than with an individual method. The fuzzy intelligent controller is designed and developed to react according to the behaviour of the system, to maintain the power flow to the load, due to its simplicity.

CHAPTER 4: SIMULATION RESULTS ANALYSIS

4.1. INTRODUCTION

This Chapter presents an analysis of a fuzzy intelligent controller, using different AC load variations in the microgrid HRES for optimal energy management algorithm. Simulated results and data are analysed from each pattern developed in the previous Chapter, under these different AC load variations. Due to the constraints set out in Chapter 3, this Chapter reports the controller's behaviour, according to the rules set out in the management of the power flowing through each component to the load. Because of the complexity of controlling power produced by hybrid system, MATLAB/SIMULINK software is used to monitor and manage the continous power flow signal behaviour within the modelled hybrid system. As the problem consisted of fluctuating energy supply the MATLAB's fuzzy, an intelligent controller is used to convey the output results.

4.2. SYSTEM SPECIFICATION

4.2.1 Typical load profile

The detailed information is shown in Table 4.1 for typical appliances to be supplied, where the daily load profile generated from an average of 5 to 6 households is assumed to contain the same appliances used by each household. The load peak demand is 1.4 kW, with the total daily energy consumption of 18.54 kWh.

Table 4.1: Summary of a typical load profile for 6 households.

Appliances	Wattage	Quantity	Wattage (kW)	Hours for daily consumption	Common sage interval(s)
Compact fluorescent light (CFL)	5W	4	0.02	5	5:00- 6:00 18:00-22:00
Radio	10W	1	0.01	12	5:00-17:00
Refrigerator	100W	1	0.1	24	00:00-00:00

Figure 4.1. indicates the behaviour of the assumed load profile, with a load demand of 0.6kW between 00:00 to 04:00 a.m.. Thereafter, the demand increased to 0.78 kW between 05:00 to 06:00 a.m.. From 07:00 a.m to 4:00 p.m., the demand for the load is steady, showing that most electricity consumers are at work during that period. The power consumption starts to increase again to 1.08 kW at 17:00 and the power consumtpion reaches its peak from 6:00 to 10:00 p.m., as during that time most consumers are back from work and start utilizing electricity. The power consumption goes back to normal at 23:00, with most consumers currently asleep.

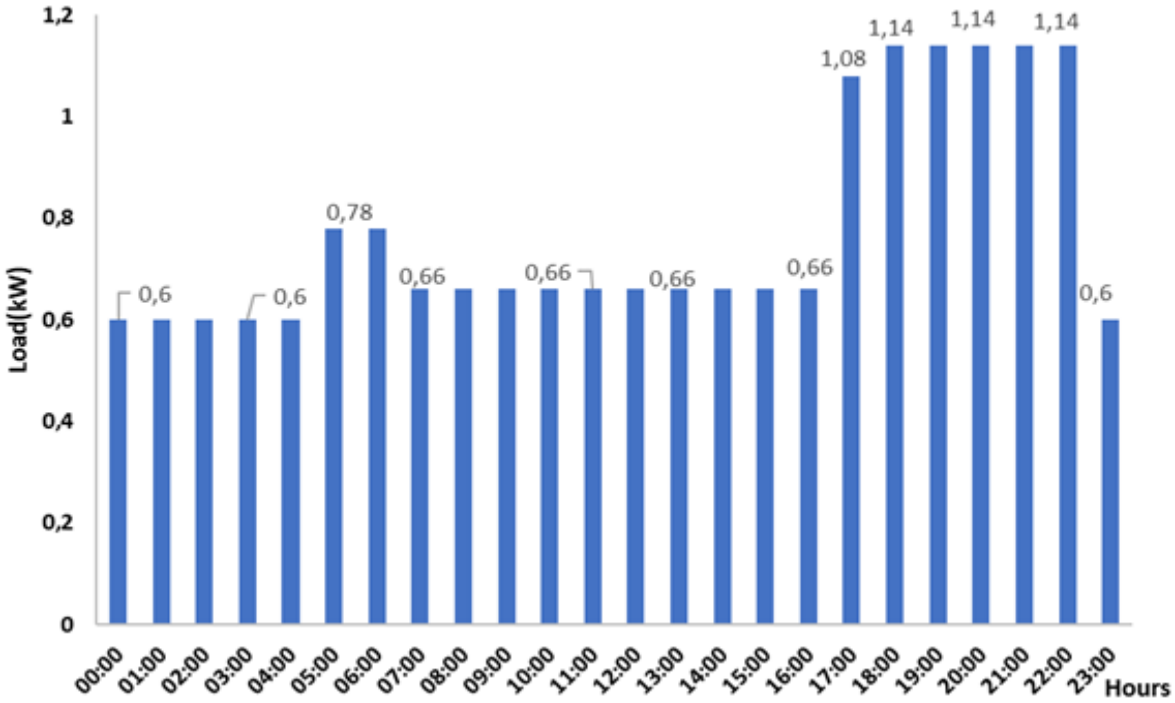

Figure 4.1: Typical total demanded load per day.

4.2.2 System specification

The proposed hybrid system specifications and parameters are shown in Table 4.2. for each component below. The components involved are approximately, three renewable energy sources, with two backup systems. The parameters of the system are comprised of Solar PV system of SunPower SPR-415-WHT-D of a 16-module in series strings and one parallel string. The synchronous machine with hydraulic turbine governor represented the PHK of the proposed system, Asynchronous machine for WT. Another synchronous machine governor and excitation machine for DG and two lithium-ion batteries with up to 50% SoC and 15s response time.

Table 4.2: Specification and parameters for PV/PHK/WT and backup system.

Components description	Parameter	Value
PV	SunPower SPR-415-WHT-D	16-module string 1 parallel strings
PHK	Synchronous machine with hydraulic turbine and governor	3-phase machine, 500VA, 400V,50Hz
WT	Asynchronous machine	400V/1.35kVA
DG	Synchronous machine with diesel governor and excitation machine	3-phase machine, 400V/1.425kVA
BT	Lithium-Ion	12V,800Ah,50% SoC, 15s response time

4.3. FUZZY LOGIC SIMULATION RESULTS

4.3.1 Fuzzy logic surface

Figure 3.4. basically depicts the output surfaces of the system against three inputs and two outputs of the system. Upon opening the surface viewer, a three-dimensional curve represents time (hrs) mapping, power consumption (W) mapping and two backup systems (W) mapping. The 18 rules set out previously, are designed to meet the objective set out in the figure below and clearly illustrate the significance of prioritizing , first and foremost, the use of the three hybridised renewable energy sources, rather than the use of battery storage and diesel generator, as well as minimizing the fuel costs and the level of carbon

dioxide emissons. As may be seen, the power consumption is met by all the renewable energy sources, while the diesel generator and battery power supply are off. This backup system solely takes over when there is an emergency.

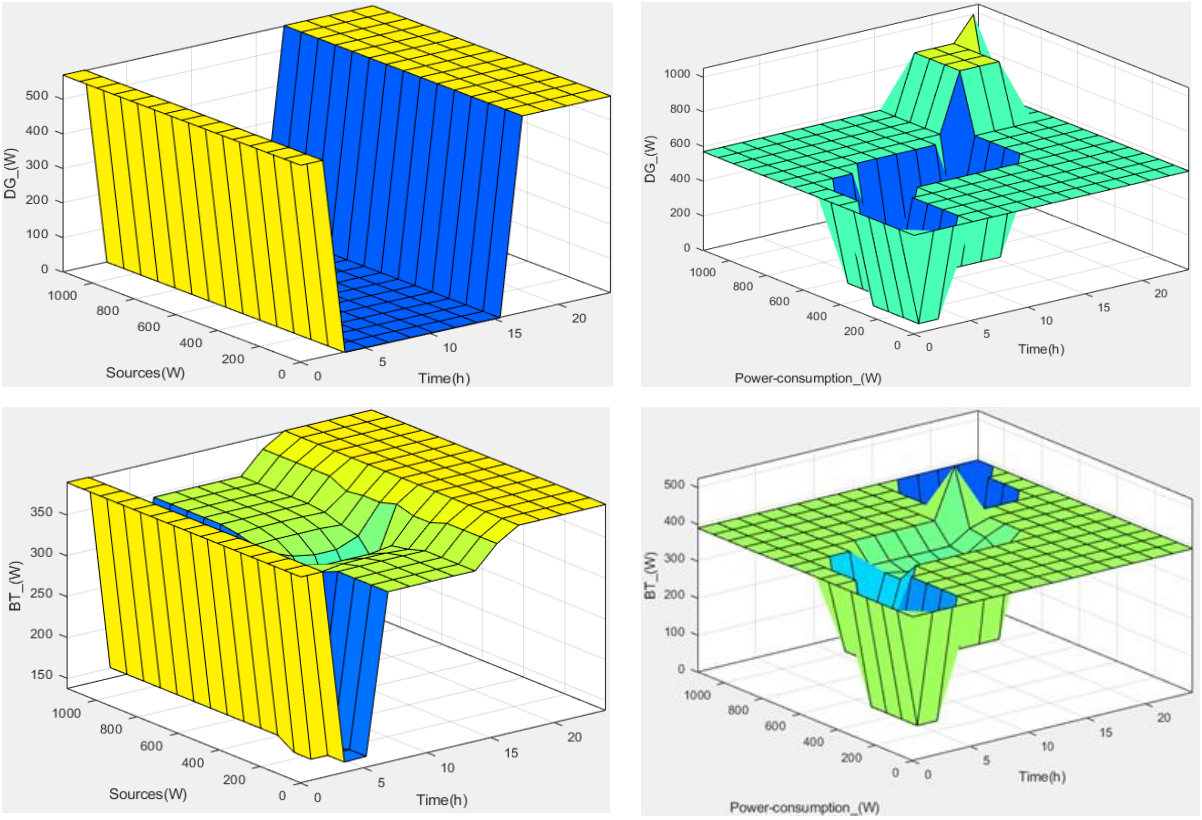

Figure 4.2: Surface function with BT and DG output.

4.3.2 Input and output fuzzy results set

The input and output variables in Figure 4.3, depict details influenced by the membership functions, in order to view the entire surface of the fuzzy inference system as to how the system, will operate in SIMULINK and plots every part of every rule. However, for a more accurate analysis of the results, input and output data and graphs are analyzed by MATLAB software. The timing of the connection of each source to the load and the value of the power used by these sources are determined and, finally, the area under the curves is calculated, which is the amount of watt-hours consumed.

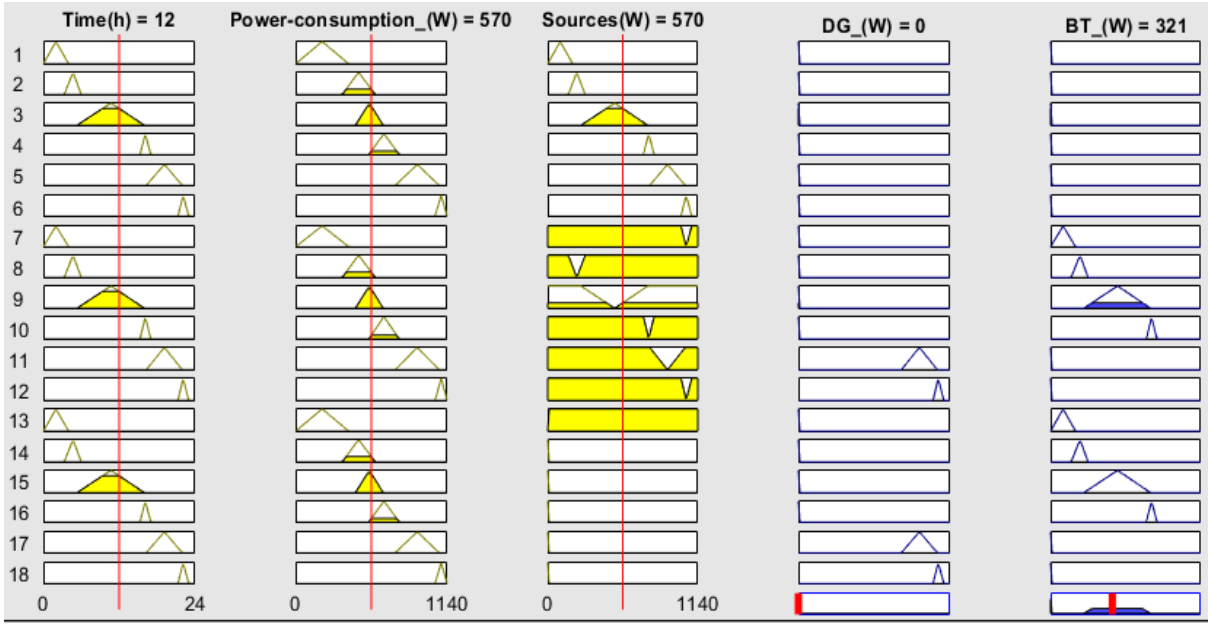

Figure 4.3: FLC input and output results set

4.4. RESULTS ANALYSIS

4.4.1 Hybrid system output power

The WT and PHK have the ability to operate throughout the day and PV operate particularly during the day. FLC is programmed to send a signal to each RE at a specific time for load balancing or maintaining stable power output, in order to avoid the use of BT and DG timeously, unless there's an emergency or when the system fails to meet the load. The IF and THEN FLC rule send a signal to the PHK at VLC, to operate between 00:00 to 04:00 a.m. Thereafter, the WT will receive a signal to take over between 03:30 to 06:00 a.m, to start operating at LC. Between 05:30a.m and 4:00 a.m at MC, the controller once again sends a signal to the combination of PHK and PV. However, PHK will begin to operate from 05:30 to 7:30 a.m and the PV takes over until 5:00 p.m, at AC. Between 16:30 and 22:00p.m, where there is HC, WT will resume operating. PHK takes over from WT between 9:30 to 11:00p.m, after receiving a signal from FLC at VHC. The battery is charged as each component starts operating and is discharged whenever there are shortfalls or emergencies in the HRES operation. Any power source that is below the zero-reference line, such as PV and WT, indicating that the source is not producing energy and does not supply any load at that time, as shown in Figure 4.4.

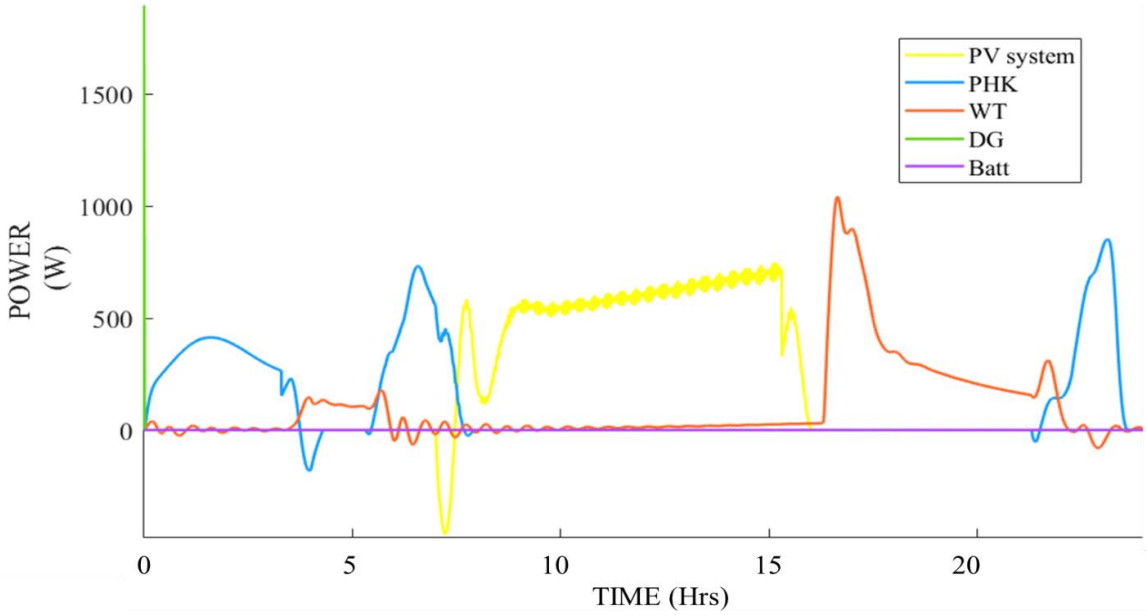

Figure 4.4: Output power produced by RES during FLC mode without backup

4.4.2 Voltage and current waveforms

Figure 4.5. illustrates the power consumption behaviour of the end user on a daily basis. It may be seen that power, which is resembled by the product of voltage and current, is used by end-users early in the day, between 04:00 and 07:00 a.m and in the late afternoon, when the load demand starts to reach its peak from 5:00 to 10:00 p.m. However, it remains stable in mid-day, from approximately 7:00 a.m. to 4:00 p.m and at 11:00 p.m in the evening.

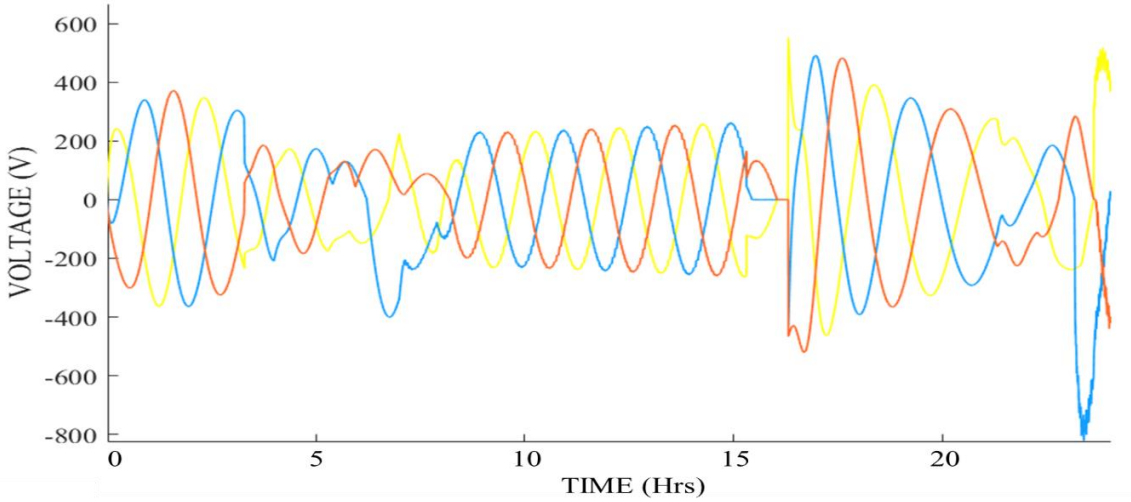

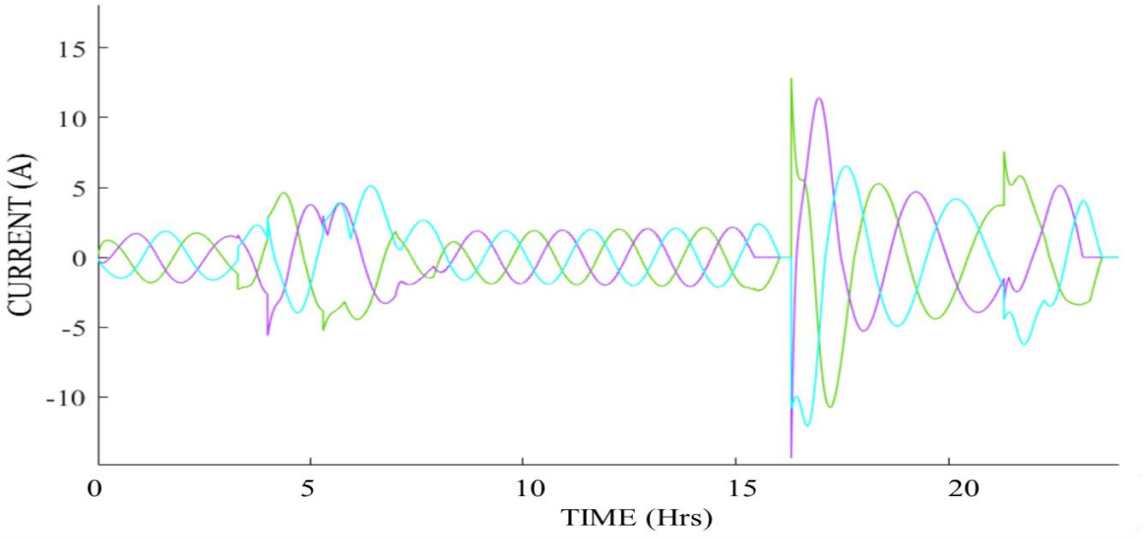

Figure 4.5: Voltage and Current waveforms during the fuzzy model

4.4.3 Switching times

Figure 4.6. describes which RES is to be operational at which time, to maintain the load demand balance. Both the PHK and WT, as stated above, have the ability to operate on a day-day basis. However, they are programmed by a fuzzy based controller, to supply energy if the resource of any source is unable to supply sufficient power at the required time. PHK will switch ON in the morning, then WT. In the middle of the day both PHK and PV will switch ON as the controller receives the signal and send it to the source. PHK and WT will then take over the load in the afternoons and evenings. However, BT and DG are both off and as they are solely on standby.

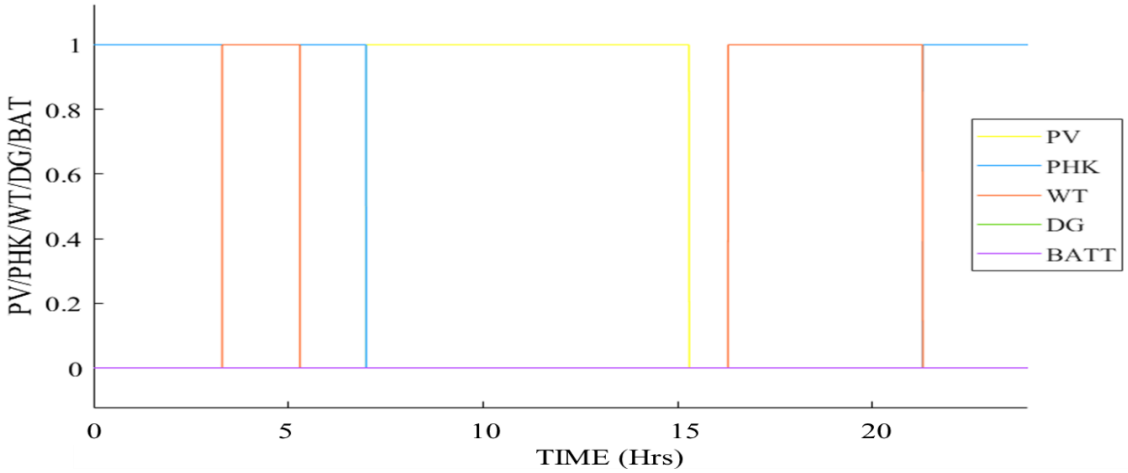

Figure 4.6: System switching times

4.5. SUMMARY

The FLC was developed to successfully operate the power system control, due to the difficulty of load fluctuation. A PV/PHK/WT hybrid system, with a backup system based FLC, was introduced for this study. The findings of the simulation showed that a FLC-based management strategy does not only provide the load, it further helps to maintain charged batteries, without allowing DG to operate fully, but only when the system experiences unpredictable power failure. Moreover, the power system has improved the operating performance, though further ideas are to be involved, to create a smoother and better performance.

CHAPTER 5: LABORATORY PRACTICAL SETUP

5.1. INTRODUCTION

This Chapter discusses the implementation of a real-time automated energy management control in a RE hybrid system, integrated with backup and validated in a laboratory setup. The experimental setup used a fuzzy intelligent controller in Chapters 3 and 4 for energy management on the software tool platform, the control board layout designed with aid of the Proteus Design Suite 8.1 software and the Arduino MEGA2560 hardware platform board, uploaded from Arduino integrated development Environment (IDE). The utilized hardware platform has the ability to monitor the real-time voltage dissipated by each component and is balanced by the controller via the voltage regulator, by adjusting it to an acceptable and readable voltage of 5V by Arduino to the load. Arduino IDE has been programmed and uploaded to the hardware platform using C++ language. Furthermore, there are two different Arduino types, Arduino MEGA and Arduino UNO. Arduino MEGA2650 was selected in this study, as it has a more pin size compared to UNO and it may further accommodate a hybridized system with more components.

5.2. DESCRIPTION AND SPECIFICATIONS OF HARDWARE DESIGN

Table 5.1 presents the proposed simulated rural microgrid system hardware specifications. Different components for hardware design have been listed and used. Due to availability and compatibility, all listed components have been integrated with the microcontroller AT2560 Arduino MEGA and simulated in Proteus Design Suite 8.1 software, as illustrated in Figure 5.2, whereby the system was simulated to verify, monitor and visualize the functionality of microgrid system in real-time.

Table 5.1: Hardware specification

Hardware components	**Description**	**Specifications**	**Quantity**
PV system	Produce DC voltage	6V, monocrystalline, 165x135x2mm, 583mA 12V,7A 12-35 VOUT 150W	1
WT system	Dynamo Lantern kit	95x110x52mm	1
PHK system	Vert Rotor Dynamo	0.01-5.5V, 100-600rpm, 0.01-100mA	1
DG system	Battery (Acts as a DG)	Rechargeable Battery 12V, 1.4Ah, (L=151 W=65 H=94mm) F1 Terminal 4.8mm 1.9kg	1
Battery	Battery (Acts as a source)	Rechargeable Battery 12V, 1.4Ah, (L=151 W=65 H=94mm) F1 Terminal 4.8mm 1.9kg	1
5 channel relay module	Switch high voltages and high current loads	3.75V-6V, 5V coil	1
Transistor	Used to switch between different loads	TIP122	4
7805 Voltage regulators, integrated circuit (IC)	Step down any voltage of generated by different sources to 5V	+5V, 1.5A	5
SD card module	Transferring data to and from a standard SD card	4.5-5.5V, 0.2-200mA, 42 x 24 x 12mm	1

SD card	Store /Login data from the system	3GB	1
Arduino Mega 2560	Brain of the hardware system -microcontroller board based on the AT2560	2560 Rev3, 54 digital input/output pins, 16 analog inputs, 4 UARTSs (hardware serial ports), 16MHz crystal oscillator, USB connection, power jack, ICSP header and reset button.	1
20x4 Liquid-crystal display (LCD)	Display different parameters	Blue, 5V, 12C NOT	1
Diode	Prevent generating a back feed of current in the system	1N4007 PN junction	5
Light emitting diodes (LED's)	Resembles which residential load is ON/OFF	5mm, 5V, Red, yellow, Blue	5
Heatsink	Dissipate heat from the transistors	24.4°C/W, 19.05 x 13.21 x 12.7mm	9
AC/DC adapter	Supply the prototype system	500mA, 3V-12V	1
Resistors	Current limiting resistors	10kΩ, 100Ω	19
Universal serial bus (USB) cable	Used to upload data from the software to hardware	Blue	1

5.3. SYSTEM DESIGN

5.3.1 System overview

Below is the overview of hardware and software tools used for the power control system that have been implemented on an embedded platform, such as Arduino MEGA. To implement the hardware, software tools were used. Softwares such as, MATLAB R2019b (FUZZY & SIMULINK), which was simulated in Chapter 3, Proteus 8 professionals and Arduino IDE playing various roles. Software tools will be programmed to communicate continuously with hardware tools, in order to control and monitor power of the proposed hybrid system in real time, transmitting the information from the sources to Arduino MEGA, through the components that are integrated on the system for controller optimization.

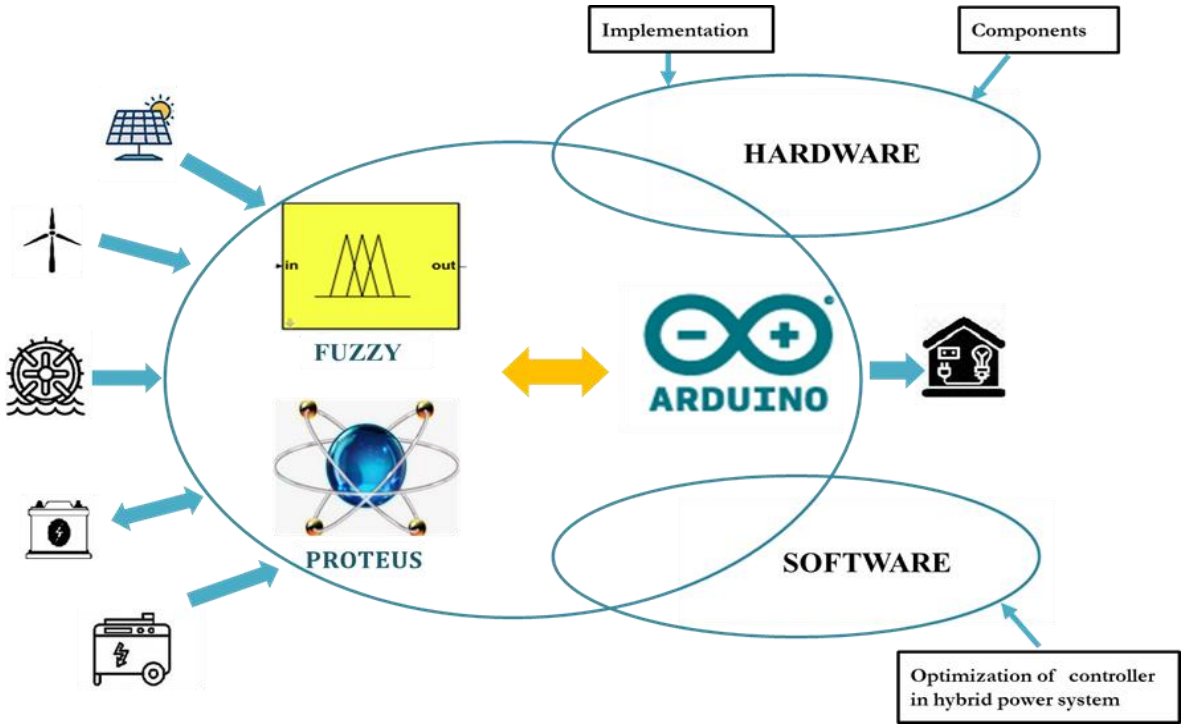

Figure 5.1: Overview of software and hardware tool

5.3.2 System considerations

The flowchart shown in Figure 5.2, presents the developed control method used in the proposed hybrid system, whereby the Arduino board sends raw data from the output power generated by each source to the PC as a sensor and transmitter. The information logged on the proteus is precisely the same as the output results yielded from IF/THEN fuzzy rules and burnt into Arduino IDE. At the end of the process, the micro-controller applies and perform decisions on the hybrid system for balanced output power to supply the load, managed by the controller.

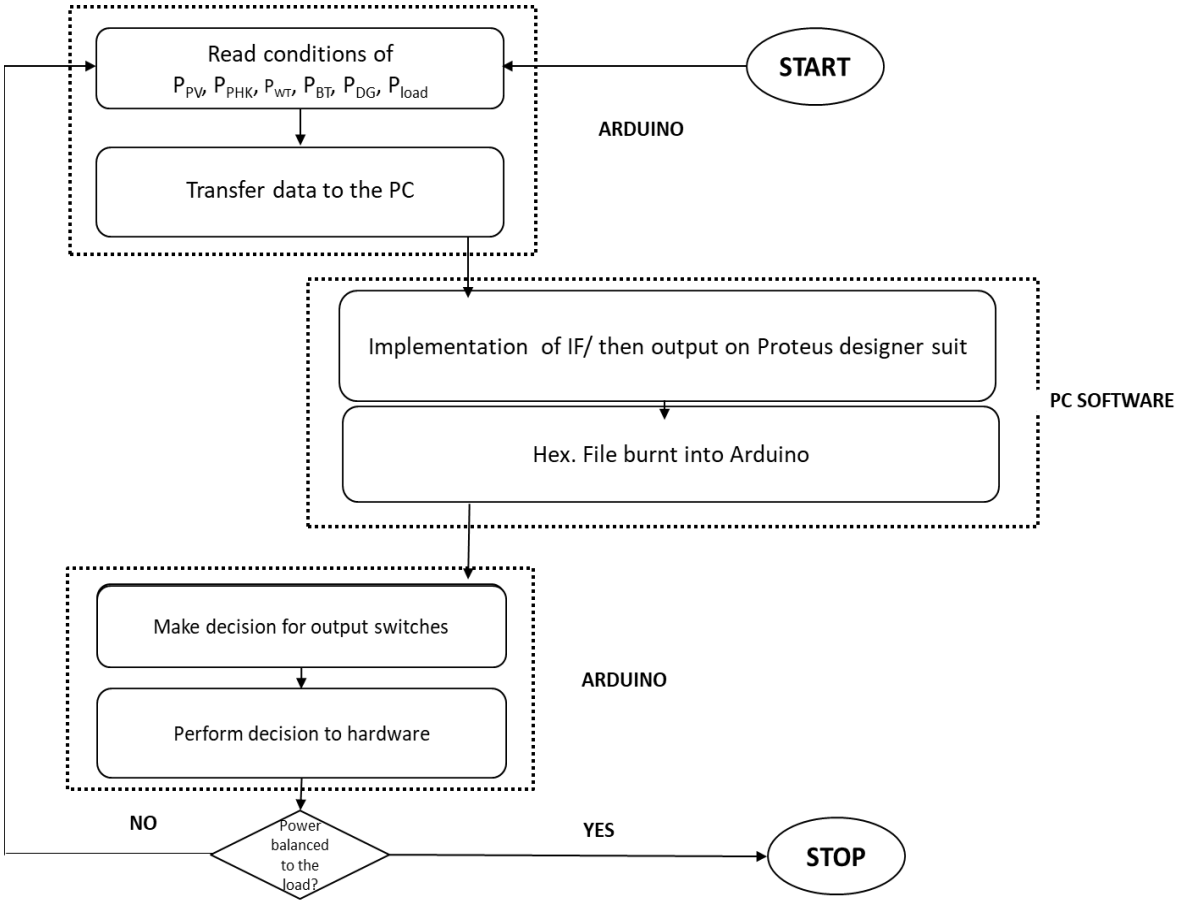

Figure 5.2: Flowchart of the intelligent controller

5.4. SOFTWARE DESIGN CONSIDERATION

5.4.1 Proteus designer suit simulations

The layout of the control in a hybridised system was developed using Proteus Designer Suite 8.1 software. The design of the proposed system, with components to build the printable circuit board layout and the 3D visualization of the circuit layout, were shown in Figure 5.3. Proteus 8 was selected, as it has many advantages compared to other programming methods, including the ability to control the process as the system was tested. The circuit connections on the proteus circuit are particularly similar to those of the hardware and are used to simulate real-time values and further tested the performance of the hardware module in Arduino MEGA. Using Proteus Design Suite, the simulated circuit yielded a satisfactory result. The Proteus 8 interacts with the Arduino micro controller through the designed circuit, with the front panel. The front panel includes components such as the control board, switches (for backup system), LED lights, RES voltage, backup voltage indicator and time indicator.

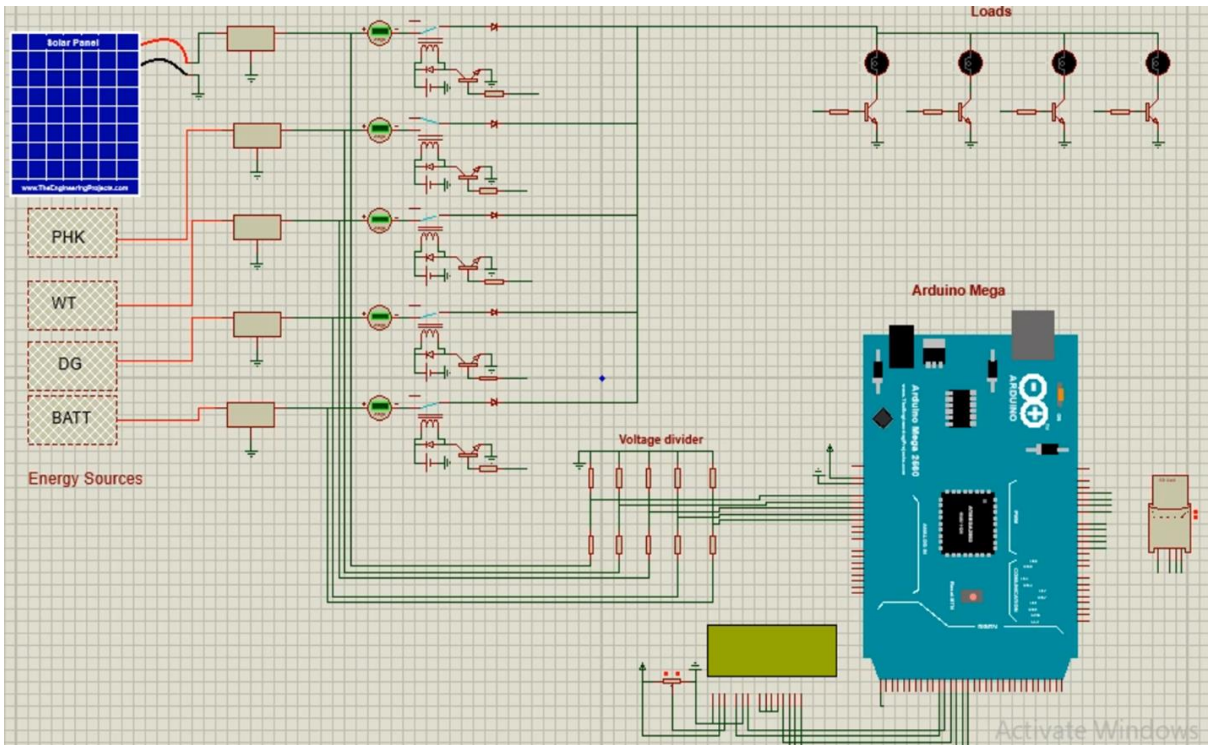

Figure 5.3: Proteus circuit

5.5. HARDWARE IMPLEMENTATION PROCESS

5.5.1 Arduino IDE

The application of Arduino IDE facilitated the development of the prototype-integrated system, shown in Figure 5.4, below. This means that the program is written in Arduino IDE and created in a.hex file, for the operation of the controller. There were libraries that were not available on Arduino when it was initially installed. However, new libraries were installed for availability of additional components to be found and utilized on the board. The library required a detailed study to be carried out in order to design an appropriate circuit and make use of compatible and available components in the designing of the proposed hybrid prototype system. Arduino IDE has made it easy to write and upload the code to the Arduino board. The software has its own default settings, which was Arduino Uno, which changed to Arduino Mega 2560. Since, Arduino Mega 2560 board has been selected, the processor will further default to Arduino Mega 2560.

Figure 5.4: Arduino IDE

Basically, a. hex file that was generated when running the code. There are three programming languages, namely C, java and C++. However, in this study, C++ was selected for the instructions on the Arduino IDE, as Arduino IDE has made it simple to write the code and upload/burn the program to the Arduino compatible board. The code was programmed according to the output results of fuzzy logic software.

In order to transfer the data from the PC to the hardware, the USB cable should be used, which will further require the port settings on the Arduino IDE to be changed, depending on how often the data has been uploaded to the SD card. The default settings are either COM 1 or COM 2, however, COM 4 has been selected. Before the code was uploaded, it was ensured that the simulation results indicated "done compiling", otherwise problems would be encountered. Once the system has finished compiling results, the code is ready to be uploaded to the hardware.

5.5.2 Arduino microcontroller programming

Arduino is a circuit in which its principal component is a microcontroller programmable to perform various tasks, as presented in Figure 5.5. The programming of microcontroller used Arduino IDE as previously mentioned. The Arduino microcontroller does not know how to perform on its own, unless the instructions are written as per demand of any study. The first step was to write the program code, compiled code on IDE with the microcontroller compiler and was uploaded to the microcontroller. The programmed microcontroller used Arduino C++ code, used for the generated power from each source, in terms of voltage to maintain energy supply to the loads and to be energized at a given time. Arduino programming language was selected, due to uncomplicated programming languages, as compared to others.

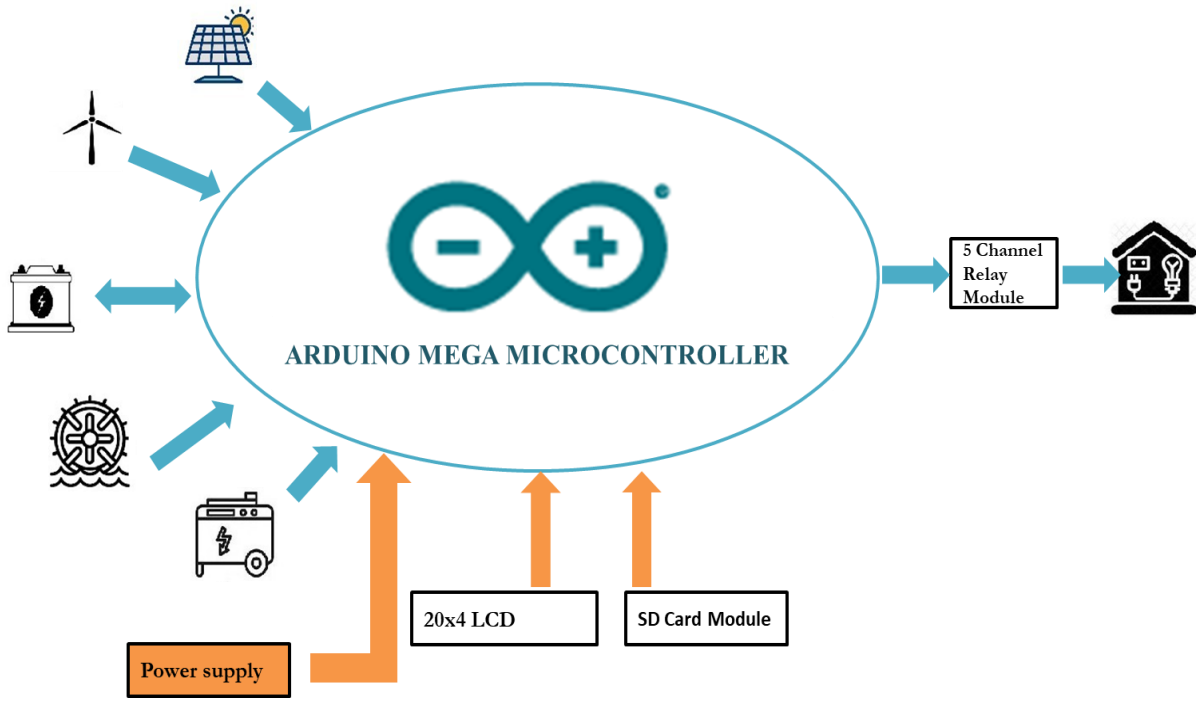

Figure 5.5: Block diagram of Arduino.

5.5.2.1 Power supply

The power supply used was from a variety of renewable energy systems, with a backup system ranging from 12V, that powered the loads through the relays connected to the microcontrollers.

5.5.2.2 Microcontroller

The main controller of the system that received signal from the renewable sources and backup system and converted the voltage produced by each component into readable voltage. Thereafter, it sends a signal to the relay, to determine which load and power sources to be ON or OFF.

5.5.2.3 5 Channel relay

This consists of a relay switch and a relay coil. It is an electronic switch connected in a series with the sources, so that it may change over from one source to the other. The switch

is usually closed when the load is supplied by RE sources and, under abnormal conditions, the switch opens up and permits the backup system to take over the load.

5.5.2.4 Voltage regulator (7805) or power module

The voltage regulator in this circuit was used to regulate the generated voltage of each source to stable 5V, which the microcontroller and other system components in this design use. However, the voltage produced under normal conditions in any household is 220V. The reason for including these components is, generally, when various sources are used to supply the load, they do not generate the same output power at simultaneously. Therefore, the hybrid system required a component to control or balance the output voltage of these sources.

5.5.2.5 Diode

The diode played a role of allowing the unidirectional power flow in the circuit, by avoiding back feed of power, by blocking the path of voltage back to the sources. The diode may therefore further be seen as an electronic version of a validation valve or switch, preventing damage of the relay coil by the electronic transients of the inductance.

5.5.2.6 SD card

The system results may be obtained from the SD card in the system. It will require an SD card adapter, so that data may be read and captured on the SD card. The data captured on the SD card is the voltage of all sources, with respect to time that may be converted to Excel spreadsheet or MATLAB plotting and construct a graphical representation of the results, with respect to time.

5.5.2.7 20x4 LCD display

This component was used to display all the parameters of the system to be used, such as the voltage, period of power consumption, sources used and their transition at a specific time.

5.5.2.8 Loads

Four appliances, such as a refrigerator, stove, geyser and lights, were considered loads in this system. The loads were energized, depending on the available energy sources, balanced by the controller, by opening and closing the relay to supply the load demand 24 hours a day.

5.5.2.9 Resistor

The main function of the resistor in this circuit, is to limit the flow of current to other system components and avoid the burning away of the component in the system.

5.5.2.10 Voltage sensor

It was used to measure the variable input voltage and scales it down to the required system voltage(5V).

5.5.2.11 LED's

In the proposed system, LEDs were used to resemble typical household appliances, i.e. geyser, refrigerator, stove and lights. The load that switched ON or OFF were reflected by these LED's, showing which appliance is ON. As shown in the experimental figure below, the refrigerator was ON throughout the day.

5.5.2.12 USB cable

The USB cable transmits and receives data to and from the microcontroller.

5.5.2.13 Arduino board

The board was used to read the signal that comes from various sensors.

5.6. EXPERIEMENTAL OUTPUT RESULTS

5.6.1 System functionality

The control board operated on a 5V alternating current voltage and controls current draw loads of up to 1,5A, corresponding to approximately 5 units of 5mm, 5V red, yellow and blue emitting diode (LED) lamps, indicating a least of different rural residential loads for a practical setup, as illustrated in Figures 5.6 & 5.7 below. The interface contains a liquid-crystal display (LCD) with a 20x4 display, which enabled the user to view the voltage, time, source ON/OFF status and input and output variables. In this circuit, the LCD display is configured to use 7-bit data, to send commands through two digital pins. The data reported on the LCD display is obtained by means of sensors installed on the board and by means of calculations made by uploaded programming, such as the voltage value.

The module that contains a 10kΩ and a 100Ω resistor and acts as a voltage divider, containing a 7805 voltage regulator IC to stabilize the output values, further has 4 channel relay module that may open and close. The relay board contains a built-in TIP122 transistor, diode and resistor; the transistor is used to control the relay, by enabling it to switch between the loads; the diode is used to prevent generation of power backfeed to the sources, as they will be producing power resistors used to limit the current. Heatsink was installed in the circuit to dissipate heat from the transistors. SD card used for storing of data and SD card module used for transferring of data, thereafter, the data was uploaded from the Arduino IDE software, via USB cable, to the hardware. However, the developed

board has only one control option, which is an automatic option, with no human interference, informing the LCD to display all different parameters in real-time.

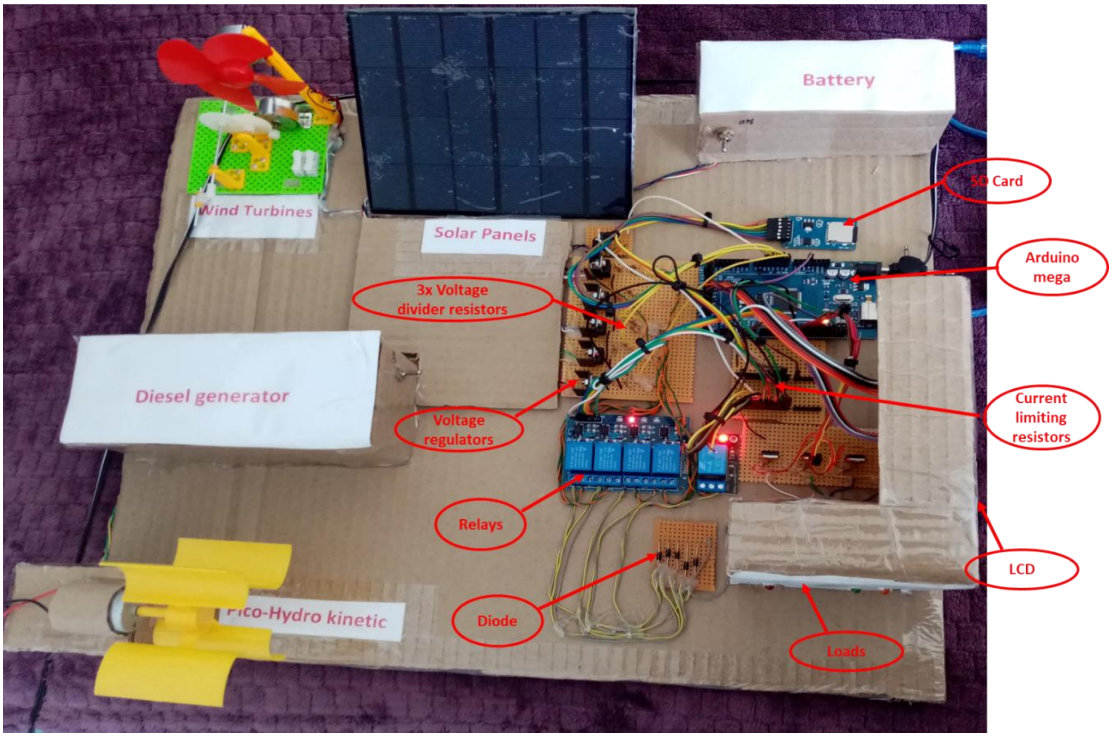

Figure 5.6: Practical Setup

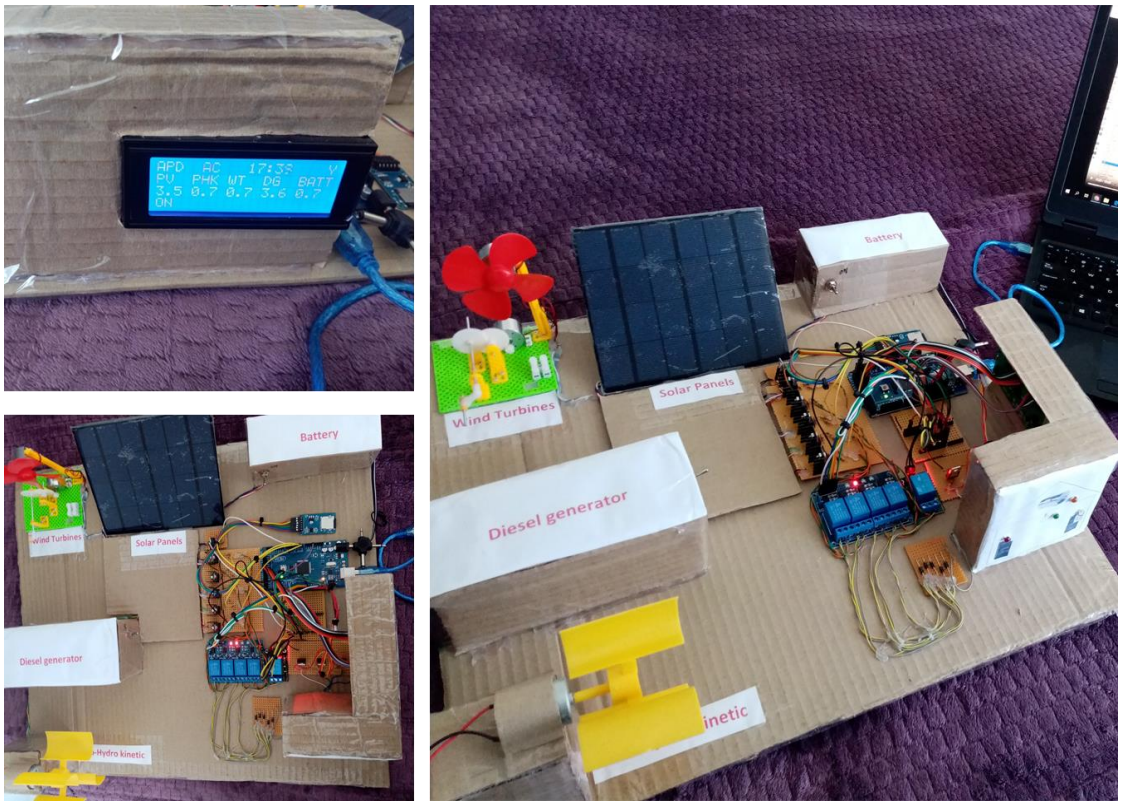

Figure 5.7 Overall overview of Practical Setup

5.6.2 Output results

The LCD displayed the status parameters of all sources in Figure 5.8, including PV, PHK, WT DG and Batt, with Arduino used to measure the maximum output voltage up to 5V. Randomly, 17:33 p.m. was selected to present the practical behaviour of the system displayed on the LCD. PV was the primary source of energy generated at 3.5V at that time, with an ON indicator on the LCD screen, indicating which source of the proposed hybridized system supplied the load during the average consumption. PHK and WT were readily available to supply the load at 0.7V, which was solely insufficient to supply the load, despite the fact that PHK was the secondary supply during that period and did not switch ON, as the energy generated by the PV was exclusively sufficient to supply the load. The standby diesel generator was available at 3.7V, in case the programmed RE source, at that time, failed during that average consumption to supply the load as expected, the backup DG was readily available to take over the load. The battery was also charged at 0.7V, since it is the excess voltage produced during that period. Y=Yes shows that the raw information has been logged and processed as programmed.

Figure 5.8: Load supplied

Table 5.2 below illustrates the behaviour of the loads in real-time, which is visualized in Figure 5.7, where four appliances, such as light, geyser, fridge and stove were connected to be supplied over a 24 hours' period. The load was carried out in the form of fuzzy logic IF/THEN rules, programmed in Arduino IDE and was capable of achieving the practical expected functionality. The load is low from 00:00 to 04:00a.m, as it is solely a morning off-peak, where the load is supplied by PHK. The light, geyser and stove are all turned OFF, however, the fridge is ON.

Table 5.2: Status of rural loads

TIME RANGE (24hrs)	FUZZY INPUT	OUTPUT LOADS			
		Light	Fridge	Geyser	Stove
00:00-4:00	MOP	OFF	ON	OFF	OFF
03:30 -6:00	MP	OFF/ON	ON	OFF/ON	OFF/ON
05:30-16:00	MD	ON/OFF	ON	ON/OFF	ON/OFF
15:30-17:00	APD	OFF	ON	OFF	OFF
16:30-22:00	EP	OFF/ON	ON	OFF/ON	OFF/ON
21:30-23:00	EOP	OFF	ON	OFF	OFF

As the load reaches a medium peak between 03:30 and 6:00a.m, the fridge remains turned ON and the light, geyser and stove switch from an OFF position to ON (OFF/ON), shown in the table below. During this time, most residents are beginning to prepare for work, schools, etc. These loads are powered by PHK and WT. WT is ready to merge with the other source, depending on the sufficient energy resource of the source generating power.

PHK and PV from 05:30 to 16:00, supplied the light, geyser and stove, which switch from ON/OFF, with the fridge remaining ON, after the load has dropped from the medium peak. PHK initially supplied the load, as PV has not yet reached its maximum

potential to generate power during that period. The stove, however, is turned OFF after the rural residents have completed their preparations in the early hours of the day.

Between 15:30 and 17:00, the light, geyser and stove are ready to be switched from OFF to ON, while the fridge is turned ON and PV is in charge of generating power to the load. During the evening peak, the OFF appliances such as geyser, stove and light switches ON, as most appliances are being used, powered by WT with PHK, further ready to supply the load if ever the demand exceeds expectations and the fridge remains ON, though the other appliances, such as the stove and geyser, will be turned OFF.

Finally, the system experiences off peak hours, which are from 21:30 to 23:00, when the load drops again, with PHK solely supplying the fridge, which is still ON at the time, as well as the geyser, stove, and lights, which are all turned OFF. Basically, the appliances are expected to transition from ON/OFF or OFF/ON while the fridge remains ON throughout the day during the specified period.

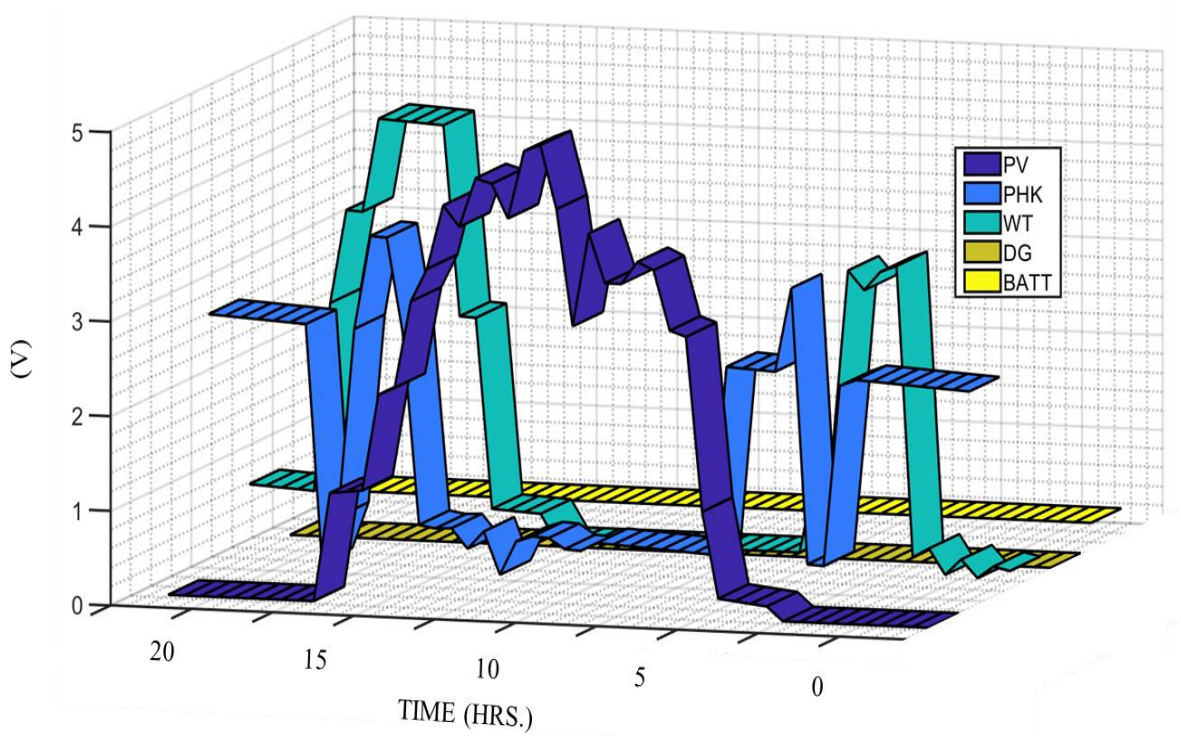

Figure 5.9: Real time hybrid RE system behaviour

Figure 5.9 further reflects the real-time behaviour of the system, as extracted from the SD card, allowing the logged data to be displayed on the LCD and validated in MATLAB plotting to visualize the system's experimental behaviour. According to the programmed

code uploaded on Arduino Mega, the system responded well and the microcontroller sent signals to the sources accordingly, as we have observed that during the day, PV takes over the load, while charging the battery. WT and PHK are readily available to supply the load in the early hours of the day and evenings, since PV during that period is unable to operate fully, as it is dependent on solar irradiation. The battery stores some of the excess or output power generated by each source, while they are producing power. From the afternoon to the evening power consumption increases. WT responds, by supplying the load, with PHK taking over in the evening. WT supplies the highest demand of power consumption in our system.

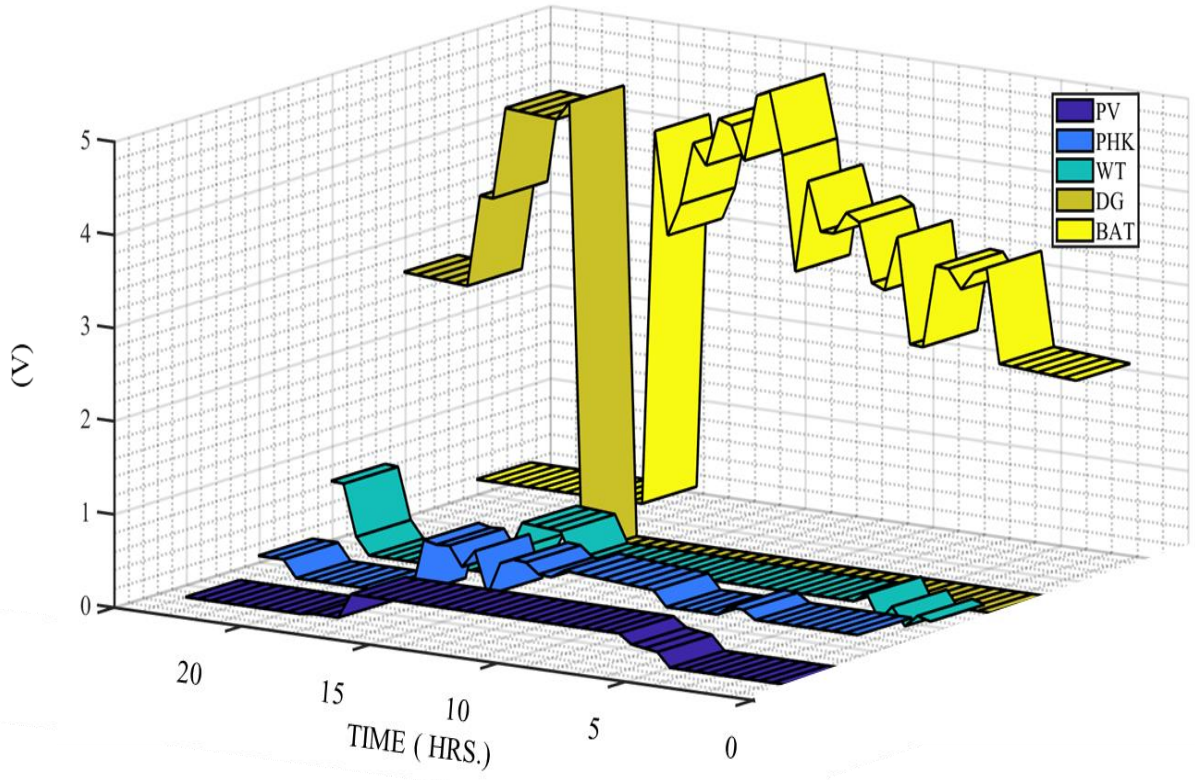

Figure 5.10: Backup system behaviour in case RE fails

The voltage dissipated in Figure 5.10, is the voltage stored in the battery during the time each source, including DG, was operational. During the night, the PV was not operational, however, if the WT and PHK fail to respond due to equipment failure or another defect that may cause the system to fail to discharge power to the load. The battery was modelled in MATLAB to discharge power up to its maximum capacity. However, the battery dissipated the majority of the power, in cases where the defects were experienced in the

system, due to a lack of power to the load, the certainty of the use of battery generated power was ensured to avoid the regular use of DG. The stored power was programed to be released in response to the load's demand. The DG system was operating at a minimal rate to avoid maximizing the increase in CO2 emissions, as the primary goal was to utilize more RE in our hybrid system, to provide power to the rural resident continuously.

5.7. SUMMARY

The circuit of the proposed system was designed in the Proteus designer suit 8.1, tested and yielded a satisfactory result, as it was burnt into a.hex file. The prototype system was observed in real-time through practical work, based on Arduino Mega2560 control preferences. The microcontroller was able to automatically maintain and provide balanced load power, without human interference, irrespective of the variable load power supply. All sources were readily available to supply power the load as programmed, using C++ language in Arduino IDE.

With adequate resources as proven in various studies, the sources were able to produce sufficient energy to the load throughout the day in the proposed system. The main priority of the system was to supply the load primarily with RE sources, then alternatively with the readily available backup system, which was fully controlled by the Arduino Mega2560 board. The microcontroller obeyed the priority control settings programed as the input. As a result, the backup system, particularly the DG, was used as little as possible. The controller enabled the user to continuously supply the load, despite the RE failure interruption caused by energy resources limitations, through the backup system. The current implementation of the hybridized system may effectively solve the lack energy supply to rural residents, which may increase severe ESKOM problems encountered in the country. With minor modifications, a larger project may be implemented, where natural resources are sufficient.

The implementation of real-time EMS, minimizes the use of the DG, while maximizing the use of available renewables. The system served the load through a controller with an off grid HRES made of PV, WT, PHK, a battery storage system and a diesel generator in a laboratory based that was designed, simulated and implemented in real time. The system's power management unit was based on a fuzzy intelligent controller, which was carried out

by the Arduino Mega2560 board, aiming to provide a widely available, cost-effective and efficient hardware platform.

The appropriate power flow control, on the other hand, was initially developed using Proteus designer suit 8.1 software and embedded in a suitable real-time platform such as the Arduino Mega2560. The numerical voltage results on the LCD and MATLAB plotting, demonstrated that the designed controller successfully followed the design goals and made the appropriate decision in real-time situations under various load and resources conditions. The developed EMS was tested and validated through a small-scale application, which accurately represented the expected results that, may be implemented in rural areas of South Africa. It is a critical step towards increasing the use of renewable energies, reducing environmental pollutants and achieving sustainable energy resources.

CHAPTER 6: CONCLUSION

6.1. SUMMARY

The Chapter presents the findings of a study on the practical implementation of an optimal controller in a proposed PV, WT, PHK with DG and battery storage system. To power remote rural households, where power grid extension is not possible. The work focused on the relevant controls in managing the power flow of energy to the rural loads, where the controller demonstrates its capabilities of monitoring and controlling the system, by maximizing the use of RE, rather than the backup system, as the use of RE is there to mitigate the increase of carbon emissions. The research study further demonstrates the viability of using hybrid RE sources for powering energy to residential loads through the intelligent controller.

Chapter 2, reviewed details of existing microgrid prototype controls for optimum operation, classifications, their disadvantages and benefits. To enable us to determine an optimal controller in real-time application or hardware platform. It further identified gaps and potential directions for future research work in this field.

In Chapter 3, the optimal controller was selected and developed in Simulink to control the proposed hybrid and to supply the load with varying supplies, under variable resources. Each source was modelled in SIMULINK, using existing and proven adequate resource data of the PV, PHK and WT from other researchers in South African context.

In Chapter 4**,** all the modelled MATTLAB simulation results were examined and the results obtained indicated that the FLC is capable of controlling the power flow of the proposed prototype standalone hybrid PV, PHK, WT, with backup for the electrification of small rural loads. The desired output power was generated to satisfy the load continuously in 24 hours.

Chapter 5 covers the practical experiment in the laboratory of the proposed hybrid system, in which a prototype system was designed and a circuit was built in Proteus software and then tested. The prototype system was implemented in real time, using an Arduino Mega2560 and the experimental result proved that the microcontroller modeled in Arduino Mega is capable of providing satisfactory output results. The status of various

load consumption and voltage supplied with respect to time, was displayed on the LCD. Arduino was utilized for decision making and operation, as per uploaded code and data logged into the SD card. It is observed through experimental work that. based on the Arduino control preferences; the model is further capable of providing an automatic supply of power to the load, without human interferences.

6.2. FUTURE WORK

Despite the successful implementation of a real-time FL controller in hybridized microgrid system, fuzzy has been criticized for its limitations, including a lack of formal methodology, difficulty in predicting stability and the robustness of the FL-controlled system. FL is not always accurate; the results are perceived or regarded based on assumptions that may not be widely accepted. Fuzzy systems do not have the machine learning capabilities of a neural network-type pattern recognition. Extensive testing with hardware is required for the validation and verification of a fuzzy knowledge-based system. It is difficult to set precise fuzzy rules and membership functions, since fuzzy has been gradually replaced by other advanced artificial intelligent controllers.

The future work, however, is to look at neuro fuzzy (NF), since neuro fuzzy is able to use combination advantages of artificial neural network (ANN) and FL for advanced output results, as it is gaining more popularity. The control provided by NF is far better compared to that provided by FL.as NF algorithm is undeniably superior to the FL algorithm, as it retains adaptability and learning. The NF model's performance may be improved further by training the neural networks with a wider variety of input and output combinations.

REFERENCES

[1] J. C. Nkomo, "Energy and economic development: Challenges for South Africa," *Journal of Energy in Southern Africa*, vol. 16, no. 3. pp. 94–103, 2005.

[2] A. Nickless, R. J. Scholes, and E. Filby, "Spatial and temporal disaggregation of anthropogenic CO2 emissions from the City of Cape Town," *S. Afr. J. Sci.*, vol. 111, no. 11–12, 2015.

[3] G. Montmasson-Clair and G. Ryan, "Repositioning Electricity Planning at the Core: An Evaluation of South Africa's Integrated Resource Plan," *SSRN Electron. J.*, 2016.

[4] A. M. Omer, "Energy, environment and sustainable development," *Renewable and Sustainable Energy Reviews*, vol. 12, no. 9. pp. 2265–2300, 2008.

[5] P. W. Van Niekerk, "The Renewable Energy Resource and Research Base in South Africa," 2008.

[6] J. Krupa and S. Burch, "A new energy future for South Africa: The political ecology of South African renewable energy," *Energy Policy*, vol. 39, no. 10, pp. 6254–6261, 2011.

[7] K. Menyah and Y. Wolde-Rufael, "Energy consumption, pollutant emissions and economic growth in South Africa," *Energy Econ.*, vol. 32, no. 6, pp. 1374–1382, 2010.

[8] T. S. Ustun, C. Ozansoy, and A. Zayegh, "Recent developments in microgrids and example cases around the world - A review," *Renew. Sustain. Energy Rev.*, vol. 15, no. 8, pp. 4030–4041, 2011.

[9] "Eskom launches ground-breaking microgrid pilot plant in Ficksburg," 2018. [Online]. Available: https://www.eskom.co.za/news/Pages/2018Nov3.aspx. [Accessed: 03-Sep-2020].

[10] S. K. Mudziwepasi and M. S. Scott, "Towards the exploration of renewable energy technologies as an alternative to grid extension for rural electrification in South Africa," *Proc. 22nd Conf. Domest. Use Energy, DUE 2014*, no. April, pp. 1–6, 2014.

[11] S. Upadhyay and M. P. Sharma, "A review on configurations, control and sizing methodologies of hybrid energy systems," *Renewable and Sustainable Energy Reviews*. pp. 47–63, 2014.

[12] M. . Siti, Tiako, and B. R.C, "A model predictive control strategy for grid-connected

solar-wind with pumped hydro storage," pp. 79–6, 2016.

[13] K. Kusakana and H. J. Vermaak, "Hybrid renewable power systems for mobile telephony base stations in developing countries," *Renew. Energy*, vol. 51, pp. 419–425, 2013.

[14] K. Kusakana, "Optimal scheduled power flow for distributed photovoltaic/wind/diesel generators with battery storage system," *IET Renew. Power Gener.*, vol. 9, no. 8, pp. 916–924, 2015.

[15] K. Kusakana and H. J. Vermaak, "Hybrid diesel generator/ renewable energy system perfomance modeling," *Renew. Energy*, vol. 67, pp. 97–102, 2014.

[16] P. Ganguly, A. Kalam, and A. Zayegh, "Fuzzy logic-based energy management system of stand-alone renewable energy system for a remote area power system," *Aust. J. Electr. Electron. Eng.*, vol. 1, no. 16, pp. 21–32, 2019.

[17] C. Ameur, S. Faquir, and A. Yahyaouy, "Intelligent optimization and management system for renewable energy systems using multi-agent," *IAES Int. J. Artif. Intell.*, vol. 8, no. 4, pp. 352–359, 2019.

[18] S. Faquir, A. Yahyaouy, H. Tairi, and J. Sabor, "Implementing a fuzzy logic based algorithm to predict solar and wind energies in a hybrid renewable energy system," *Renew. Altern. Energy Concepts, Methodol. Tools, Appl.*, pp. 1220–1235, 2016.

[19] S. Faquir, A. Yahyaouy, H. Tairi, and J. Sabor, "Energy management in an electrical hybrid system using a fuzzy inference control system," *n Proc. 2013 Int. Conf. Ind. Eng. Syst. Manag. (IESM),* pp. 1–5, 2013.

[20] W. M. Lin, C. M. Hong, and C. H. Chen, "Neural-network-based MPPT control of a stand-alone hybrid power generation system," *IEEE Trans. Power Electron.*, vol. 26, no. 12, pp. 3571–3581, 2011.

[21] H. Yang, W. Zhou, L. Lu, and Z. Fang, "Optimal sizing method for stand-alone hybrid solar-wind system with LPSP technology by using genetic algorithm," *Sol. Energy*, vol. 82, no. 4, pp. 354–367, 2008.

[22] H. W. D. Hettiarachchi, K. T. M. U. Hemapala, and A. G. B. P. Jayasekara, "Review of Applications of Fuzzy Logic in Multi-Agent-Based Control System of AC-DC Hybrid Microgrid," *IEEE Access*, vol. 7, pp. 1284–1299, 2019.

[23] A. Shemshadi, S. M. T. Bathaee, A. A. Azirani, and S. J. Kashani, "Design of sugeno-type fuzzy logic controller for torque distribution in a Parallel Hybrid Vehicle," *Int.*

Rev. Electr. Eng., vol. 5, no. 2, pp. 536–541, 2010.

[24] D. Abd-El Baset, H. Rezk, and M. Hamada, "Fuzzy Logic Control Based Energy Management Strategy for Renewable Energy System," *2020 Int. Youth Conf. Radio Electron. Electr. Power Eng. (REEPE),IEEE*, pp. 1–5, 2020.

[25] L. Olatomiwa, S. Mekhilef, M. S. Ismail, and M. Moghavvemi, "Energy management strategies in hybrid renewable energy systems: A review," *Renew. Sustain. Energy Rev.*, vol. 62, pp. 821–835, 2016.

[26] G. Kyriakarakos, A. I. Dounis, K. G. Arvanitis, and G. Papadakis, "A fuzzy logic energy management system for polygeneration microgrids," *Renew. Energy*, vol. 41, pp. 315–327, 2012.

[27] J. Wang and X. Lu, "Sustainable and Resilient Distribution Systems with Networked Microgrids," *Proceedings of the IEEE*, vol. 108, no. 2. pp. 238–241, 2020.

[28] M. Warneryd, M. Håkansson, and K. Karltorp, "Unpacking the complexity of community microgrids: A review of institutions' roles for development of microgrids," *Renew. Sustain. Energy Rev.*, vol. 121, 2020.

[29] M. Gough, S. F. Santos, M. Javadi, R. Castro, and J. P. S. Catalão, "Prosumer flexibility: A comprehensive state-of-the-art review and scientometric analysis," *Energies*, vol. 13, no. 11, p. 2710, 2020.

[30] J. Najafi, A. Peiravi, A. Anvari-Moghaddam, and J. M. Guerrero, "An efficient interactive framework for improving resilience of power-water distribution systems with multiple privately-owned microgrids," *Int. J. Electr. Power Energy Syst.*, vol. 116, 2020.

[31] Q. Fu, A. Nasiri, A. Solanki, A. Bani-Ahmed, L. Weber, and V. Bhavaraju, "Microgrids: Architectures, Controls, Protection, and Demonstration," *Electr. Power Components Syst.*, vol. 43, no. 12, pp. 1453–1465, 2015.

[32] S. Mishra, K. Anderson, B. Miller, K. Boyer, and A. Warren, "Microgrid resilience: A holistic approach for assessing threats, identifying vulnerabilities, and designing corresponding mitigation strategies," *Appl. Energy*, vol. 264, 2020.

[33] M. Stadler and A. Naslé, "Planning and implementation of bankable microgrids," *Electr. J.*, vol. 32, no. 5, pp. 24–29, 2019.

[34] S. Ladide, A. E. L. Fathi, M. Bendaoud, H. Hihi, and K. Faitah, "Hybrid renewable power supply for typical public facilities in six various climate zones in Morocco,"

Int. J. Renew. Energy Res., vol. 9, no. 2, pp. 893–912, 2019.

[35] D. N. Luta and A. K. Raji, "Performance and Cost Analysis of Lithium-Ion Battery for Powering Off-Grid Telecoms Base Stations in Africa," *Int. J. Eng. Res. Africa*, vol. 43, pp. 101–111, 2019.

[36] P. C. D. Goud and R. Gupta, "Solar PV based nanogrid integrated with battery energy storage to supply hybrid residential loads using single-stage hybrid converter," *IET Energy Syst. Integr.*, vol. 2, no. 2, pp. 161–169, 2020.

[37] F. Katiraei, R. Iravani, N. Hatziargyriou, and A. Dimeas, "Microgrids management," *IEEE Power Energy Mag.*, vol. 6, no. 3, pp. 54–65, 2008.

[38] M. Borghei, M. Ghassemi, and C. C. Liu, "Optimal capacity and placement of microgrids for resiliency enhancement of distribution networks under extreme weather events," in *2020 IEEE Power and Energy Society Innovative Smart Grid Technologies Conference, ISGT 2020*, 2020.

[39] K. R. Khan, M. S. Siddiqui, Y. Al Saawy, N. Islam, and A. Rahman, "Condition Monitoring of a Campus Microgrid Elements using Smart Sensors," *Procedia Comput. Sci.*, vol. 163, pp. 109–116, 2019.

[40] D. E. Olivares *et al.*, "Trends in microgrid control," *IEEE Trans. Smart Grid*, vol. 5, no. 4, pp. 1905–1919, 2014.

[41] M. Caruso *et al.*, "Experimental Prototyping of a Microgrid with Mechanical Point of Common Coupling," 2020, pp. 214–219.

[42] N. H. van der Blij, L. M. Ramirez-Elizondo, M. T. J. Spaan, and P. Bauer, "Grid sense multiple access: A decentralized control algorithm for DC grids," *Int. J. Electr. Power Energy Syst.*, vol. 119, 2020.

[43] K. Kusakana, "Optimal Operation Control of Hybrid Renewable Energy Systems. PhD Diss.," Central University of Technology, 2015.

[44] M. Stadler *et al.*, "Value streams in microgrids: A literature review," *Applied Energy*, vol. 162. pp. 980–989, 2016.

[45] A. Cagnano, E. De Tuglie, and P. Mancarella, "Microgrids: Overview and guidelines for practical implementations and operation," *Applied Energy*, vol. 258. 2020.

[46] D. Mayorga González and J. Myrzik, "Probabilistic determination of the operational flexibility of active distribution networks with high penetration of full-converter interfaced renewable distributed generation units," in *Proceedings of the Universities*

Power Engineering Conference, 2015, vol. 2015-Novem.

[47] G. Platt, B. Adam, and C. David, "What role for microgrids?," 2012.

[48] Y. S. Kim, E. S. Kim, and S. Il Moon, "Frequency and voltage control strategy of standalone microgrids with high penetration of intermittent renewable generation systems," *IEEE Trans. Power Syst.*, vol. 31, no. 1, pp. 718–728, 2016.

[49] M. F. Zia, E. Elbouchikhi, and M. Benbouzid, "Microgrids energy management systems: A critical review on methods, solutions, and prospects," *Appl. Energy*, vol. 222, no. June, pp. 1033–1055, 2018.

[50] Y. E. G. Vera, R. Dufo-López, and J. L. Bernal-Agustín, "Energy management in microgrids with renewable energy sources: A literature review," *Applied Sciences (Switzerland)*, vol. 9, no. 18. 2019.

[51] L. Meng, E. R. Sanseverino, A. Luna, T. Dragicevic, J. C. Vasquez, and J. M. Guerrero, "Microgrid supervisory controllers and energy management systems: A literature review," *Renewable and Sustainable Energy Reviews*, vol. 60. pp. 1263–1273, 2016.

[52] E. Bullich-Massagué, F. Díaz-González, M. Aragüés-Peñalba, F. Girbau-Llistuella, P. Olivella-Rosell, and A. Sumper, "Microgrid clustering architectures," *Appl. Energy*, 2018.

[53] A. Sharma, V. Chintala, and S. Kumar, "Feasibility Analysis of Photovoltaic (PV) Grid Tied System for Indian Military Station Considering Economic & Grid Cyber-Security Aspects," 2020, pp. 153–162.

[54] E. W. Prehoda, C. Schelly, and J. M. Pearce, "U.S. strategic solar photovoltaic-powered microgrid deployment for enhanced national security," *Renew. Sustain. Energy Rev.*, vol. 78, pp. 167–175, 2017.

[55] M. Guarnieri, A. Bovo, A. Giovannelli, and P. Mattavelli, "A Real Multitechnology Microgrid in Venice: A Design Review," *IEEE Ind. Electron. Mag.*, vol. 12, no. 3, pp. 19–31, 2018.

[56] A. Parrado-Duque, G. Osma-Pinto, R. Rodríguez-Velásquez, and G. Ordóñez-Plata, "Considerations for the Assessment Resilience in Low Voltage Electrical Network with Photovoltaic Systems - Part i," in *2019 FISE-IEEE/CIGRE Conference - Living the Energy Transition, FISE/CIGRE 2019*, 2019.

[57] O. Mohammed, T. Youssef, M. H. Cintuglu, and A. Elsayed, "Design and simulation

issues for secure power networks as resilient smart grid infrastructure," *Smart Energy Grid Eng.*, no. November, pp. 245–342, 2017.

[58] M. H. Nazari, S. H. Hosseinian, and E. Azad-Farsani, "Shapley value-based techno-economic framework for harmonic and loss mitigation," *IEEE Access*, vol. 7, pp. 119576–119592, 2019.

[59] F. Arrigo, E. Bompard, M. Merlo, and F. Milano, "Assessment of primary frequency control through battery energy storage systems," *Int. J. Electr. Power Energy Syst.*, vol. 115, 2020.

[60] J. Salazar, F. Tadeo, and C. De Prada, "A microgrid library in a general simulation language," *IFAC Proc. Vol.*, vol. 19, pp. 3599–3604, 2014.

[61] L. Palacin, C. De Prada, F. Tadeo, and J. Salazar, "Operation of medium-size reverse osmosis plants with optimal energy consumption," in *IFAC Proceedings Volumes (IFAC-PapersOnline)*, 2010, vol. 9, no. PART 1, pp. 841–846.

[62] R. Darbali-Zamora, J. E. Quiroz, J. Hernández-Alvidrez, J. Johnson, and E. I. Ortiz-Rivera, "Implementation of a Dynamic Real Time Grid-Connected DC Microgrid Simulation Model for Power Management in Small Communities," *2018 IEEE 7th World Conf. Photovolt. Energy Conversion, WCPEC 2018 - A Jt. Conf. 45th IEEE PVSC, 28th PVSEC 34th EU PVSEC*, pp. 1179–1184, 2018.

[63] B. Riar, J. Lee, A. Tosi, S. Duncan, M. Osborne, and D. Howey, "Energy management of a microgrid: Compensating for the difference between the real and predicted output power of photovoltaics," in *2016 IEEE 7th International Symposium on Power Electronics for Distributed Generation Systems, PEDG 2016*, 2016.

[64] E. Mostacciuolo, L. Iannelli, S. Sagnelli, F. Vasca, R. Luisi, and V. Stanzione, "Modeling and power management of a LEO small satellite electrical power system," *2018 Eur. Control Conf. ECC 2018*, pp. 2738–2743, 2018.

[65] M. Jain, S. Gupta, D. Masand, G. Agnihotri, and S. Jain, "Real-Time Implementation of Islanded Microgrid for Remote Areas," *J. Control Sci. Eng.*, vol. 2016, 2016.

[66] M. A. Hannan, M. G. M. Abdolrasol, M. Faisal, P. J. Ker, R. A. Begum, and A. Hussain, "Binary Particle Swarm Optimization for Scheduling MG Integrated Virtual Power Plant Toward Energy Saving," *IEEE Access*, vol. 7, pp. 107937–107951, 2019.

[67] P. J. Binduhewa, M. Barnes, and A. Renfrew, "Standard microsource interface for a

microgrid," PhD Diss., University of Manchester (United Kingdom), 2008.

[68] M. Sechilariu and F. Locment, *Urban DC Microgrid: Intelligent Control and Power Flow Optimization*. 2016.

[69] T. Gunaratne, D. Wijesinghe, K. Wijerathne, P. J. Binduhewa, and J. Ekanayake, "AC-DC Multi-port domestic distribution interface," in *MERCon 2018 - 4th International Multidisciplinary Moratuwa Engineering Research Conference*, 2018, pp. 288–293.

[70] N. M. Mudiyanselage Herath Herath, "Operation , Control , and Simulation of Modular Multilevel Converters with Embedded Energy Storage," 2019.

[71] M. Sechilariu, F. Locment, and L. T. Dos Santos, "A conceptual framework for full optimal operation of a grid-connected DC microgrid," in *Proceedings - 2018 IEEE International Conference on Industrial Electronics for Sustainable Energy Systems, IESES 2018*, 2018, vol. 2018-Janua, pp. 296–301.

[72] M. Sechilariu, "Urban DC Microgrids for Advanced Local Energy Management with Smart Grid Communication," 2017, pp. 3–9.

[73] T. Aziz, S. R. Deeba, and Nahid-Al-Masood, "Investigation of post-fault voltage recovery performance with battery-based energy storage system in a microgrid," in *Proceedings of the 2016 Australasian Universities Power Engineering Conference, AUPEC 2016*, 2016.

[74] C. Ding and K. L. Lo, "Microgrid control and management of state transition period," in *Proceedings of the Universities Power Engineering Conference*, 2012.

[75] J. Alam, T. Hossen, B. Paul, and R. Islam, "Modified Sinusoidal Voltage & Frequency Control of Microgrid in Island Mode Operation," *Int. J. Sci. Eng. Res.*, vol. 4, no. 2, pp. 1–6, 2013.

[76] N. Gupta, "Generation scheduling at PCC in grid connected microgrid," *Int. Conf. Recent Adv. Innov. Eng. ICRAIE 2014*, pp. 9–13, 2014.

[77] F. A. Gervasio, E. Bueno, R. A. Mastromauro, M. Liserre, and S. Stasi, "Voltage control of microgrid systems based on 3lnpc inverters with LCL-filter in islanding operation," in *2015 International Conference on Renewable Energy Research and Applications, ICRERA 2015*, 2015, pp. 827–832.

[78] P. Asmus, "Microgrids, Virtual Power Plants and Our Distributed Energy Future," *Electr. J.*, vol. 23, no. 10, pp. 72–82, 2010.

[79] D. E. Albrecht, *Our energy future: Socioeconomic implications and policy options for rural America*. 2014.

[80] F. Pallas, "Data protection and smart grid communication - The European perspective," in *2012 IEEE PES Innovative Smart Grid Technologies, ISGT 2012*, 2012.

[81] M. Peik-Herfeh, H. Seifi, and M. K. Sheikh-El-Eslami, "Decision making of a virtual power plant under uncertainties for bidding in a day-ahead market using point estimate method," *Int. J. Electr. Power Energy Syst.*, vol. 44, no. 1, pp. 88–98, 2013.

[82] C. K. Sao and P. W. Lehn, "Control and power management of converter fed microgrids," *IEEE Trans. Power Syst.*, vol. 23, no. 3, pp. 1088–1098, 2008.

[83] T. Jain and E. S. N. P. Raju, "Hybrid AC / DC Micro Grid : An Overview," *Fifth Int. Conf. Power Energy Syst. Kathmandu,* no. October 2014, pp. 1–7, 2013.

[84] Y. Li and Y. W. Li, "Power management of inverter interfaced autonomous microgrid based on virtual frequency-voltage frame," *IEEE Trans. Smart Grid*, vol. 2, no. 1, pp. 30–40, 2011.

[85] S. Mishra, S. R. Lenka, P. Satapathy, and P. Nayak, "Optimum design of PV-battery-based microgrid with mutation volatilization-dependent water cycle algorithm," in *Lecture Notes in Electrical Engineering*, 2020, vol. 630, pp. 609–621.

[86] A. Alanazi, H. Lotfi, and A. Khodaei, "Coordinated AC/DC microgrid optimal scheduling," *2017 North Am. Power Symp. NAPS 2017*, pp. 1–6, 2017.

[87] A. Alanazi, H. Lotfi, and A. Khodaei, "Market clearing in microgrid-integrated active distribution networks," *Electr. Power Syst. Res.*, vol. 183, 2020.

[88] K. Lummi, A. Rautiainen, L. Peltonen, S. Repo, P. Jarventausta, and J. Rintala, "Microgrids as part of electrical energy system - Pricing scheme for network tariff of DSO," in *International Conference on the European Energy Market, EEM*, 2018, vol. 2018-June.

[89] E. Unamuno and J. A. Barrena, "Hybrid ac/dc microgrids - Part I: Review and classification of topologies," *Renew. Sustain. Energy Rev.*, vol. 52, pp. 1251–1259, 2015.

[90] H. Lotfi and A. Khodaei, "Hybrid AC/DC microgrid planning," *Energy*, vol. 118, pp. 37–46, 2017.

[91] I. Patrao, E. Figueres, G. Garcerá, and R. González-Medina, "Microgrid architectures for low voltage distributed generation," *Renewable and Sustainable Energy Reviews*, vol. 43. pp. 415–424, 2015.

[92] A. Alfergani, A. Khalil, and Z. Rajab, "Networked control of AC microgrid," *Sustain. Cities Soc.*, vol. 37, pp. 371–387, 2018.

[93] X. Liu, P. Wang, and P. C. Loh, "A Hybrid AC / DC Microgrid and Its," vol. 2, no. 2, pp. 278–286, 2011.

[94] M. Farzinfar, N. K. C. Nair, and M. Bahadornejad, "A new adaptive load-shedding and restoration strategy for autonomous operation of microgrids: A real-time study," *Int. J. Eng. Trans. A Basics*, vol. 33, no. 1, pp. 82–91, 2020.

[95] D. Kumar, F. Zare, and A. Ghosh, "DC Microgrid Technology: System Architectures, AC Grid Interfaces, Grounding Schemes, Power Quality, Communication Networks, Applications, and Standardizations Aspects," *IEEE Access*, vol. 5, pp. 12230–12256, 2017.

[96] A. Chub, D. Zinchenko, D. Vinnikov, and A. Blinov, "Three-port flyback converter for photovoltaic module integration in bipolar DC microgrids," in *Proceedings of the IEEE International Conference on Industrial Technology*, 2020, vol. 2020-Febru, pp. 909–914.

[97] S. Zheng, Z. Ni, and M. Chinthavali, "A Flexible and Secure Evaluation Platform for Overvoltage Protection in Power Electronics Systems," 2020, pp. 877–882.

[98] C. Ndukwe and T. Iqbal, "Sizing and dynamic modelling and simulation of a standalone PV based DC microgrid with battery storage system for a remote community in Nigeria," *J. Energy Syst.*, vol. 3, no. 2, pp. 67–85, 2019.

[99] M. S. Bin Arif and M. A. Hasan, "Microgrid architecture, control, and operation," *Hybrid-renewable energy Syst. microgrids Integr. Dev. Control*, pp. 23–37, Jan. 2018.

[100] T. Dragicevic, X. Lu, J. C. Vasquez, and J. M. Guerrero, "DC Microgrids - Part I: A Review of Control Strategies and Stabilization Techniques," *IEEE Transactions on Power Electronics*, vol. 31, no. 7. pp. 4876–4891, 2016.

[101] S. A. Wakode, A. A. Sheikh, R. R. Deshmukh, and M. S. Ballal, "Oscillation Frequency Based Protection Scheme for Ring Type DC Microgrid," in *2020 IEEE International Conference on Power Electronics, Smart Grid and Renewable Energy, PESGRE 2020*, 2020.

[102] S. J. Williamson, J. Kitson, A. Griffo, and W. Macêdo, "Universal droop controller for DC–DC converter interfaces onto a modular multi-tiered DC microgrid," *J. Eng.*, vol. 2019, no. 17, pp. 3469–3473, 2019.

[103] A. Makkieh, A. Emhemed, D. Wang, A. Junyent-Ferre, and G. Burt, "Investigation of different system earthing schemes for protection of low-voltage DC microgrids," *J. Eng.*, vol. 2019, no. 18, pp. 5129–5133, 2019.

[104] F. Nejabatkhah and Y. W. Li, "Overview of Power Management Strategies of Hybrid AC/DC Microgrid," *IEEE Trans. Power Electron.*, vol. 30, no. 12, pp. 7072–7089, 2015.

[105] A. Gupta, S. Doolla, and K. Chatterjee, "Hybrid AC-DC Microgrid: Systematic Evaluation of Control Strategies," *IEEE Trans. Smart Grid*, vol. 9, no. 4, pp. 3830–3843, 2018.

[106] B. Liang *et al.*, "Coordination control of hybrid AC/DC microgrid," *J. Eng.*, vol. 2019, no. 16, pp. 3264–3269, 2019.

[107] P. Wang, C. Jin, D. Zhu, Y. Tang, P. C. Loh, and F. H. Choo, "Distributed control for autonomous operation of a three-port ac/dc/ds hybrid microgrid," *IEEE Trans. Ind. Electron.*, vol. 62, no. 2, pp. 1279–1290, 2015.

[108] Y. Xia, W. Wei, M. Yu, X. Wang, and Y. Peng, "Power Management for a Hybrid AC/DC Microgrid with Multiple Subgrids," *IEEE Trans. Power Electron.*, vol. 33, no. 4, pp. 3520–3533, 2018.

[109] K. Sun, X. Wang, Y. W. Li, F. Nejabatkhah, Y. Mei, and X. Lu, "Parallel Operation of Bidirectional Interfacing Converters in a Hybrid AC/DC Microgrid Under Unbalanced Grid Voltage Conditions," *IEEE Trans. Power Electron.*, vol. 32, no. 3, pp. 1872–1884, 2017.

[110] D. W. Gao, "Basic Concepts and Control Architecture of Microgrids," in *Energy Storage for Sustainable Microgrid*, 2015, pp. 1–34.

[111] X. Feng, A. Shekhar, F. Yang, R. E. Hebner, and P. Bauer, "Comparison of Hierarchical Control and Distributed Control for Microgrid," *Electr. Power Components Syst.*, vol. 45, no. 10, pp. 1043–1056, 2017.

[112] M. Saleh, Y. Esa, and A. A. Mohamed, "Communication-Based Control for DC Microgrids," *IEEE Trans. Smart Grid*, vol. 10, no. 2, pp. 2180–2195, 2019.

[113] M. Saleh, Y. Es, and A. Mohamed, "Hardware based testing of communication based control for DC microgrid," in *2017 6th International Conference on Renewable Energy Research and Applications, ICRERA 2017*, 2017, vol. 2017-Janua, pp. 902–907.

[114] E. Pashajavid, F. Shahnia, and A. Ghosh, "A decentralized strategy to remedy the

power deficiency in remote area microgrids," in *Proceedings of the Universities Power Engineering Conference*, 2015, vol. 2015-Novem, no. December.

[115] M. D. Ilic and S. Liu, *Hierarchical power systems control : its value in a changing industry*. London: Springer., 1996.

[116] J. M. Guerrero, J. C. Vasquez, J. Matas, L. G. De Vicuña, and M. Castilla, "Hierarchical control of droop-controlled AC and DC microgrids - A general approach toward standardization," *IEEE Trans. Ind. Electron.*, vol. 58, no. 1, pp. 158–172, 2011.

[117] A. J. Wood, B. F. Wollenberg, and G. B. Sheblé, *Problem Solutions For POWER GENERATION OPERATION AND CONTROL From https://passtest.eu/Complete-Solution-Manual-for-Power-Generation-Operation-and-Control-3rd-Edition-by-Allen-J-Wood-Bruce-F-Wollenberg*, no. August. 2013.

[118] F. Shahnia, R. P. S. Chandrasena, S. Rajakaruna, and A. Ghosh, "Primary control level of parallel distributed energy resources converters in system of multiple interconnected autonomous microgrids within self-healing networks," *IET Gener. Transm. Distrib.*, vol. 8, no. 2, pp. 203–222, 2014.

[119] S. Bacha, D. Picault, B. Burger, I. Etxeberria-Otadui, and J. Martins, "Photovoltaics in microgrids: An overview of grid integration and energy management aspects," *IEEE Ind. Electron. Mag.*, vol. 9, no. 1, pp. 33–46, 2015.

[120] A. Bidram and A. Davoudi, "Hierarchical structure of microgrids control system," *IEEE Trans. Smart Grid*, vol. 3, no. 4, pp. 1963–1976, 2012.

[121] R. P. S. Chandrasena, F. Shahnia, A. Ghosh, and S. Rajakaruna, "Secondary control in microgrids for dynamic power sharing and voltage/frequency adjustment," in *2014 Australasian Universities Power Engineering Conference, AUPEC 2014 - Proceedings*, 2014.

[122] M. S. Saleh, A. Althaibani, Y. Esa, Y. Mhandi, and A. A. Mohamed, "Impact of clustering microgrids on their stability and resilience during blackouts," in *Proceedings - 2015 International Conference on Smart Grid and Clean Energy Technologies, ICSGCE 2015*, 2016, pp. 195–200.

[123] M. Jin, W. Feng, P. Liu, C. Marnay, and C. Spanos, "MOD-DR: Microgrid optimal dispatch with demand response," *Appl. Energy*, vol. 187, pp. 758–776, 2017.

[124] H. Belmili, S. Boulouma, B. Boualem, and A. M. Fayçal, "Optimized Control and

Sizing of Standalone PV-wind Energy Conversion System," in *Energy Procedia*, 2017, vol. 107, no. September 2016, pp. 76–84.

[125] M. Marzband, A. Sumper, J. L. Domínguez-García, and R. Gumara-Ferret, "Experimental validation of a real time energy management system for microgrids in islanded mode using a local day-ahead electricity market and MINLP," *Energy Convers. Manag.*, vol. 76, pp. 314–322, 2013.

[126] P. García, J. P. Torreglosa, L. M. Fernández, and F. Jurado, "Optimal energy management system for stand-alone wind turbine/photovoltaic/ hydrogen/battery hybrid system with supervisory control based on fuzzy logic," *Int. J. Hydrogen Energy*, vol. 38, no. 33, pp. 14146–14158, 2013.

[127] B. Bhandari, K. T. Lee, C. S. Lee, C. K. Song, R. K. Maskey, and S. H. Ahn, "A novel off-grid hybrid power system comprised of solar photovoltaic, wind, and hydro energy sources," *Appl. Energy*, vol. 133, pp. 236–242, 2014.

[128] S. Upadhyay and M. P. Sharma, "Selection of a suitable energy management strategy for a hybrid energy system in a remote rural area of India," *Energy*, vol. 94, pp. 352–366, 2016.

[129] S. Berrazouane and K. Mohammedi, "Parameter optimization via cuckoo optimization algorithm of fuzzy controller for energy management of a hybrid power system," *Energy Convers. Manag.*, vol. 78, pp. 652–660, 2014.

[130] R. Dai and M. Mesbahi, "Optimal power generation and load management for off-grid hybrid power systems with renewable sources via mixed-integer programming," *Energy Convers. Manag.*, vol. 73, pp. 234–244, 2013.

[131] R. R. Obaid, "Grid-Tied Solar Panel and Controller for Small Residential Applications," *Int. J. Therm. Environ. Eng.*, vol. 2, no. 2, pp. 103–106, 2010.

[132] S. D. Patil, S. G. Kadwane, and S. P. Gawande, "Current Control of Grid Tied Inverter through SHEPWM Method," in *Energy Procedia*, 2017, vol. 117, pp. 643–650.

[133] C. T. Ma, "Investigation on integrated control strategies for grid-tied inverters under unbalanced grid voltage," in *Lecture Notes in Engineering and Computer Science*, 2018, vol. 2.

[134] M. Hojabri, A. Z. Ahmad, A. Toudeshki, and M. Soheilirad, "An Overview on Current Control Techniques for Grid Connected Renewable Energy Systems," in

2nd International Conference on Power and Energy Systems (ICPES 2012), 2012, pp. 119–126.

[135] A. Kihal, F. Krim, B. Talbi, A. Laib, and A. Sahli, "A robust control of two-stage grid-tied PV systems employing integral sliding mode theory," *Energies*, vol. 11, no. 10, 2018.

[136] P. Rajendran, A. S. Kalpanadevi, and U. G. S. K. Radha, "Design and Development of Fuzzy Based Inverter Controller for Solar / Battery Hybrid Power System," vol. 6, no. 2, pp. 937–942, 2020.

[137] S. Mahjoub, M. Ayadi, and N. Derbel, "Comparative study of smart energy management control strategies for hybrid renewable system based dual input-single output DC-DC converter," *J. Electr. Syst.*, 2020.

[138] V. Syrotiuk *et al.*, "A hybrid system with intelligent control for the processes of resource and energy supply of a greenhouse complex with application of energy renewable sources," *Prz. Elektrotechniczny*, vol. 96, no. 7, pp. 149–152, 2020.

[139] I. Abadlia, L. Hassaine, A. Beddar, F. Abdoune, and M. R. Bengourina, "Adaptive fuzzy control with an optimization by using genetic algorithms for grid connected a hybrid photovoltaic–hydrogen generation system," *Int. J. Hydrogen Energy*, vol. 45, no. 43, pp. 22589–22599, 2020.

[140] S. Al-Chlaihawi, M. A. T. Alrubei, A. Al-Gizi, M. Al-Saadi, and M. Louzazni, "Fuzzy Logic Power Flow Control in divide Full Bridge Three-Port Converter," in *IOP Conference Series: Materials Science and Engineering*, 2020, vol. 881, no. 1.

[141] D. A. El Baset, H. Rezk, and M. Hamada, "Fuzzy Logic Control Based Energy Management Strategy for Renewable Energy System," *Proc. 2nd 2020 Int. Youth Conf. Radio Electron. Electr. Power Eng. REEPE 2020*, vol. 3, no. 2, pp. 2–6, 2020.

[142] A. Alshahir, W. Collings, R. Molyet, and R. Khanna, "Transient Enhancement of Smart Grid Using SMES Controlled by PID and Fuzzy Logic Control," *Eng. Appl. Sci.*, vol. 5, no. 3, p. 56, 2020.

[143] N. Blair *et al.*, "System advisor model, sam 2014.1. 14: General description," *NREL Rep. No. TP-6A20-61019, Natl. Renew. Energy Lab. Golden, CO*, no. February, p. 13, 2014.

[144] M. R. A. Kashkooli and S. M. Madani, "Reducing Torque and Flux Ripples in Direct Torque Control of DFIG Operation at Constant Switching Frequency for Wind

Generation Application," *Majlesi J. Energy Manag.*, vol. 5, no. 4, pp. 27–32, 2016.

[145] X. Y. Wang, J. L. Wang, and H. Wang, "Improvement of the efficiency and power output of solar cells using nanoparticles and annealing," *Sol. Energy*, vol. 101, pp. 100–104, 2014.

[146] F. P. de Mello *et al.*, "Hydraulic turbine and turbine control models for system dynamic studies working group on prime mover and energy supply models for system dynamic performance studies," *IEEE Trans. Power Syst.*, vol. 7, no. 1, pp. 167–179, 1992.

[147] "Mathsworks." [Online]. Available: https://www.mathworks.com/help/examples.html. [Accessed: 18-Jan-2021].

[148] I. M. Canay, "Causes of Discrepancies on Calculation of Rotor Quantities and Exact Equivalent Diagrams of the Synchronous Machine," *IEEE Trans. Power Appar. Syst.*, vol. PAS-88, no. 7, pp. 1114–1120, 1969.

[149] A. Moeini, I. Kamwa, P. Brunelle, and G. Sybille, "Synchronous Machine Stability Model, an Update to IEEE Std 1110-2002 Data Translation Technique," in *IEEE Power and Energy Society General Meeting*, 2018, vol. 2018-Augus.

[150] I. P. and E. Society, *IEEE Guide for Synchronous Generator Modeling Practices and Applications in Power System Stability Analyses*, vol. 2002, no. November. 1991.

[151] D. Kosterev, "Hydro turbine-governor model validation in pacific northwest," *IEEE Trans. Power Syst.*, vol. 19, no. 2, pp. 1144–1149, 2004.

[152] A. Acakpovi, E. Ben Hagan, and F. Xavier Fifatin, "Review of Hydropower Plant Models," *Int. J. Comput. Appl.*, vol. 108, no. 18, pp. 33–38, 2014.

[153] H. Goyal, M. Hanmandlu, and D. P. Kothari, "A three gate optimal flow control approach for automatic control of small hydro power plants using neural networks," *Int. Energy J.*, vol. 7, no. 2, pp. 91–102, 2006.

[154] PES, *IEEE Recommended Practice for Excitation System Models for Power System Stability Studies*, vol. 2005, no. April. 2006.

[155] S. P. Koko, K. Kusakana, and H. J. Vermaak, "Techno-Economic Analysis of an Off-Grid Micro- Hydrokinetic River System for Remote Rural Electrification," 2014.

[156] A. A. H. Hussein and I. Batarseh, "An overview of generic battery models," in *IEEE Power and Energy Society General Meeting*, 2011.

[157] E. M. Krieger, J. Cannarella, and C. B. Arnold, "A comparison of lead-acid and lithium-based battery behavior and capacity fade in off-grid renewable charging applications," *Energy*, vol. 60, pp. 492–500, 2013.

APPENDICES

Appendix A: Load system

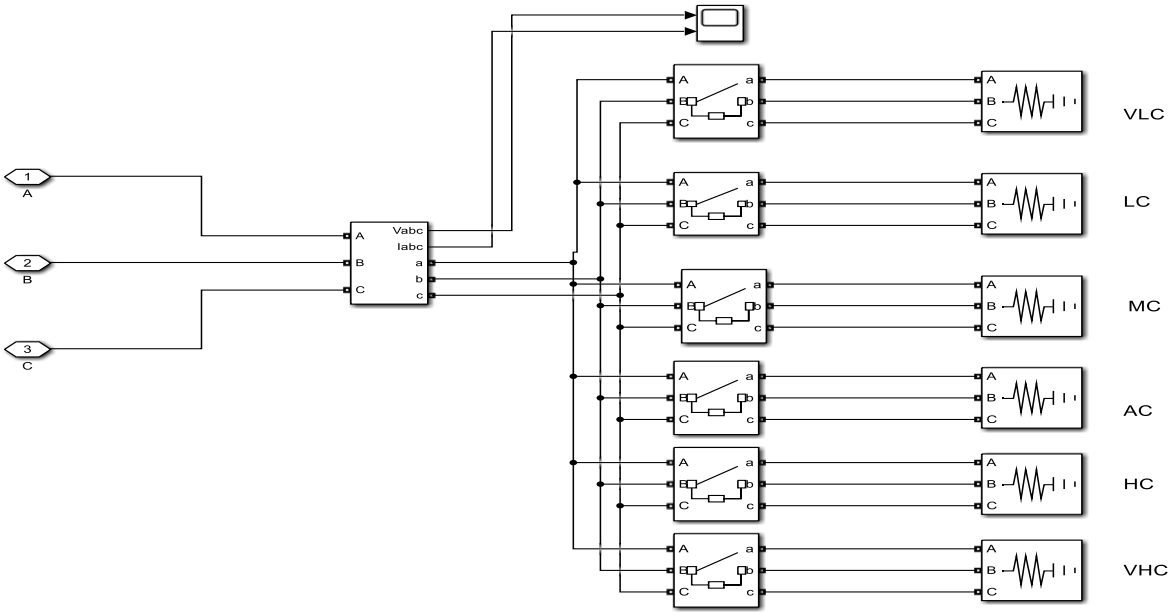

Appendix B: Externally hybrid control switch

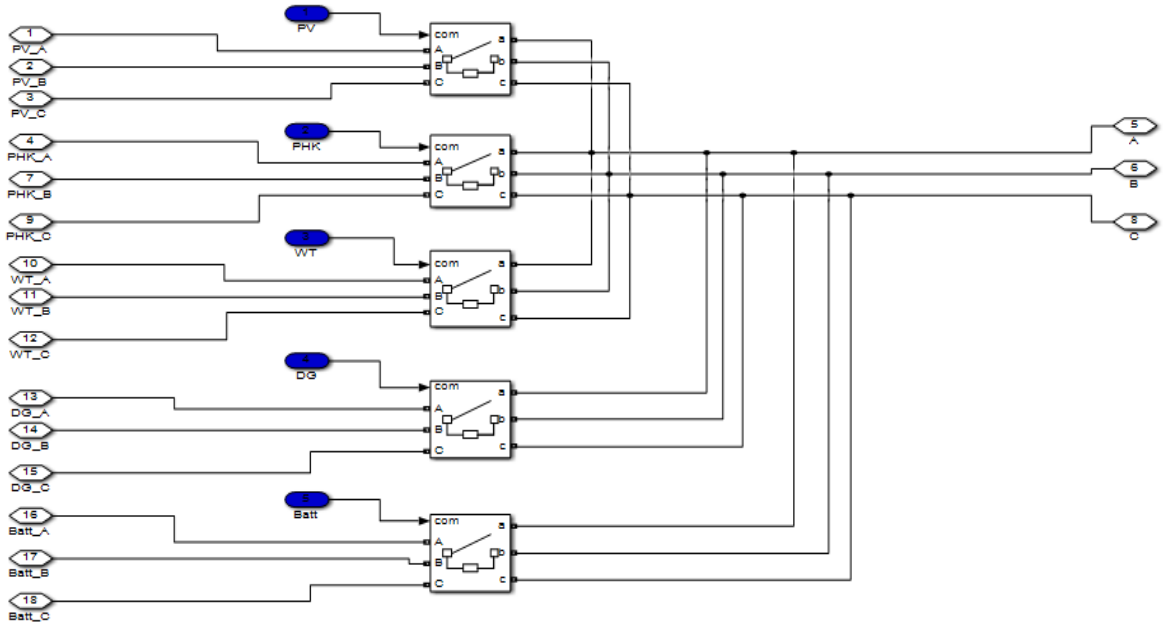

Appendix C: MATLAB function code

```
function CONTR = fcn(time,DG, Batt)

      CONTR=[0 0 0 0 0];
      if time>=0 && time<=4
          CONTR = [0 1 0 0 0];
      end
         if time>=3.3 && time<=6
          CONTR = [0 0 1 0 0];
         end
             if time>=5.3 && time<=11
               CONTR = [0 1 0 0 0];
             end

             if time>=7 && time<=15.30
               CONTR = [1 0 0 0 0];
             end
                     if time>=16.3 && time<=22
                         CONTR = [0 0 1 0 0];
                     end
                         if time>=21.3 && time<=24
                             CONTR = [0 1 0 0 0];
                         end

end
```

Appendix D: Arduino C++ code

```
#include <LiquidCrystal.h>
#include <SD.h>
#include <SPI.h>

File myFile;
int pinCS = 53;

const int rs = 43, en = 42, d4 = 41, d5 = 40, d6 = 39, d7 = 38;
LiquidCrystal lcd(rs, en, d4, d5, d6, d7);
```

```
//Time
int Hours= 0 ;
int Minutes=0 ;
int Seconds=0;
float R1=20000;
float R2=10000;
float Vout, Vin1, Vin2, Vin3, Vin4, Vin5;
float Vref=12.73;

//Fuzzy logic input(time in hrs)
int MOP=4;
int MP=6;
int MD=16;
int APD=17;
int EP=22;
int EOP=23;

void setup()
{
  Serial.begin(9600);
  pinMode(pinCS, OUTPUT);
  pinMode(A0, INPUT); //PV
  pinMode(A1, INPUT); //PHK
  pinMode(A2, INPUT); //WT
  pinMode(A3, INPUT); //DG
  pinMode(A4, INPUT); //BATT

//Relay outputs
  pinMode(3, OUTPUT); //PV
  pinMode(4, OUTPUT); //PHK
  pinMode(5, OUTPUT); //WT
  pinMode(6, OUTPUT); //DG
```

```
  pinMode(7, OUTPUT); //BATT

//Loads
  pinMode(8, OUTPUT); //S
  pinMode(9, OUTPUT); //L
  pinMode(10, OUTPUT); //F
  pinMode(11, OUTPUT); //G

  pinMode(13, OUTPUT); //LCD
  pinMode(12, OUTPUT);
  analogWrite(13,130);
  analogWrite(12,130);
  lcd.begin(20, 4);
  lcd.clear();
}

void loop()
{

 Time();
  lcd.setCursor(10, 0);
  lcd.print(Hours);
  lcd.print(":");
  lcd.print(Minutes);

  lcd.setCursor(0, 1);
  lcd.print("PV  PHK WT  DG  BATT");

//Voltage calculations
  //PV
  Vout = (5.00/ 1023.00)*analogRead(A0);
  Vin1 = Vout / (R2/(R1+R2));
```

```
//PHK
Vout = (5.00/ 1023.00)*analogRead(A1);
Vin2 = Vout / (R2/(R1+R2));
//WT
Vout = (5.00/ 1023.00)*analogRead(A2);
Vin3 = Vout / (R2/(R1+R2));
//DG
Vout = (5.00/ 1023.00)*analogRead(A3);
Vin4 = Vout / (R2/(R1+R2));
//BATT
Vout = (5.00/ 1023.00)*analogRead(A4);
Vin5 = Vout / (R2/(R1+R2));

if(Hours>=17 && Hours<=7)
{
  Vin1=0;
}

//Loads config
digitalWrite(10,HIGH); //F
if(Hours>=16 && Hours<=22)
{
  digitalWrite(8,HIGH); //S
  digitalWrite(11,HIGH); //G
}
else
{
  digitalWrite(8,LOW); //S
  digitalWrite(11,LOW); //G
}
if(Hours>=17 && Hours<=6)
{
```

```
   digitalWrite(9,HIGH); //L
  }
  else
  {
   digitalWrite(9,LOW); //L
  }

if(Minutes==10 || Minutes==20 || Minutes==30 || Minutes==40 || Minutes==50
|| Minutes==59 || Minutes==1)
{
 lcd.setCursor(0, 2);
 lcd.print(Vin1,1); lcd.print(" ");
 lcd.print(Vin2,1); lcd.print(" ");
 lcd.print(Vin3,1); lcd.print(" ");
 lcd.print(Vin4,1); lcd.print(" ");
 lcd.print(Vin5,1); lcd.print(" ");

 if(Hours>=0 && Hours<=4)  //MOP
 {
  lcd.setCursor(0, 0);
  lcd.print("MOP");
  lcd.setCursor(5, 0);
  lcd.print("VLC");
  if(Vin2>=3) //PHK on
  {
   digitalWrite(3,1);  //PV
   digitalWrite(4,0);  //PHK on
   digitalWrite(5,1);  //WT
   digitalWrite(6,1);  //DG
   digitalWrite(7,1);  //Batt

   lcd.setCursor(0,3);
```

```
   lcd.print("    ON             ");
  }
  else  //Batt on
  {
   digitalWrite(3,1);  //PV
   digitalWrite(4,0);  //PHK on
   digitalWrite(5,1);  //WT
   digitalWrite(6,1);  //DG
   digitalWrite(7,0);  //Batt on

   lcd.setCursor(0,3);
   lcd.print("    ON         ON  ");
  }
 }
if(Hours>4 && Hours<=6)  //MP
{
 lcd.setCursor(0, 0);
 lcd.print("MP ");
 lcd.setCursor(5, 0);
 lcd.print("LC ");
 if(Vin3>=3) //WT in
 {
  digitalWrite(3,1);  //PV
  digitalWrite(4,1);  //PHK
  digitalWrite(5,0);  //WT on
  digitalWrite(6,1);  //DG
  digitalWrite(7,1);  //Batt

  lcd.setCursor(0,3);
  lcd.print("        ON         ");
 }
 else  //Batt in
```

```
  {
   digitalWrite(3,1);  //PV
   digitalWrite(4,1);  //PHK
   digitalWrite(5,0);  //WT on
   digitalWrite(6,1);  //DG
   digitalWrite(7,0);  //Batt on

   lcd.setCursor(0,3);
   lcd.print("       ON       ON ");
  }
}
if(Hours>6 && Hours<=15)  //MD
{
 lcd.setCursor(0, 0);
 lcd.print("MD ");
 lcd.setCursor(5, 0);
 lcd.print("MC ");
 if(Vin1>=3 || Vin2>=3) //PV and PHK on
 {
   digitalWrite(3,0);  //PV on
   digitalWrite(4,0);  //PHK on
   digitalWrite(5,1);  //WT
   digitalWrite(6,1);  //DG
   digitalWrite(7,1);  //Batt

   lcd.setCursor(0,3);
   lcd.print("ON  ON             ");
 }
 else  //Batt in
 {
   digitalWrite(3,0);  //PV on
   digitalWrite(4,0);  //PHK on
```

```
    digitalWrite(5,1);  //WT
    digitalWrite(6,1);  //DG
    digitalWrite(7,0);  //Batt on

    lcd.setCursor(0,3);
    lcd.print("ON  ON          ON ");
   }
}
if(Hours>15 && Hours<=17)  //APD
{
  lcd.setCursor(0, 0);
  lcd.print("APD");
  lcd.setCursor(5, 0);
  lcd.print("AC ");
  if(Vin1>=3) //PV in
  {
    digitalWrite(3,0);  //PV
    digitalWrite(4,1);  //PHK
    digitalWrite(5,1);  //WT
    digitalWrite(6,1);  //DG
    digitalWrite(7,1);  //Batt

    lcd.setCursor(0,3);
    lcd.print("ON                ");
  }
  else  //Batt in
  {
    digitalWrite(3,0);  //PV
    digitalWrite(4,1);  //PHK
    digitalWrite(5,1);  //WT
    digitalWrite(6,1);  //DG
    digitalWrite(7,0);  //Batt
```

```
      lcd.setCursor(0,3);
      lcd.print("ON              ON ");
    }
  }
if(Hours>17 && Hours<=22)  //EP
  {
    lcd.setCursor(0, 0);
    lcd.print("EP ");
    lcd.setCursor(5, 0);
    lcd.print("HC ");
    if(Vin3>=3) //WT in
    {
      digitalWrite(3,1);  //PV
      digitalWrite(4,1);  //PHK
      digitalWrite(5,0);  //WT
      digitalWrite(6,1);  //DG
      digitalWrite(7,1);  //Batt

      lcd.setCursor(0,3);
      lcd.print("       ON         ");
    }
    else  //DG in
    {
      digitalWrite(3,1);  //PV
      digitalWrite(4,1);  //PHK
      digitalWrite(5,0);  //WT
      digitalWrite(6,0);  //DG
      digitalWrite(7,1);  //Batt

      lcd.setCursor(0,3);
      lcd.print("       ON  ON     ");
```

```
   }
  }
  if(Hours>22 && Hours<=23)  //EOP
  {
   lcd.setCursor(0, 0);
   lcd.print("E0P");
   lcd.setCursor(5, 0);
   lcd.print("VHC ");
   if(Vin2>=3) //PHK in
   {
    digitalWrite(3,1);  //PV
    digitalWrite(4,0);  //PHK
    digitalWrite(5,1);  //WT
    digitalWrite(6,1);  //DG
    digitalWrite(7,1);  //Batt

    lcd.setCursor(0,3);
    lcd.print("    ON              ");
   }
   else  //DG in
   {
    digitalWrite(3,1);  //PV
    digitalWrite(4,0);  //PHK
    digitalWrite(5,1);  //WT
    digitalWrite(6,0);  //DG
    digitalWrite(7,1);  //Batt

    lcd.setCursor(0,3);
    lcd.print("    ON      ON      ");
   }
  }
}
```

```
// SD Card Initialization
 if (SD.begin())
 {
   lcd.setCursor(19, 0);
   lcd.print("Y");
  }
  else
 {
   lcd.setCursor(19, 0);
   lcd.print("N");
   Serial.println("SD card initialization failed");
   return;
 }
  //data logging
  if(Minutes==30 || Minutes==59)
   {
     datalogging();
   }
}

void datalogging()
{
 // Create/Open file
 myFile = SD.open("test.txt", FILE_WRITE);

 // if the file opened okay, write to it:
 if (myFile)
 {
   // Write to file
   myFile.print(" ");
   myFile.print(Hours);
```

```
  Serial.print(" ");
  Serial.print(Hours);
  myFile.print(":");
  myFile.print(Minutes);
  Serial.print(":");
  Serial.print(Minutes);
  myFile.print("    ");
  myFile.print((Vin1/5)*100);
  Serial.print("    ");
  Serial.print((Vin1/5)*100);
  myFile.print("    ");
  myFile.print((Vin2/5)*100);
  Serial.print("    ");
  Serial.print((Vin2/5)*100);
  myFile.print("    ");
  myFile.print((Vin3/5)*100);
  Serial.print("    ");
  Serial.print((Vin3/5)*100);
  myFile.print("    ");
  myFile.print((Vin4/5.2)*100);
  Serial.print("    ");
  Serial.print((Vin4/5.2)*100);
  myFile.print("    ");
  myFile.println((Vin5/5.2)*100);
  Serial.print("    ");
  Serial.println((Vin5/5.2)*100);

  myFile.close(); // close the file
}
// if the file didn't open, print an error:
else
{
```

```
    Serial.println("error opening test.txt");
    lcd.setCursor(19, 0);
    lcd.print("N");
  }
}

void Time()
{
   Minutes=Minutes+1;
     if(Minutes==60)
     {
      lcd.clear();
      Minutes=0;
      Hours=Hours+1;
        if(Hours==23)
         {
          lcd.clear();
          Hours=0;
         }
     }
  //delay(100);
}
```

Appendix E: Cost of experiment

Central University of Technology has managed to provide grant for the material of the prototype system shown in the appendix for the development and the design of the proposed hybrid system. The system can be implemented in SA's rural standalone microgrid hybrid systems.

Table A.E.6.1: Prototype material costs

Item no.	**Components**	**Quantity**	Unit cost (ZAR)	Amount (ZAR)
1	PV system, 6V, monocrystalline, 165x135x2mm, 583mA 12V,7A 12-35 VOUT 150W	1	R 1 799.99	R 1 799.99
2	WT system, Dynamo Lantern kit, 95x110x52mm	1	R 749.00	R 749.00
3	PHK system, Vert Rotor Dynamo, 0.01-5.5V, 100-600rpm, 0.01-100mA	1	R 759.00	R 759.00
4	DG & battery system, rechargeable battery 12V, 1.4Ah, (L=151 W=65 H=94mm) F1 Terminal 4.8mm 1.9kg	2	R 359.13	R 718.26
5	5 channel relay module, 3.75V-6V, 5V coil	1	R 149	R 149
6	Transistor, TIP122	4	R 386.00	R 716.26

7	7805 Voltage regulators, +5V, 1.5A	5	R 176.00	R 880.00
8	SD card module, 4.5-5.5V, 0.2-200mA, 42 x 24 x 12mm	1	R 339.00	R 339.00
9	SD card, 3GB	1	R 75.00	R 75.00
10	Arduino Mega, 2560 Rev3, 54 digital input/output pins, 16 analog inputs, 4 UARTSs (hardware serial ports), 16MHz crystal oscillator, USB connection, power jack, ICSP header and reset button.	1	R 762.54	R 762.54
11	20x4 LCD, Blue, 5V, 12C NOT	1	R 339.00	R 339.00
12	Diode, 1N4007 PN junction	5	R 50.00	R 250.00
13	LED, 5mm, 5V, Red, yellow, Blue	5	R 66.75	R 333.75
14	Heatsink, 24.4°C/W, 19.05 x 13.21 x 12.7mm	9	R 54.24	R 488.16
15	AC/DC adapter, 500mA, 3V-12V	1	R 474.00	R 474.00
16	Resistors, 10kΩ, 100Ω	19	R 103.00	R 1 957.00
17	Universal serial bus (USB) cable, Blue	1	R 109.00	R 109.00